

2007

Engineering a Photo-Control Mechanism for RNA Interference

Richard Andrew Blidner

Louisiana State University and Agricultural and Mechanical College

Follow this and additional works at: https://digitalcommons.lsu.edu/gradschool_dissertations



Part of the [Engineering Science and Materials Commons](#)

Recommended Citation

Blidner, Richard Andrew, "Engineering a Photo-Control Mechanism for RNA Interference" (2007). *LSU Doctoral Dissertations*. 1331.

https://digitalcommons.lsu.edu/gradschool_dissertations/1331

This Dissertation is brought to you for free and open access by the Graduate School at LSU Digital Commons. It has been accepted for inclusion in LSU Doctoral Dissertations by an authorized graduate school editor of LSU Digital Commons. For more information, please contact gradetd@lsu.edu.

ENGINEERING A PHOTO-CONTROL MECHANISM
FOR RNA INTERFERENCE

A Dissertation

Submitted to the Graduate Faculty of the
Louisiana State University and
Engineering College
in partial fulfillment of the
requirements for the degree of
Doctor of Philosophy

in

The Interdisciplinary Program
in Engineering Science

by

Richard Andrew Blidner
B.S., Tulane University, 2001
M.S., The Ohio State University, 2003
December 2007

ACKNOWLEDGMENTS

I would like to begin by thanking my primary advisor, Dr. W. Todd Monroe for providing valuable direction and support throughout the course of this work. I have learned a great deal under his tutelage, which expands beyond the subjects of basic sciences and engineering to include strategies for management, facilitating collaborations within multidisciplinary applications, written and verbal communication styles, and more. His patience and confidence in me while I was learning the biochemical and chemical techniques required for this work have allowed me the room to grow and learn which would have otherwise been restricted without this support.

Next I would like to thank the complete dissertation committee: Dr. Mark A. Batzer, Dr. Robert P. Hammer, Dr. Richard L. Bengtson, Dr. Michael C. Murphy, and Dr. Richard F. Shaw. Each individual provided insights that guided and challenged my thinking, substantially improving the design this research project. Special thanks are owed to Dr. Robert Hammer for providing chemical expertise and advice that was critical to nearly every aspect of this work. I would also like to mention Dr. Mark Batzer for agreeing to serve as my minor advisor in biochemistry and for providing a wealth of both equipment and knowledge based resources.

Finally, I would like to thank all of the faculty, graduate student, and undergraduate student collaborators who helped with this project. The interdisciplinary nature of this work would have been impossible without the help from those in other research focus areas. I would like to thank Drs. Kurt Svoboda and Mandi Lopez along with the students and personnel in their laboratories for providing expertise in zebrafish and PCR, respectively. I would also like to thank Julianne Audiffred for agreeing to

continue on with her Ph.D. and providing help in managing the day to day operations of the lab. Last but certainly not least, I would like to thank the collection of master's students and undergraduates who worked beside me to achieve the end goals of this project.

TABLE OF CONTENTS

| | |
|--|------|
| ACKNOWLEDGEMENTS | ii |
| LIST OF TABLES | vii |
| LIST OF FIGURES | viii |
| LIST OF ABBREVIATIONS | x |
| ABSTRACT | xii |
| CHAPTER 1: Introduction | 1 |
| 1.1 Purpose and Significance | 1 |
| 1.2 RNA Interference | 3 |
| 1.2.1 Known Mechanism of RNA Interference | 4 |
| 1.2.1.1 Small Interfering RNA Generation | 6 |
| 1.2.1.2 RISC Assembly | 7 |
| 1.2.1.3 RISC Maturation | 9 |
| 1.2.1.4 RISC Targeting and mRNA Degradation | 10 |
| 1.2.1.5 Downstream RNAi Processes | 12 |
| 1.2.2 Chemical Modifications to siRNAs | 14 |
| 1.2.2.1 Terminal Modifications | 14 |
| 1.2.2.2 Backbone Modifications | 17 |
| 1.2.2.3 Base Modifications | 20 |
| 1.2.2.4 2' Modifications | 20 |
| 1.2.3 Current RNAi Therapeutic Developments | 25 |
| 1.3 Caging | 28 |
| 1.3.1 Definition and Historical Perspective | 28 |
| 1.3.2 Common Cage Groups | 32 |
| 1.3.2.1 2-Nitrobenzyl Caging Group | 32 |
| 1.3.2.2 <i>p</i> -Hydroxyphenacyl Caging Group | 35 |
| 1.3.2.3 Coumarinyl Caging Group | 38 |
| 1.3.2.4 Benzoin Caging Group | 41 |
| 1.3.3 Caging of Nucleic Acids | 43 |
| 1.3.4 Special Considerations | 48 |
| 1.3.4.1 Two-Photon Excitation | 48 |
| 1.3.4.2 Convertible Nucleoside Approach | 49 |
| CHAPTER 2: Initial Feasibility Studies for Caging RNA | 52 |
| 2.1 Determination of Caging Efficiency | 52 |
| 2.2 Determination and Optimization of Caging Protocol | 54 |
| 2.3 Caging of 700bp dsRNA | 60 |
| 2.4 Design of the siRNA for the pAcGFP Reporter System | 62 |
| CHAPTER 3: 2'-Fluoro Nucleic Acids Induce RNA Interference | 64 |
| 3.1 Introduction | 64 |

| | | |
|------------|---|-----|
| 3.2 | Materials and Methods | 68 |
| 3.2.1 | siRNA Design | 68 |
| 3.2.2 | siRNA and siFNA Preparation | 69 |
| 3.2.3 | Hybridization Analysis..... | 70 |
| 3.2.4 | Nuclease Digestions | 71 |
| 3.2.5 | Cell Culture and Transfection | 71 |
| 3.2.6 | Flow Cytometry RNAi Analysis | 72 |
| 3.2.7 | Semiquantitative PCR Analysis | 73 |
| 3.3 | Results | 75 |
| 3.3.1 | FNA Generation..... | 75 |
| 3.3.2 | Hybridization Analysis..... | 76 |
| 3.3.3 | Nuclease Digestions | 77 |
| 3.3.4 | RNAi of GFP Expression in Cell Cultures | 78 |
| 3.4 | Discussion | 83 |
| 3.4.1 | FNA Generation..... | 84 |
| 3.4.2 | Digestion Assays | 86 |
| 3.4.3 | RNAi of GFP Expression in Cell Cultures | 87 |
| 3.5 | Conclusions and Future Works | 91 |
| CHAPTER 4: | Caging 2'-Fluoro Nucleic Acids for RNAi | 94 |
| 4.1 | Introduction | 94 |
| 4.2 | Materials and Methods | 97 |
| 4.2.1 | 2'-Deoxy-2'-Fluoro Nucleic Acid Synthesis and Caging..... | 97 |
| 4.2.2 | Evaluation of Caged Nucleic Acids <i>In Vitro</i> | 98 |
| 4.2.3 | Nuclease Digestions | 99 |
| 4.2.4 | Photoexposure | 99 |
| 4.2.5 | Cell Culture and Transfection | 100 |
| 4.2.6 | Flow Cytometry RNAi Analysis | 101 |
| 4.2.7 | Zebrafish Embryo RNAi | 102 |
| 4.3 | Results | 103 |
| 4.3.1 | Spectrophotometric Evaluation of Caged FNA | 103 |
| 4.3.2 | HPLC Separation of Caged FNAs | 105 |
| 4.3.3 | Nuclease Digestions | 106 |
| 4.3.4 | Control of RNAi in Cell Culture with Caged FNAs | 107 |
| 4.3.5 | Control of RNAi in Zebrafish Embryos | 110 |
| 4.4 | Discussion | 113 |
| CHAPTER 5: | Base-Caged ATP: an Alternative to γ -Phosphate Caged ATP | 123 |
| 5.1 | Introduction | 123 |
| 5.2 | Materials and Methods | 125 |
| 5.3 | Results | 128 |
| 5.4 | Discussion..... | 133 |
| CHAPTER 6: | Conclusions and Future Directions | 135 |
| 6.1 | Conclusions..... | 135 |
| 6.2 | Future Directions | 141 |

| | |
|----------------------------|-----|
| REFERENCES | 145 |
| LETTER OF PERMISSION | 167 |
| VITA | 168 |

LIST OF TABLES

| | | |
|-----|---|-----|
| 1.1 | Caging efficiencies of various NA targets | 55 |
| 5.1 | Luciferase ATP assay with caged effectors | 132 |
| 5.2 | % of RLU from ATP co-incubated with caged effectors | 132 |

LIST OF FIGURES

| | | |
|------|--|-----|
| 1.1 | RNAi mechanism | 5 |
| 1.2 | Sugar and backbone chemical modifications | 19 |
| 1.3 | 2-Nitrobenzyl γ -phosphate caged ATP and photolytic release | 30 |
| 1.4 | 2-nitrobenzyl derivatives | 33 |
| 1.5 | Proposed photolytic mechanism of 2-nitrobenzyl..... | 35 |
| 1.6 | <i>p</i> -hydroxyphenacyl cage group | 36 |
| 1.7 | <i>p</i> -hydroxyphenacyl photolytic mechanism | 38 |
| 1.8 | The coumarinyl cage group | 39 |
| 1.9 | Coumarinyl proposed photolytic mechanisms..... | 40 |
| 1.10 | The benzoin cage group | 42 |
| 1.11 | One versus two-photon uncaging | 48 |
| 1.12 | Convertible nucleoside approach..... | 50 |
| 2.1 | Caging efficiency by cage concentration and reaction temperature..... | 56 |
| 2.2 | LH-20 sephadex resolution | 58 |
| 2.3 | Capillary electrophoresis of caged 700bp dsRNA..... | 61 |
| 3.1 | Melt-curve analysis of FNA hybridization | 76 |
| 3.2 | Capillary electrophoresis of nuclease treated RNAs and FNAs | 77 |
| 3.3 | Brightfield and fluorescent microscopy of cell cultures | 79 |
| 3.4 | RNAi analysis of siRNA and siFNA in cell culture..... | 81 |
| 3.5 | RNAi analysis of antisense RNA and FNA in cell culture..... | 82 |
| 3.6 | Semiquantitative PCR analysis of RNAi knockdown of GFP vs. GAPDH | 83 |
| 4.1 | Spectrophotometric analysis of caged FNAs | 104 |

| | | |
|-----|---|-----|
| 4.2 | HPLC separation of caged FNAs..... | 105 |
| 4.3 | Nuclease digestion (BAL-31) of control and caged FNAs..... | 106 |
| 4.4 | RNAi using caged siFNAs in cell culture..... | 108 |
| 4.5 | Response of cells to various doses of 365 nm light..... | 109 |
| 4.6 | Zebrafish injection analysis..... | 110 |
| 4.7 | GFP expression is unaffected by UVA light exposure | 111 |
| 4.8 | RNAi of caged versus control siFNA in zebrafish | 111 |
| 4.9 | Toxicity evaluation of control versus caged siFNAs..... | 112 |
| 5.1 | Base-caged adenosine scheme..... | 127 |
| 5.2 | NMR of DMNB-NH ₂ | 128 |
| 5.3 | HPLC monitoring of CPR and NB-NH ₂ cage reaction | 129 |
| 5.4 | HPLC monitoring of CPR and DMNB-NH ₂ cage reaction | 130 |

LIST OF ABBREVIATIONS

| | |
|----------------------|---|
| 2'-F | deoxy-2'-fluoro |
| 2'-MOE | 2'-O-Methoxyethyl |
| 2-NB | 2-Nitrobenzyl |
| <i>Aci</i> -nitro | Z-nitronic acid |
| AGO | arginate |
| AMD | age-related macular degeneration |
| ATP | adenosine 5'-triphosphate |
| BHK-21 | Baby Hamster Kidney |
| BLAST | Basic Local Alignment Search Tool |
| cDNA | complementary DNA |
| CNB | α -carboxy-2-nitrobenzyl |
| Dcr-1 | Dicer-1 |
| Dcr-2 | Dicer-2 |
| DMEM-RS | Dulbecco's Modified Eagle's Medium - Reduced Serum |
| DMF | Dimethylformamide |
| DMNB | 4,5-dimethoxy-2-nitrobenzyl |
| DMNB-NH ₂ | 4,5-dimethoxy-2-nitrobenzylamine |
| DMNPE | 1-(4,5-dimethoxy-2-nitrophenyl)diazoethane |
| DMSO | dimethyl sulfoxide |
| DNA | deoxyribonucleic acid |
| dsRNA | double-stranded RNA |
| ESI-MS | electrospray ionization mass spectroscopy |
| FASC-Scan | fluorescence activated cell sorter |
| FNA | 2'-deoxy-2'-fluoro substituted nucleic acid |
| FSC | forward angle light scatter |
| GAPDH | Glyceraldehyde 3-phosphate dehydrogenase |
| GFP | green fluorescent protein |
| hAGO2 | Human AGO protein 2 |
| HPLC | high performance liquid chromatography |
| LD50 | 50% lethal dose |
| LNA | locked nucleic acids |
| MALDI-MS | matrix-assisted laser desorption/ionization mass spectroscopy |
| miRNA | microRNA |
| mRNA | messenger RNA |
| MS | mass spectroscopy |
| NA | nucleic acid |
| NB | 2-nitrobenzyl |
| NB-NH ₂ | 2-nitrobenzylamine |
| NPE | 1-(2-nitrophenyl)ethyl |
| nt | Nucleotide |
| NTP | Nucleoside triphosphate |
| PAGE | Polyacrylamide gel electrophoresis |
| p-Body | processing body |
| PBS | phosphate buffered saline |

| | |
|--------------|--|
| PCR | polymerase chain reaction |
| <i>p</i> HP | <i>p</i> -hydroxyphenacyl group |
| <i>p</i> HPA | <i>p</i> -hydroxyphenylacetic acid |
| PS | phosphorothioate |
| PTGS | post transcriptional gene silencing |
| Rf | resolution factor |
| RISC | RNA-induced silencing complex |
| RLC | RISC loading complex |
| RLU | Relative luminescence units |
| RNA | ribonucleic acid |
| RNAi | RNA interference |
| rNTP | ribonucleotide tri-phosphate |
| RP-HPLC | Reverse phase high performance liquid chromatography |
| RSV | respiratory syncytial virus |
| RT-PCR | reverse transcription polymerase chain reaction |
| shRNA | short hairpin RNA |
| siFNA | small interfering FNA |
| siRNA | small interfering RNA |
| SSC | side angle light scatter |
| TAPS | N-Tris(hydroxymethyl)methyl-3-aminopropane sulfonic acid |
| TE | Tris-EDTA |
| TEAA | triethylammonium acetate |
| TPE | two-photon excitation |
| TRBP | TAR RNA binding protein |
| VEGF | vascular endothelial growth factor |

ABSTRACT

RNA interference (RNAi) is a phenomenon in which RNA molecules elicit potent and sequence-specific post-transcriptional gene silencing. Nucleic acid chemical modifications have been incorporated to improve their pharmacological properties. Despite numerous developments in chemical modifications for increased stability, safety, and efficiency of these therapeutic agents, they still face challenges of spatial and temporal targeting. One potential targeting strategy uses photocaging techniques, which involves the covalent attachment of photolabile compounds to the effector NA species that blocks bioactivity until exposed to near UV-light. This work demonstrates that fully-2'-fluorinated nucleic acids (FNAs) can elicit RNAi and that these effectors are resistant to sugar-specific enzymatic digestion. 1-(4,5-dimethoxy-2-nitrophenyl)diazoethane (DMNPE) was used to cage NA oligonucleotides, including FNAs for controlling RNAi. Photo-control over RNAi was demonstrated in cell culture and developing zebrafish embryos. Caging also afforded additional protection against nuclease digestion. High doses of siFNAs were toxic to fish embryos, as characterized by a developmental delay and increased mortality rate. Caging siFNAs rendered the effectors inert and eliminated the observed toxicity in the developing embryos. Building on the success of caging chemically-modified siFNAs through random phosphate alkylation, a strategy for the site-specific incorporation of an amine-based cage post-synthetically was developed. To demonstrate the feasibility of directed post-synthetic base caging, a base-caged ATP was generated and tested for photo-activation capacity. A novel cage group, 4,5-dimethoxy-2-nitrobenzylamine, was synthesized and used for the conversion of chloropurine riboside triphosphate and the corresponding

free nucleoside. Base-caged ATPs were inactive until photoexposure to 365nm light. Additionally, these compounds did not demonstrate competitive inhibition of protein-ATP interactions, as previously described for γ -phosphate caged ATP. For the site-specific incorporation of caged nucleobase derivatives, a strategy relying on amine-reactive convertible nucleotides was developed for positional substitution using 2-nitrobenzyl amine cage compounds. These convertible nucleotides can be incorporated during custom solid-phase synthesis, and may provide a reactive target for the presented amine-based cage compounds. Caging RNAi effectors will allow for spatial and temporal targeting of a controlled dose release of gene silencing agents, which has potential applications for wet-bench assays, probing developing biological systems, and potentially targeted therapeutics.

CHAPTER 1

Introduction

1.1 Purpose and Significance

The primary aim of this work was to develop a method to induce RNAi activity with an external trigger. To achieve this goal, photo-caging technology was applied to RNAi effectors to control gene silencing activity using light. Photo-caging refers to the attachment of photosensitive compounds to a biomolecule to transiently alter its activity until the caged biomolecule is exposed to light of an appropriate wavelength and intensity to remove the adducts (further defined in section 1.3.1). It was originally hypothesized that caging various forms of dsRNA would be adequate to control their activity. However, phosphate backbone photo-caging was found to be chemically incompatible with stable RNA polymers (see section 2.3). Therefore, it was necessary to develop 100% chemically modified RNA mimics that successfully elicit RNAi and are compatible with the caging strategy for controlling activity. This body of work demonstrates that these chemically modified siRNAs function as potent RNAi effectors, and the attachment of multiple cage compounds on each strand results in transiently inert small interfering duplexes. Exposure to light of the appropriate wavelength and sufficient energy restores the biological response to these compounds *in vitro*, in cell culture, and *in vivo*. These results demonstrate the potential utility of caged RNAi effectors by incorporating several simultaneous modes of control for gene silencing. Using the caging strategy, the inert RNAi effector can be delivered globally to a biological system of interest without eliciting a response. In this scenario, a photo-trigger can be used to induce gene silencing in a desired region of three-dimensional space and/or at a specific time interval, post delivery. In addition to this spatial-

temporal control, the extent of activity can be controlled using assorted doses of light energy. This level of control has potential future applications in the areas of developmental knockdown investigations, tissue specific gene silencing, and single cell gene silencing for experimental and therapeutic modeling purposes.

A secondary aim of this work was to explore chemical means of incorporating a caging group into an RNAi effector in a site-specific manner. The method described above uses a reactive intermediate for covalent attachment to the nucleic acid in a batch-style reaction, resulting in caging at random sites on the effector. Towards the aim of site-specific incorporation, a caging group with modified attachment chemistry was generated and tested for its ability to bind an adenosine residue on the nucleobase. Nucleoside model studies indicate that this attachment scheme is possible through a nucleophilic substitution of chlorine on 6-chloropurine riboside (see chapter 5). This scheme was expanded to generate base-caged ATP, which unlike γ -phosphate caged ATP, does not act as a competitive inhibitor for proteins that associate with ATP. Future studies will attempt to use this caging strategy for incorporating an amine-attached caging compound on an internal nucleobase through substitution utilizing a convertible nucleoside. Caging at a site-directed location may allow for complete inhibition of activity using a single cage compound and a more efficient photo-activation of the RNAi effectors, resulting in a binary on-off behavior profile. Caging offers the ability to modulate RNAi activity in terms of spatial and temporal resolution and as a means for light-dependant dosing of RNAi intensity, which has applications in developmental investigations of biological systems and therapeutic targeting

1.2 RNA Interference

RNA interference (RNAi) refers to a highly specific, potent, and naturally occurring post-transcriptional silencing of protein expression initiated by RNA. The first evidence of this mechanism emerged from studies attempting to genetically enhance the violet pigmentation in petunias (Napoli, Lemieux et al. 1990; van der Krol, Mur et al. 1990). The overexpression of the pigment gene unexpectedly resulted in a null phenotype. A related observation was seen in fungal systems where an over-expressed transgene retarded gene expression at the post-transcriptional level (Romano and Macino 1992). However, it took nearly a decade to discover that dsRNA is the foundation of this post-transcriptional gene silencing (PTGS) mechanism (Fire, Xu et al. 1998). The breakthrough experiment showed that the introduction of dsRNA was far more efficient in silencing a complementary target gene than either sense or antisense strands individually. This dsRNA-induced PTGS mechanism was coined RNAi. RNAi and its discovery have received a series of highly-acclaimed recognitions including Science magazine's 2002 *Breakthrough of the Year*, Fortune Magazine's 2003 *Biotech's Billion Dollar Breakthrough*, and has earned Andrew Fire and Craig Mello the 2006 Nobel Prize in Physiology or Medicine. This praise is well-deserved as the field of RNAi matures and the significance of this discovery is being realized. However, the use of RNAi for therapeutics still faces several hurdles that are discussed in the following sections. A detailed review of the RNAi mechanism along with advancements in RNA chemical modifications and current therapeutic development is given in the following sections to adequately identify these obstacles,

describe current technologies to improve the pharmacological effectiveness of RNAi, and to identify candidate positions for optimal photo-caging of RNAi effectors.

1.2.1 Known Mechanism of RNA Interference

The RNAi pathway has been extensively studied in various eukaryotic organisms. It is an active process which requires ATP at several stages to induce gene silencing. Although there are numerous differences in these pathways across various plants and animals, the basic mechanism seems to be well conserved. For this universal model, small double stranded RNAs (dsRNAs) act as the crucial substrate for the initiation of RNAi. The sources of these dsRNAs can vary widely, which is discussed in the following paragraph. Once introduced to the cytoplasm, these small RNAs associate with several proteins to form the RNA-Induced Silencing Complex (RISC) (Hammond, Bernstein et al. 2000). The nucleoprotein complex is then activated by one or several ATP-dependant processes that are not yet well understood. It is theorized that this activation process includes the unwinding of the siRNA for target recognition. However, to date a conserved ATP-dependant helicase has not been identified. Once activated, RISC recognizes the mRNA target and either clips it at a specific location, physically blocks its translation, or sequesters it to a processing body (p-Body) organelle. Although the general process can be described in a relatively straightforward manner, the full process is complex due to a high number of variations, unidentified factors, and downstream processes. For simplicity, the entire mechanism with an emphasis on the siRNA pathway will be broken down into 1) siRNA generation, 2) RISC assembly, 3) RISC maturation, 4) RISC targeting

interaction and mRNA degradation, and 5) downstream chromatin remodeling. Each of these sub-processes is described below.

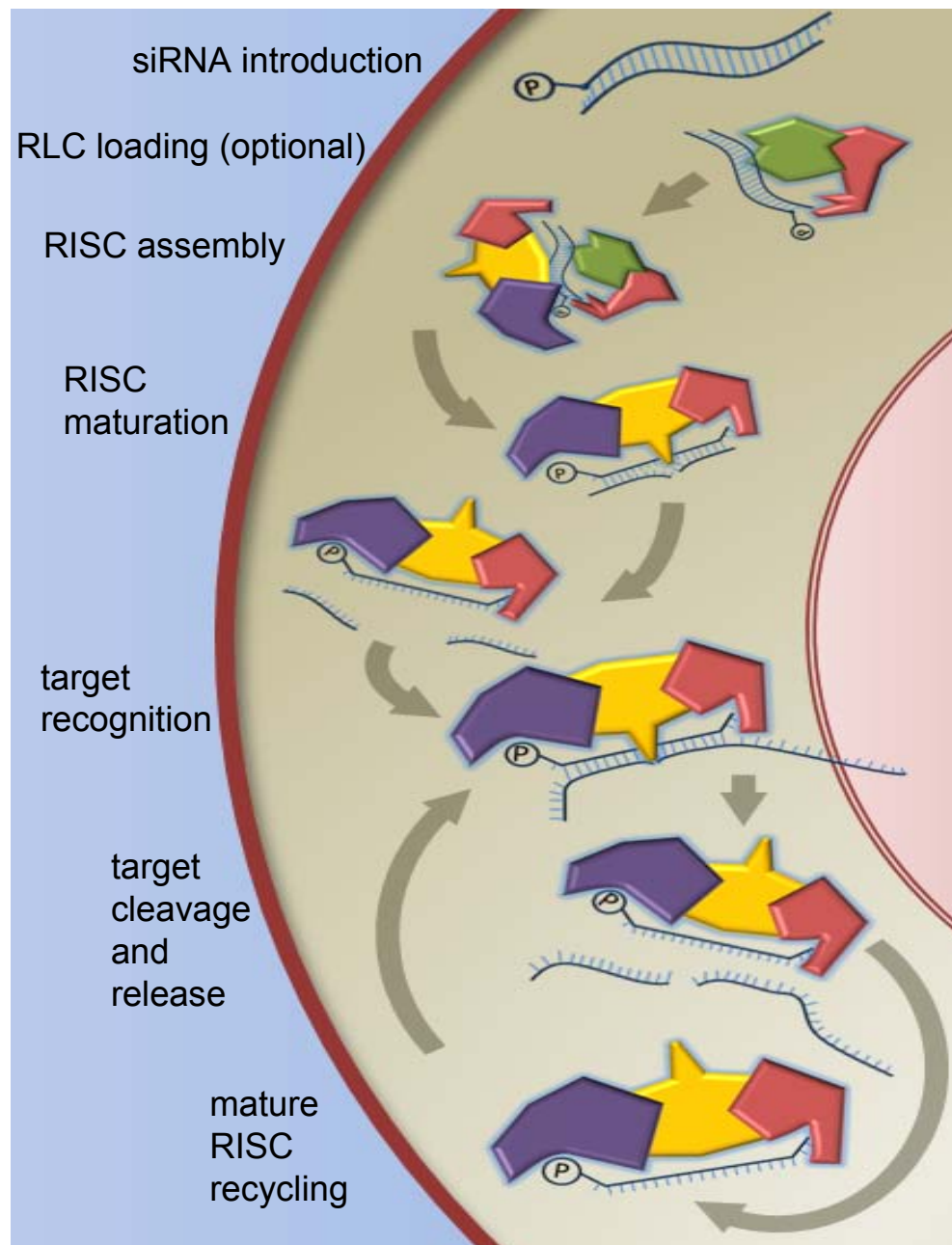


Figure 1.1: RNAi mechanism. RISC components illustrate how RNA and proteins associate with each other. Stages include siRNA generation, siRNA recognition and RISC assembly, RISC maturation, and target mRNA cleavage

1.2.1.1 Small Interfering RNA Generation

SiRNAs can be generated through several natural and synthetic methods. As was done in this work, siRNAs can be generated synthetically or enzymatically *in vitro* and then delivered to the cells or embryos in an active form. In most organisms, the introduction of long double-stranded RNA (dsRNA) prompts the enzymatic digestion of the RNA into 21-30nt length siRNAs. The highly conserved enzyme that performs this digestion was named Dicer and belongs to the RNase III family of enzymes (Hammond, Bernstein et al. 2000; Bernstein, Caudy et al. 2001; Elbashir, Lendeckel et al. 2001). This pathway is not utilized for RNAi in mammalian cells because they mount a global protein kinase response as a viral protection mechanism, which results in cellular apoptosis (Williams 1997; Gil and Esteban 2000). However, Dicer is still a critical component to the RISC pathway and is present in mammalian systems. In addition to linearized dsRNA, Dicer can process stem-loop structures to produce siRNAs. This has enabled the ability to introduce transgenic short hairpin RNAs (shRNAs) that are processed by Dicer to induce RNAi. One of the more profound discoveries that arose from RNAi studies was the existence of hundreds of endogenous stem-loop RNAs called microRNAs (miRNAs), which are theorized to play a major role in genetic regulation (Lee, Feinbaum et al. 1993; Ruvkun 2001). These miRNAs originate from non-coding regions of the genome in the form of a long primary transcript known as pri-miRNA. These are processed in the nucleus into the shorter stem-loop structures (pre-miRNA) and exported to the cytoplasm where they are processed into their mature form. Although siRNAs and miRNAs are functionally similar, small structural differences of these effectors elicit different RNAi pathways.

1.2.1.2 RISC Assembly

Once in the cytoplasm, small RNAs are assembled into RISC. This is a process in which siRNAs or miRNAs interact with a series of cellular proteins to form active complexes for target recognition and regulation. The most important factor for active RISC is the assembly of siRNAs with the argonaute (AGO) family of proteins. These are the only small binding proteins which have been found in all variations of functional RISC to date. Several studies have shown that when some AGO proteins are complexed with siRNA a functional core RISC can be formed, which drives mRNA degradation *in vitro* and *in vivo* (Martinez, Patkaniowska et al. 2002; Liu, Carmell et al. 2004; Rand, Ginalski et al. 2004). AGO proteins contain several conserved domains, that are critical for siRNA binding and RISC activity. The PAZ domain is located within a hydrophobic cleft and contains a series of aromatic and positively charged residues that enable a strong recognition of the negative charges on the siRNA 3'-end 2nt overhangs (Song, Liu et al. 2003). AGO proteins also contain a Mid domain, which is characterized by a deep basic pocket. Studies have suggested that this domain interacts with the 5'-end monophosphate of the guide RNA (Parker, Roe et al. 2004; Song, Smith et al. 2004; Ma, Yuan et al. 2005; Rivas, Tolia et al. 2005; Yuan, Pei et al. 2005). The final region of interest is the conserved PIWI domain, which is between the Mid and PAZ domains. This section contains a motif that is similar to those found in the RNase H family of endonucleases, suggesting that AGO proteins possess catalytic activity (Yang and Steitz 1995; Parker, Roe et al. 2004; Ma, Yuan et al. 2005; Parker, Roe et al. 2005; Yuan, Pei et al. 2005). However, not all AGO proteins contain a catalytically active PIWI motif. For instance, 8 AGO proteins have been discovered in

humans, which are evenly split into 2 subfamilies: PIWI and eIF2C containing AGOs (Sasaki, Shiohama et al. 2003). Among the non-PIWI containing proteins, only one, hAGO2, demonstrates catalytic ability (Liu, Carmell et al. 2004; Meister, Landthaler et al. 2004; Rivas, Tolia et al. 2005). An understanding of this family of proteins may allow for the design of siRNAs that can enter functionally different RNAi pathways. Additionally conserved requirements among all AGO variants may provide insight into potential caging sites that will disrupt all RNAi processes.

In some RISC systems, other protein factors are required for RISC assembly and RNAi activity. Not only are there variations among different organism species but there are various pathways within single organisms. One example comes from *Drosophila melanogaster*, one of the most extensively studied systems, where two dicer proteins (Dcr-1 and Dcr-2) have distinct functions (Bernstein, Caudy et al. 2001; Liu, Rand et al. 2003; Lee, Nakahara et al. 2004; Okamura, Ishizuka et al. 2004; Pham, Pellino et al. 2004). Dcr-1 is responsible for miRNA production while Dcr-2 is required only for siRNA production and therefore it is not required for normal fly development (Lee, Nakahara et al. 2004; Okamura, Ishizuka et al. 2004). In this system, siRNAs are loaded into a RISC loading complex (RLC) which is comprised of Dcr-2 and a double-stranded RNA binding protein, R2D2, before associating with AGO2 (Pham, Pellino et al. 2004; Tomari, Du et al. 2004; Tomari, Matranga et al. 2004; Tomari and Zamore 2005). One interesting phenomenon is that R2D2 and Dcr-2 bind asymmetrically to the siRNA, where R2D2 associates to the more stable end (Tomari, Matranga et al. 2004). This could be taken into account when designing siRNAs to ensure that the antisense strand is preferentially retained in RISC. The RLC

factors are gradually displaced once AGO2 has been recruited, leaving behind only the core RISC components, AGO2 and siRNA. Observations in the human system of siRNA-based RISC assembly seem to share many similarities with *Drosophila*. It has been shown that human Dicer forms a complex with TAR RNA binding protein (TRBP) (Chendrimada, Gregory et al. 2005; Haase, Jaskiewicz et al. 2005). Following this binding, siRNA is added to the assembly forming a Dicer-TRBP-siRNA complex. In this system, TRBP is required for recruiting hAGO2 to the complex for RISC formation.

1.2.1.3 RISC Maturation

The process of generating a mature RISC containing the single-stranded RNA effector is not yet well understood. It is known that the maturation process requires ATP *in vitro* (Nykanen, Haley et al. 2001). Initial models rely on an unidentified ATP-dependant helicase in the immature RISC or RLC to remove the carrier strand. This theory is supported by the fact that several DEAD-box RNA helicases, which are ATP dependant, are involved in the RNA pathway in different organisms (Dalmay, Horsefield et al. 2001; Tabara, Yigit et al. 2002; Yan, Mouillet et al. 2003; Cook, Koppetsch et al. 2004; Tomari, Du et al. 2004; Kim, Gabel et al. 2005). In this proposed mechanism it is unclear whether helicase unwinding occurs in the RLC or simultaneously with AGO protein displacement of the RLC cofactors. More recent models suggest the RLC transfers the siRNA to the AGO protein, and in a process that is analogous to mRNA enzymatic processing, the passenger strand is cleaved. Once cleaved, the two halves of the passenger strand are ejected so that RISC is free to repeat the process on another mRNA target (Matranga, Tomari et al.

2005; Miyoshi, Tsukumo et al. 2005; Leuschner, Ameres et al. 2006). The ejecting process is likely an ATP dependant process that is equivalent to releasing digested target mRNA and recycling of RISC. Additionally, if ATP is required for strand separation, there is nothing to suggest that this is a helicase independent process.

1.2.1.4 RISC Targeting and mRNA Degradation

There are two functional categories of mature RISC: those that initiate cleavage of the target and those that only participate in translational arrest. Cleavage the mRNA target by RISC is determined by three factors. First, only an AGO protein that contains an active endonuclease motif in the PIWI domain can cleave target mRNA (Liu, Carmell et al. 2004; Parker, Roe et al. 2004; Baumberger and Baulcombe 2005; Parker, Roe et al. 2005). If a non-catalytically active AGO protein is used, a non-cleaving RISC is formed. Secondly, a high degree of complementarity is needed between the incorporated strand of siRNA with the target (Chiu and Rana 2002). Lastly, the scissile phosphodiester bond of the mRNA must be directly accessible to the active endonuclease motif in the PIWI domain (Parker, Roe et al. 2004; Parker, Roe et al. 2005; Yuan, Pei et al. 2005). Only a fraction of all the AGO proteins identified contain a catalytically active motif, such as the human hAGO2 (Liu, Carmell et al. 2004; Meister, Landthaler et al. 2004; Meister and Tuschl 2004; Rivas, Tolia et al. 2005) or dAGO1 and dAGO2 in *Drosophila* (Meister and Tuschl 2004). The catalysis of AGO “slicer” activity is dependant on divalent cations such as Mg^{2+} and Ca^{2+} (Schwarz, Tomari et al. 2004; Rivas, Tolia et al. 2005). The location of cleavage is predetermined by RISC at the phosphodiester bond on the mRNA across from the

location between the nucleotides 10 and 11 from the 5'-end of the guide RNA, regardless of siRNA size (Elbashir, Lendeckel et al. 2001; Elbashir, Martinez et al. 2001; Haley, Tang et al. 2003; Rivas, Tolia et al. 2005). The hydrolysis of this phosphodiester linkage yields 3'-hydroxyl and 5'-phosphate termini on the cleavage products (Elbashir, Martinez et al. 2001; Martinez and Tuschl 2004).

Proper base-pairing is not only important for target recognition but is critical for RISC-directed cleavage. A strong association between the guide RNA strand and the target mRNA seems to correlate to more efficient target cleavage (Chiu and Rana 2003; Tang, Reinhart et al. 2003; Martinez and Tuschl 2004; Yang, Li et al. 2005). However, there does seem to be some mismatch tolerance as certain locations of partial complementarities can lead to mRNA cleavage. In nearly all cases of base mismatching, target cleavage is reduced. The exception to this rule is the first base on the 5' end. A point mismatch at this location increases the observed target cleavage *in vitro* (Rhoades, Reinhart et al. 2002; Haley, Tang et al. 2003; Lewis, Shih et al. 2003; Tang and Zamore 2004; Ma, Yuan et al. 2005), presumably by facilitating release of the processed target. Other than this location, mismatches on the 5'-half of the guide strand are less tolerated than those on the 3'-half (Haley, Tang et al. 2003; Martinez and Tuschl 2004). It has also been suggested that the A-form RNA helix is required for RISC activity (Chiu and Rana 2002; Chiu and Rana 2003). Since there are 11 base-pairs per turn in the A-form helix, a mismatch in the first 9 or 10 nucleotides of the guide strand may disrupt the helix and cause the resulting loss of activity.

The preferred association between the AGO protein with the guide RNA occurs with the 5'-end phosphate anchored in the basic pocket motif of the Mid-PIWI

domain and the 3'-end bound to the PAZ-domain (Parker, Roe et al. 2004; Ma, Yuan et al. 2005; Yuan, Pei et al. 2005). This directs the region containing the active slicer motif between the Mid-PIWI and PAZ domains, and the interaction with the guide strand likely restricts this region so that the hydrophilic side of this domain is positioned toward the solution (Ma, Yuan et al. 2005). Once bound to the target, a conformational change occurs to bring the scissile phosphodiester bond of the target into the catalytically active region (Ma, Yuan et al. 2005; Parker, Roe et al. 2005). The actual cutting of the target mRNA is not ATP dependant, but the release of the cleaved products does require ATP and likely also requires an ATPase/RNA helicase (Hunter 2000; Nykanen, Haley et al. 2001; Haley, Tang et al. 2003; Rivas, Tolia et al. 2005). In the circumstance of a non-catalytic RISC, knockdown may occur either through blockade of protein translation or by sequestering mRNA targets to cytoplasmic processing bodies (P-bodies) that are sometimes co-localized with mRNA decapping and degradation proteins (Bagga, Bracht et al. 2005; Ding, Spencer et al. 2005; Fillman and Lykke-Andersen 2005; Jabri 2005; Liu, Valencia-Sanchez et al. 2005; Pillai, Bhattacharyya et al. 2005; Rehwinkel, Behm-Ansmant et al. 2005; Sen and Blau 2005).

1.2.1.5 Downstream RNAi Processes

RNA-dependant epigenetic chromatin remodeling was first discovered in 1994 in a plant system (Wassenegger, Heimes et al. 1994). This phenomenon occurred in response to the integration of viral cDNA into the host genome. It was observed that the replicating foreign sequence triggered methylation of homologous

DNA copies. It was later shown that this process is dependant on short RNA strands that are generated from processing the replicated dsRNA, suggesting Dicer activity (Zilberman, Cao et al. 2004). This RNA-dependant DNA-methylation was found to be highly specific in that methylation is limited to the region of RNA-DNA complementarity (Wassenegger 2000; Aufsatz, Mette et al. 2002). In addition to plants, RNAi mediated chromatin remodeling was also studied in *S. Pombe*, a species of yeast. It was observed that small RNAs, which were generated from the centromeric repeat regions of chromosomes, eventually caused a silencing of these regions (Reinhart and Bartel 2002). The existence of a nucleus RISC that contains small RNAs and the AGO1 protein provided the first biochemical evidence of RNAi activity in the nucleus (Motamedi, Verdel et al. 2004; Noma, Sugiyama et al. 2004). It was subsequently found that Dicer, RNA-dependant RNA-polymerase, and a specific histone methyl transferase are also required to establish heterochromatin in *S. Pombe* centromeres (Volpe, Kidner et al. 2002; Hall, Noma et al. 2003; Volpe, Schramke et al. 2003). Unlike the plant system, chromatin methylation in yeast spreads several kilobases from the initially targeted region (Hall, Shankaranarayana et al. 2002; Schramke and Allshire 2003). Although more extensively studied in the plant and yeast systems, RNAi-related chromatin remodeling has been identified in human cells (Bayne and Allshire 2005). The phenomenon of RNA-mediated epigenetic genome modification demonstrates the utility of RNAi as an intrinsic defense mechanism to foreign genetic material from viral or transposable element sources, as well as suggesting a potential RNAi role in developmental processes.

1.2.2 Chemical Modifications to siRNAs

Although siRNAs utilizing chemical modifications have been used to determine intramolecular RNA structural requirements that are necessary to elicit RNAi and to elucidate certain protein-nucleic acid interactions, most of these studies aim to improve the pharmacological properties of siRNAs. For *in vitro*, cell culture, and some *in vivo* models, the efficacy of unmodified siRNAs is sufficient. However, the development of robust RNAi drugs faces several challenges including; chemical stability in physiological environments, improved bio-distribution, improved cellular delivery, and targeting of disease tissues. This section reviews the current literature on siRNA chemical modifications. Several excellent reviews are also available (Dorsett and Tuschl 2004; Manoharan 2004; Zhang, Du et al. 2006).

1.2.2.1 Terminal Modifications

The termini of siRNAs have different structural requirements related to how they interact with RISC components (refer to section 10.2.1 for a detailed description). The structural studies of the interactions between the PAZ and MID domains of AGO proteins with siRNAs complement studies in which terminally-modified RNAi effectors were tested for silencing ability. For example, it is known that a 5'-phosphate on the antisense, or guide strand, is required for siRNA recognition and RISC formation from both crystallography studies of AGO proteins and from incorporating modifications on siRNAs to disrupt the RNAi pathway (Nykanen, Haley et al. 2001; Martinez, Patkaniowska et al. 2002; Schwarz, Hutvagner et al. 2002; Parker, Roe et al. 2004; Song, Smith et al. 2004; Ma, Yuan et al. 2005; Rivas, Tolia et al. 2005; Yuan, Pei et al.

2005). Despite the progress made in the understanding of the RNAi pathway, different studies relating to terminal modification of siRNA often yields varying results. One of the modified termini that yields the most inconsistent reports with respect to RNAi tolerance is the 3'-antisense end. Structural studies of siRNA recognition by AGO proteins suggests that the 2-nt 3'-antisense overhang is necessary for proper RISC formation and stability (Lingel, Simon et al. 2003; Song, Liu et al. 2003; Yan, Yan et al. 2003; Ma, Ye et al. 2004). Therefore, modifications to this location should reduce RNAi activity. Indeed, both 2-hydroxyethylphosphate and 2'-O,4'-C-ethylene thymidine modifications to this location abolished all RNAi activity (Hamada, Ohtsuka et al. 2002). Other siRNA chemical modification examples, however, have demonstrated that silencing activity is retained when this terminal is modified with larger substitutions such as 3'-phosphate-aminopropyl, 3'-puromycin, 3'-biotin, or fluorescent chromophores (Chiu and Rana 2002; Schwarz, Hutvagner et al. 2002; Harborth, Elbashir et al. 2003). There is even a case in which the 3'-2nt overhang of the antisense strand was eliminated and the resulting blunt ended siRNA that exhibited RNAi activity in mammalian cell culture (Czauderna, Fechtner et al. 2003)

siRNAs tolerate terminal modifications on both ends of the sense strand (Chiu and Rana 2003; Czauderna, Fechtner et al. 2003; Harborth, Elbashir et al. 2003; Davidson, Harel et al. 2004; Lorenz, Hadwiger et al. 2004; Muratovska and Eccles 2004; Morrissey, Blanchard et al. 2005). This is expected since this strand is not retained in the active RISC effector, and as long as the siRNA forms a proper duplex structure for RISC formation, RNAi will likely be uninterrupted. These locations are the most exploited with respect to improving cellular delivery. For example, cholesterol

and lipid conjugates to the sense strand 5'-terminal nucleotide allow increased delivery to liver cells (Lorenz, Hadwiger et al. 2004; Soutschek, Akinc et al. 2004). In a similar strategy, end-conjugation to proteins that promote endocytosis has also demonstrated successful siRNA delivery and effective RNAi (Davidson, Harel et al. 2004; Muratovska and Eccles 2004). Another example employs an acid-labile linker to generate siRNA micelle complexes that are transported by triggering cell-surface receptors and subsequently released into the intracellular environment through pH-dependent breakdown (Oishi, Nagasaki et al. 2005). Although this end-conjugation strategy addresses increased delivery of siRNAs to cells, this technique has primarily been evaluated in liver cells when applied to *in vivo* models since the RNAi effectors are localized in this tissue after being introduced systemically.

Modification of the 5'-end of the antisense strand is the least tolerated by the RNAi pathway. It has been consistently demonstrated the phosphate at this location is required for RNAi. More specifically, the 5'-phosphoester bond must not be disturbed if silencing is to occur (Nykanen, Haley et al. 2001). An unmodified hydroxyl can be phosphorylated, but if this location is blocked by any conjugate attached the oxygen, RNAi will be abolished (Elbashir, Martinez et al. 2001; Martinez, Patkaniowska et al. 2002; Schwarz, Hutvagner et al. 2002). Conjugation that retains 5'-phosphate does not eliminate the necessary phosphoester and is generally tolerated. Several studies have demonstrated that silencing ability is retained after conjugation of a bulky linker to the phosphate (Schwarz, Hutvagner et al. 2002; Harborth, Elbashir et al. 2003). In fact, a photolabile linker at this location has shown to decrease but not eliminate RNAi activity (Nguyen, Chavli et al. 2006; Shah and Friedman 2007). The residual activity

was explained by an isomer that partially exposes the negative charge of the phosphate to the MID domain of the AGO protein (Shah and Friedman 2007). This allows for RISC recognition of the 5'-end, even when a large conjugate is attached to the phosphate.

1.2.2.2 Backbone Modifications

Backbone modifications have a history in providing NA stability and chemical resistance to degradation and enzymatic digestion that predates RNAi. This review is limited to the use of these chemical substitutions for synthetic siRNA knockdown. A recent review of chemical modifications to antisense and ribozyme therapies provides a more detailed record of these applications (Kurreck 2003). Since a great deal of knowledge was generated studying the effects of backbone modifications on DNA antisense therapies, only the most successful candidates have been investigated for RNAi. The most widely used phosphate modification in siRNA is the phosphorothioate (PS). The PS modification consists of a sulfur substitution in place of one of the nonbridging oxygen within the phosphate backbone.

PS substitutions were first used in siRNAs in 2000 (Parrish, Fleenor et al. 2000), shortly after the discovery of RNAi. Studies on RNAs with PS substitutions used sparingly do not report adverse effects on silencing ability (Padilla and Sousa 2002; Braasch, Jensen et al. 2003; Holen, Amarzguioui et al. 2003), but extensive modification can result in cytotoxicity (Amarzguioui, Holen et al. 2003; Holen, Amarzguioui et al. 2003). One of the more heavily cited studies also showed a decreased silencing ability of phosphorothioated compared to unmodified siRNA

independent of cytotoxicity (Chiu and Rana 2003). Alternatively one study reported that if certain locations were modified, RNAi activity would actually increase (Li, Mao et al. 2005). In addition to the aforementioned research, several incidences of the PS modification being used in conjunction with other types of chemical modifications and conjugations have been reported (reviewed by (Manoharan 2004; Zhang, Du et al. 2006)).

Another, less common, modification that has generated some recent enthusiasm is the boranophosphate substitution. These modifications consist of BH_3 substitutions of one of the non-bridging oxygen molecules of the phosphate backbone. NAs with these modifications have demonstrated nuclease stability (Hall, Wan et al. 2004; Hall, Wan et al. 2006), increased hydrophobicity (Shaw, Sergueev et al. 2000), and minimal toxicity (Hall, Burnham et al. 1993). Relative to PS modified siRNAs of the same sequence, boranophosphates used for partial modification showed the ability to increase the level of silencing activity (Hall, Wan et al. 2004). Single-stranded boranophosphate-siRNAs were also able to enter the RNAi pathway and not operate under a translational arrest pathway alone (Hall, Wan et al. 2006). This is appealing as it is demonstrated in chapter 2 that fully modified 2'-fluoro RNAs were unable to elicit single-stranded RNAi. This suggests that single-stranded RNA recognition by RISC components may involve an intermediate factor that requires the 2'-hydroxyl instead of identifying the negative charge of the phosphate. Although this modification shows promise, it should be noted that all boranophosphate RNAi studies have been conducted by the same research group and further studies are needed.

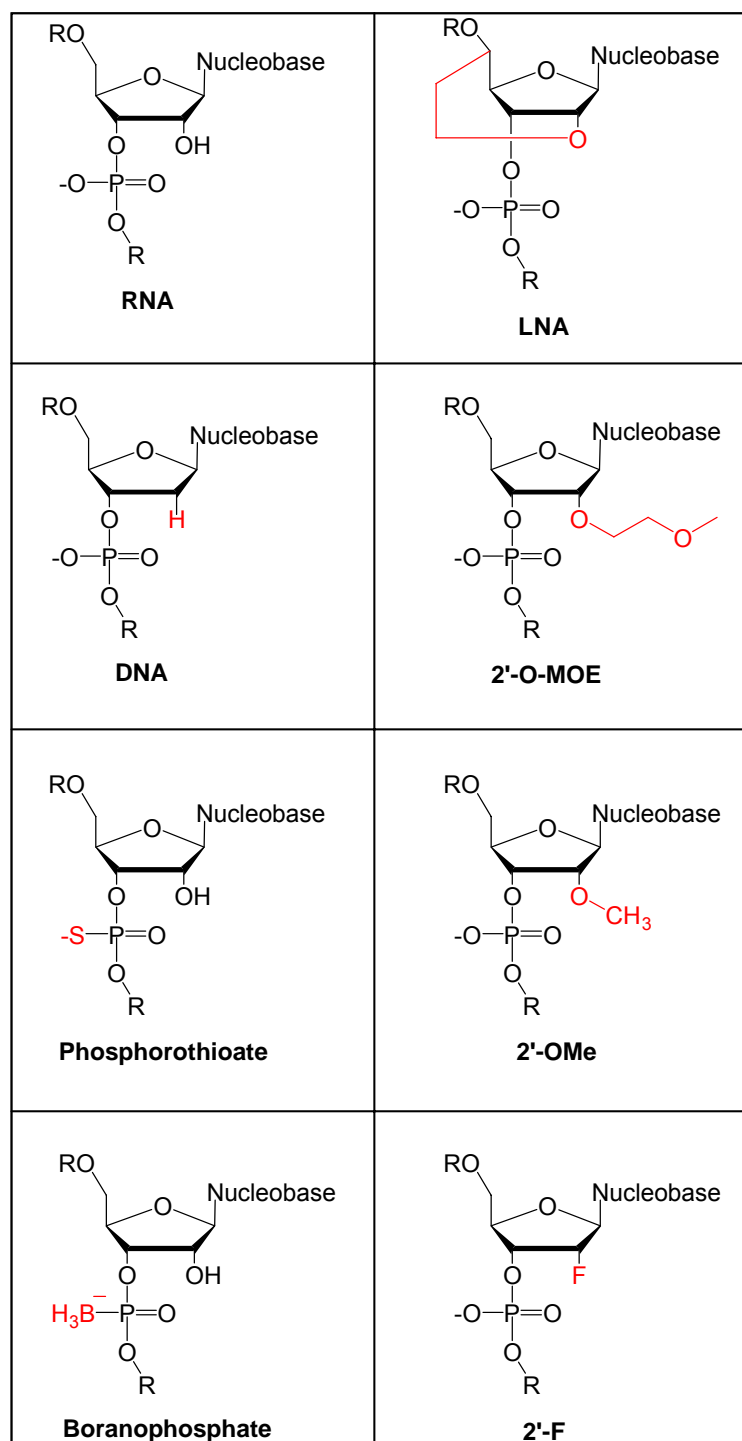


Figure 1.2: Sugar and backbone chemical modifications used for RNAi

1.2.2.3 Base Modifications

Surprisingly, nucleobase chemical modifications have not been extensively studied in siRNAs. Base modifications that have been attempted thus far include 5'-bromo uracil, 5'-iodo uracil, 2,6-diaminopurine, N3-methyl-uridine, inosine, and 5-(3-aminoallyl) (Parrish, Fleenor et al. 2000; Chiu and Rana 2003). In general, each of these substitutions reduced RNAi activity to varying degrees. To complement reports on nucleobase substitution are studies that have investigated single base mismatching. A recent comprehensive investigation was carried out by systematically inserting a single base mutation at all locations of the siRNA target site (Du, Thonberg et al. 2005). This study provides insight into which locations are most sensitive to mismatches. Additionally, it was discovered that the identity of the mismatch also influenced silencing ability. Reduction in silencing activity caused by single base mismatches varied depending on which nucleobase was inserted as the mismatch. This study differed from others which inserted point mutations into the siRNA rather than the target (Boutla, Delidakis et al. 2001; Holen, Amarzguioui et al. 2002; Amarzguioui, Holen et al. 2003). However, the results of these two substitution techniques were consistent. Together, these studies suggest that complementarity in the central region of the siRNA is the most critical for efficient RNAi activity, whereas mismatches at the terminal ends are better tolerated.

1.2.2.4 2' Modifications

Modifications to the 2'-hydroxyl of RNA have been widely utilized in siRNAs. These substitutions are generally well tolerated by the RNAi pathway because the 2'-

hydroxyl is not necessary for RISC recognition or target cleavage (Chiu and Rana 2003). Additionally these modifications increase the chemical and enzymatic stability of the NAs, relative to unmodified RNA. For these reasons, many chemical substitutions at this location have been evaluated for RNAi activity and improved resistance to nuclease degradation.

2'-O-Methoxyethyl (2'-MOE) modifications had previously shown promise for antisense applications due to their enhanced blood stability and adequate retention of activity (reviewed by (Kurreck 2003)). Therefore, they seemed likely candidates for introduction into siRNAs. However, pervasive use of this modification is not well tolerated by the RNAi pathway, suggesting that the cumbersome side chain interferes with the process. In the central region of the duplex across from the cleavage site, it appears that the size of a 2'-substitution is inversely proportional to the level of RNAi activity of the effector (Chiu and Rana 2003; Prakash, Allerson et al. 2005). The 2'-MOE modification was also not tolerated on the on either end of the antisense strand, but RNAi activity was maintained surprisingly well when this modification was used on either end of the sense strand (Prakash, Allerson et al. 2005). Another study showed favorable results by increasing end duplex stability with several 2'-MOE modifications on each side of the siRNA (Vickers, Koo et al. 2003). Despite the potential for improved stability, these studies suggest that this modification reduces RNAi efficiency and can only be used sparingly.

Initial studies using 2'-O-methyl (2'-OME) substitutions demonstrated unfavorable results with respect to maintaining RNAi efficiency (Elbashir, Martinez et al. 2001; Chiu and Rana 2003). However, the use of this modification has

subsequently been studied in great detail (reviewed by (Manoharan 2004; Zhang, Du et al. 2006)). Like other bulky modifications, 2'-OME nucleotides can only be used sparingly. Heavy utilization results in a decrease in silencing activity, presumably through disruption of the major groove of the RNA A-type helix (Chiu and Rana 2003). This study that gradually increased the number of 2'-OME substitutions determined that four nucleotide substitutions per strand are well tolerated. Additionally, limited use of this substitution appears to increase RNAi ability, presumably through increase duplex stability and/or improved resistance to enzymatic digestion (Czauderna, Fechtner et al. 2003). The benefits obtained by using a small number of the 2'-OME modification in a siRNA have made this substitution popular for use in siRNAs with combinations of various chemical modifications.

Locked nucleic acids (LNA) are a family of ribose modified compounds in which the 2'-oxygen is bridged to the 4'-carbon, locking the ribose in the C3'-endo conformation. LNAs have been studied in detail to determine their nuclease resistance, duplex stability, and RNAi functionality (Braasch, Jensen et al. 2003; Jepsen and Wengel 2004; Elmen, Thonberg et al. 2005). End-modification using LNAs is tolerated well on all but the 5'-end of the antisense strand. In another example of a comprehensive evaluation, a single LNA substitution was evaluated at each location of the antisense strand of an otherwise active siRNA (Elmen, Thonberg et al. 2005). This study identified four locations that resulted in a significant loss of silencing activity, which comprised of the 5'-end, nucleotide 10, nucleotide 12, and nucleotide 14. However, these positional effects were only tested on a single siRNA sequence. As with other bulky modifications, extensive use of these modifications results in a loss

of RNAi activity. It was proposed that this decrease might be a result of increased thermal stability and a reduction in helicase unwinding ability (Elmen, Thonberg et al. 2005). However, 2'-fluoro substitutions result in a similar thermal stability without diminishing silencing capacity (see chapter 2). Even with the limitations of LNAs, careful placement of this modification can improve the properties of the resulting siRNAs for use in *in vivo* systems.

Of all the chemical modifications tested, deoxy-2'-fluoro (2'-F) modifications seem to be the best-tolerated alteration with respect to retaining the silencing activity of unmodified siRNAs. These substitutions have several characteristics that make them ideal for RNAi applications. Fluorine is small enough to fit within the minor groove without inhibiting duplex recognition by certain proteins, and the electronegativity of the halide reinforces the A-type helix through the preferred C3'-endo ribose pucker conformation (Guschlbauer and Jankowski 1980; Chiu and Rana 2003). In addition to not disrupting the global structure of a RNA duplex, 2'-F substitutions increase thermal stability of the modified NAs when annealed to DNA or RNA (Kawasaki, Casper et al. 1993; Yazbeck, Min et al. 2002). 2'-F modified oligonucleotides and siRNAs have also demonstrated improved resistance to enzymatic degradation relative to their unmodified counterparts (reviewed by (Manoharan 2004; Zhang, Du et al. 2006)). Several studies have shown similar levels of RNAi elicited between unmodified siRNA and these synthetic counterparts that contain fluorine on every pyrimidine (Braasch, Jensen et al. 2003; Chiu and Rana 2003; Harborth, Elbashir et al. 2003; Layzer, McCaffrey et al. 2004; Manoharan 2004; Soutschek, Akinc et al. 2004). Sullenger and colleagues showed that 2'-F pyrimidine-

modified siRNAs and unmodified siRNAs have similar activity over a range of concentrations and silencing durations (Layzer, McCaffrey et al. 2004). Chiu and Rana compared silencing potency of various siRNA modifications and found that siRNA completely modified with 2'-F pyrimidines and 2'-H purines showed only a 50% decrease in knockdown ability relative to an unaltered siRNA counterpart (Chiu and Rana 2003). In addition to improving resistance to enzymatic degradation while maintaining silencing efficiency, 2'-modifications have been shown to reduce off-target effects normally observed following siRNA delivery (Jackson, Burchard et al. 2006; Cekaite, Furset et al. 2007). Until recently, 2'-F modified purine phosphoramidite building-blocks for solid phase synthesis were unavailable. Therefore, the aforementioned studies investigated pyrimidine only 2'-F NAs. Chapter 2 demonstrates the first use of fully-modified 2'-F siRNAs generated through synthetic and enzymatic methods. Alternatively, 2'-deoxy-2'fluoro- β -D-arabinonucleic acid modifications, in which the 2'-fluoro is inverted, have been used to partially modify siRNA and successfully induce RNAi (Dowler, Bergeron et al. 2006). The combination of these results suggests that the 2'-OH is not necessary for RNAi, but changes at this location that either alter the global duplex structure or disrupt the minor groove can abolish interference. Therefore, this modification is ideal for either global 2'-F substitution or for use in conjunction with other chemical modifications for the development of efficient and persistent RNAi effectors.

The combination of several types of chemical modifications into a single siRNA molecule is becoming increasingly common in efforts to improve the pharmacological efficacy of RNAi. Bhat and colleagues demonstrated that fully-modified duplexes which included 2'-F pyrimidine nucleotides and 2'-O-methyl purine

nucleotides actually increased RNAi efficiency, and in one case they achieved a 500-fold increase in silencing ability (Allerson, Sioufi et al.). The grouping of these two modifications is popular in studies that utilized more than one type of chemical substitution (Allerson, Sioufi et al. 2005; Morrissey, Blanchard et al. 2005; Morrissey, Lockridge et al. 2005; Prakash, Allerson et al. 2005; Kraynack and Baker 2006). In one of the more heavily modified examples, Morrissey and colleagues (Morrissey, Blanchard et al. 2005) created a siRNA targeting hepatitis B that contained 2'-deoxy, 2'-F, 2'-O-ME, PS, and 3'-5'-inverted deoxy-abasic substitutions. Combining these types of modifications may improve efficacy and effector half-life, but it may also provide means to achieve targeted delivery or inducible activity with the use of alternative modifications such as receptor ligands or caging compounds conjugated to the stabilized siRNAs.

1.2.3 Current RNAi Therapeutic Developments

RNAi has demonstrated potent gene silencing in laboratory studies, making it an exciting alternative approach for treating a wide variety of medical conditions. The strategy of repressing protein translation with NAs has several advantages over small molecule pharmaceuticals. Most notably is the flexibility and ease of targeting the specific gene that is causing a pathological state. There are a whole host of diseases in which the protein responsible has been identified, but no compound has been developed for effective treatment. Using RNAi and antisense techniques, several sequences could be developed for the specific disease-causing gene or allele, and candidate effectors could be generated in sufficient quantities for evaluation in a matter of days once the problem gene is identified. Despite these benefits and general

optimism surrounding this technology, few examples exist of siRNA being tested clinically in humans. In addition to the fact that RNAi is still a relatively young technology, the primary reason that RNAi drugs are rare is the inability to overcome the problems of biodistribution, siRNA stability, cellular delivery, and tissue targeting, as discussed in the prior sections. For this reason, all clinical trials to date rely on localized delivery of the siRNA-based drugs.

Three companies are currently in the process of conducting clinical trials of RNAi drugs. Acuity Pharmaceuticals (recently merged with Fropix Corp. and eXegenics, Inc.) was the first to begin a phase I clinical trial for a siRNA drug in November of 2004. This siRNA targets the gene for vascular endothelial growth factor (VEGF) to halt angiogenesis in the macula. Up-regulation of this gene is one of the major factors in causing wet age-related macular degeneration (AMD). The drug, called bevasiranib, is delivered intra-ocularly to stop the progression of the disease. This drug was also the first to reach the milestone of a double-blinded phase II study in July of 2005. Although it is not yet on the market, Acuity has reported positive results relating to halting the disease progression and maintaining safety. SiRNA Therapeutics (recently acquired by Merck & Co.) has also completed phase I trials using a siRNA drug, Sirna-027, targeting wet AMD. In addition, they are moving rapidly toward clinical trials of a hepatitis C targeting siRNA, Sirna-034. Lastly, Alnylam Pharmaceuticals have developed a siRNA drug, ALN-RSV01, which targets nucleocapsid protein to prevent viral replication against respiratory syncytial virus (RSV). Phase I clinical trials for this compound began in December of 2005, and a human experimental infection model was initiated in November of 2006. However, to achieve RNAi by systemic delivery, some of the technologies discussed in the prior

section will need to be applied. Indeed, many of these techniques have been adopted outside of academia. A strong commercial contingent is actively pursuing techniques that will improve the pharmacological potential of siRNAs.

The development of delivery systems is of paramount importance to the successful generation of RNAi therapeutics. Several companies have adopted a lipid-mediated approach to this problem. Silence Therapeutics (formerly SR Pharma) has developed siRNA-lipoplexes that function very similar to cationic liposomes that are used to transfect cell culture. In addition to complexing the NAs with a lipid delivery system, this company has developed a siRNA structure that is blunt-ended and contains alternating 2'-modifications to impart enzymatic stability. A similar lipid approach has been adopted by SiRNA Therapeutics in which lipid nanoparticles are used to physically encase the effector for delivery. For both of these cases, the siRNA complexes are endocytosed and then released intracellularly. A more tissue-specific version of this strategy was developed by Calando Pharmaceuticals. In their strategy, siRNAs are end-conjugated to a polymer, which are complexed into nanoparticle structures. These polymers have the ability to target specific cell surface receptors and induce endocytosis. Nantech Pharmaceutical Company Inc., has taken this cellular targeting strategy one step further to promote siRNA delivery specifically at tight junctions of epithelial and endothelial cells. High-throughput screening is used to identify compounds that interact with these tight junctions and then candidate compounds are used as carriers for delivery of siRNAs. Nantech also uses siRNA sequences that are screened for natural enzyme resistance and replaces ribouracil with ribothymine to reduce off-target silencing through improved hybridization properties. Due to the known enzyme susceptibility of siRNAs and the complications

associated with global and specific cellular delivery, it is reasonable to assume that systemic application of RNAi drugs will require the combination of several technological advancements.

If the hurdles associated RNAi drugs are overcome, the therapeutic applications are nearly limitless. Three of the most important areas of RNAi potential applications include antivirals, treatments for neurodegenerative disorders, and cancer therapies. For example, the development of vaccines is severely limited when the virus of interest proves to be highly mutagenic. RNAi offers the alternative of targeting highly conserved regions of the genome, as opposed to targeting viral surface antigens. Examples of viruses that may one day be treatable with RNAi drugs include influenza, hepatitis C, and HIV. As aforementioned, Alnylam has already completed phase I clinical trials with a siRNA against RSV, a viral target. Alnylam is also working with Medtronic toward a technology that would allow for local delivery of siRNAs to treat neurodegenerative diseases via an implantable infusion pump. As a final example, Calando is expected to file a new drug application for a cancer targeting siRNA, CALAA-01. Despite the guarded optimism for RNAi drugs, they are fundamentally untested in therapeutic applications. In order to truly estimate the impact of RNAi, more validation in human trials are necessary.

1.3: Caging

1.3.1: Definition and Historical Perspective

Traditional chemical modulators of biological processes are unable to achieve the necessary spatiotemporal control required for some experimental investigations and targeting for therapeutics. One strategy to achieve this control is to

develop compounds whose activity is dependant on a conditional trigger. Light exemplifies an ideal external trigger for inducing mechanisms with extraordinary spatial and temporal resolution. Light-induced activation of biological molecules is typically accomplished by first rendering the molecule of interest inert through conjugation of a photoprotecting group, or “caging”, which can later be removed by exposure to an appropriate light source. Caging is very specific term, which describes the use of a photolytic chromophore for the rapid release of a biologically active substrate (Kaplan, Forbush et al. 1978). The covalent attachment of a photosensitive compound produces a photo-caged compound when the attachment of this group blocks native biochemical or biological activity and the blocked activity can be restored by light treatment. Therefore, the term “caged,” in this context, is descriptive of the photo-activation property and does not refer to physical trapping of the inactivated substance within a crystal lattice or shell. For the purposes of this work, the term caging is more narrowly defined. Caging refers to the covalent attachment of one or multiple chromophores to a biomolecule, and the attachment of the caging compound(s) must alter the normal biological activity of the substrate. In nearly all cases, it is desired that the caged molecule is functionally inert. Attachment of the cage and inactivation of the biomolecule must be transient and reversible in the presence of the appropriate incident light. This restriction eliminates stable photo-responsive elements, such as biological photoswitches (Reviewed by (Mayer and Heckel 2006)). Finally, the photo-responsive biomolecule must not be naturally occurring. Although the definition of caging requires that the photochemistry be used to release a biochemically active substrate, the initial findings by Kaplan and colleges was inspired by earlier reports in

which photolabile residues were used as protecting groups in synthetic chemistry for carboxylic acids, alcohols, amines, ketones, or phosphates (reviewed by (Pillai 1980)).

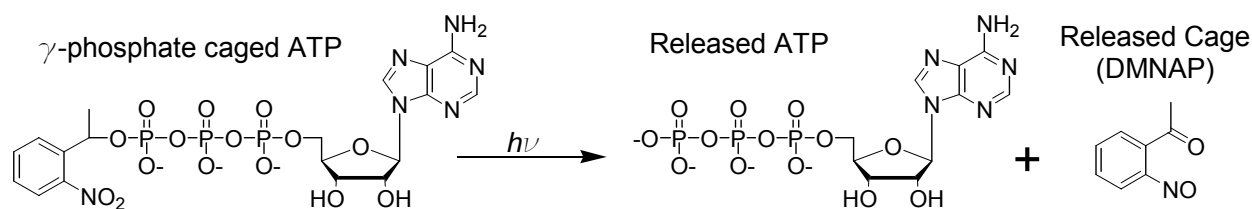


Figure 1.3: 2-Nitrobenzyl γ -phosphate caged ATP and photolytic release

Classically, caged compounds have been used to study the time course of cellular responses induced by a millisecond step increase in the intracellular concentration of a bioactive compound of interest. As aforementioned, Kaplan et al. (Kaplan, Forbush et al. 1978) was the first to apply this type of photochemistry to release an inducer to a biological system, the Na:K ion pump from erythrocytes (e.g. ATP, Fig. 1.3). Time course experiments using caged compounds have been used to study a wide range of biological processes *in vitro* and *in vivo*, including studies of cell motility, muscle fibers, active transport proteins, biological membranes and other intracellular responses (reviewed by (McCray and Trentham 1989; Pelliccioli and Wirz 2002; Mayer and Heckel 2006; Ellis-Davies 2007)). Applications of cage groups have expanded beyond their beginnings in organic synthesis and step increases in concentration of biological inducers to play an important role in the inactivation of macro-biomolecules. While the early biochemical studies were limited to evaluating the time course of brief biological responses *in vitro* and *in situ*, caged macromolecules afford control to a broad range of wet-bench and potentially therapeutic applications. Examples of caged macromolecules include proteins, neurotransmitters, fluorophores,

lipids, and nucleic acids (Mayer and Heckel 2006; Ellis-Davies 2007). Photoprotected species can be dispersed throughout the biological target without eliciting the normal bioactivity, which is a major advantage over conventional methods for substrate release. Additional benefits of this strategy include control over the local concentration and spatial distribution, and the temporal release of the effector can be varied from seconds to nanoseconds (Givens, Weber et al. 1998).

In order to be effective in biological systems, cage compounds must exhibit various characteristics to achieve the desired response while avoiding unwanted-effects (reviewed by (Mayer and Heckel 2006; Ellis-Davies 2007; Tang and Dmochowski 2007)). The chromatic properties of the caged species must allow for efficient and non-toxic substrate release. Therefore the cage should have both a high extinction coefficient at non-damaging wavelengths, corresponding to strong light absorption characteristics, as well as a high quantum yield, which dictates energy conversion efficiency. For applications in which a rapid biological response is being measured, the rate at which the product is released through dark-reaction intermediates may also be a significant factor. The caged molecule should be water soluble and resistant to hydrolysis in order to be properly utilized under aqueous conditions in physiological pH ranges. Additionally, the caged molecule and the released byproduct(s) should be physiologically inert to avoid potentially toxic side-responses. Lastly, in order to progress beyond proof-of-concept studies, the mode of covalent attachment between the cage and biomolecule should be relatively simple, reproducible, and cost efficient. Although many caging systems adequately adhere to these characteristics, no single cage exhibits the ideal properties for all categories.

Many types of caging groups have been developed in efforts to improve the aforementioned properties. However, most of these are simple conjugations to already known photoprotecting groups. For instance, nitrobenzyl derivatives are often adorned with electron donating functional moieties to achieve a hyperchromatic absorbance shift into the near UV-light range (Aujard, Benbrahim et al. 2006). Nitrobenzyl derivatives are the most extensively studied of all the caging groups and were selected for this study. A review of caging groups for nucleic acids is presented in the following section.

1.3.2 Common Cage Groups

The number of incidences in which photoprotection groups have been used to cage biomolecules has been rapidly expanding since ATP was first caged by Kaplan in 1978. For the purposes of this study, emphasis is placed a general review of various categories of cage compounds while providing periodic examples of applications. Although the experimental section of this work only utilizes one of these caging groups, an understanding of available alternatives is paramount to future works that may improve upon this body of work.

1.3.2.1 2-Nitrobenzyl Caging Group

The 2-nitrobenzyl (2-NB) caging group and its derivatives are the most widely utilized cage molecules to date, and therefore are the best characterized (Goeldner and Givens 2006). The pervasiveness in the literature is not necessarily an indicator that this caging group has ideal photochemical properties or is the easiest to

use via synthetic or biochemical methods, but rather its' widespread use first type of cage compound applied to biological systems. Kaplan's pioneering work using caged ATP for controlling the NA:K pump utilized 2-NB cages from this category (Kaplan, Forbush et al. 1978). They were also the first used to study millisecond time-scale induction of the actin-myosin response to photolysed caged ATP (McCray, Herbette et al. 1980; Goldman, Hibberd et al. 1982). The basic structure that defines the group is a benzyl structure with an ortho-located nitro substitution. Variants of this structure commonly include substitutions directly on the carbon ring and/or alternative attachment chemistry on the methyl group (fig. 1.4a).

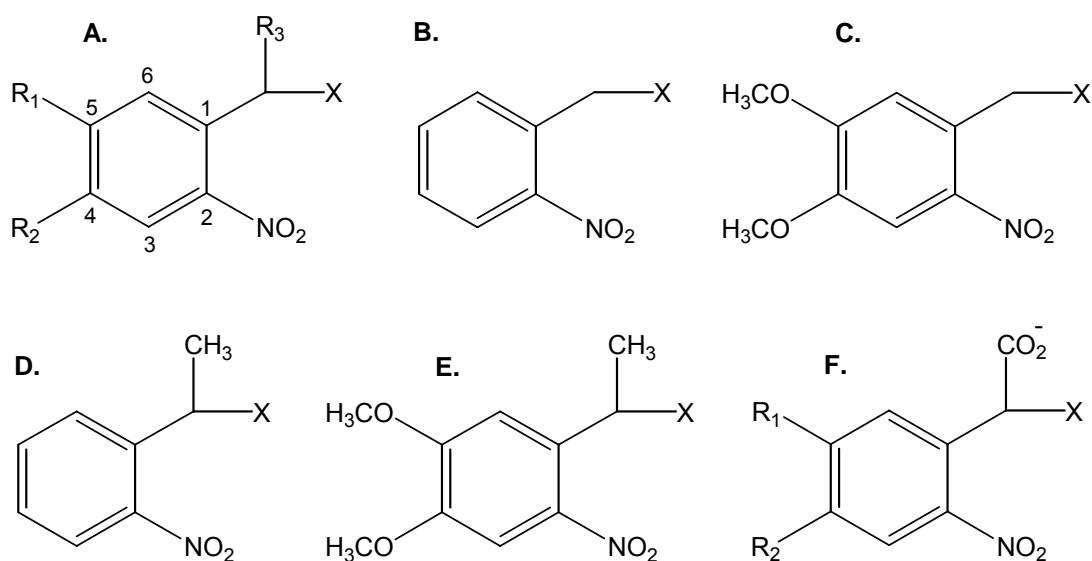


Figure 1.4: 2-nitrobenzyl derivatives

Cage compounds in the 2-NB family of can be further subdivided based on different substitutions at positions 4 and 5 as well as the exocyclic linker, as illustrated in figure 1.4a. Common subdivisions include 2-nitrobenzyl (NB) (fig. 1.4b), 4,5-dimethoxy-2-nitrobenzyl (DMNB) (fig. 1.4c), 1-(2-nitrophenyl)ethyl (NPE) (fig. 1.4d), 1-

(4,5-dimethoxy-2-nitrophenyl)ethyl (DMNPE) (fig. 1.4e), and α -carboxy-2-nitrobenzyl (CNB) (fig. 1.4f). The driving motivation for developing derivatized forms of the cage compound is to improve either the rate or efficiency of photolysis. Generally, electron donating ring substitutions result a hyperchromatic absorbance shift, allowing photolysis at longer wavelengths that are less damaging to biological systems. However, these substitutions often significantly reduce the efficiency of photolysis (Aujard, Benbrahim et al. 2006; Goeldner and Givens 2006). Benzylic carbon α -substitutions presumably affect the C-H bond at the site of attachment in the excited state, which may affect the rate of hydrogen transfer that forms the *aci*-nitro intermediate, illustrated below (Goeldner and Givens 2006). However, the decay process of 2-NB photo-cleavage is complex, and the rate constants at each stage depend heavily on pH, make up of the media or buffer, the nature of the substrate, as well as derivations to the cage compound (Il'ichev, Schworer et al. 2004).

The currently theorized mechanism of 2-NB photolysis begins with the delivery of a photon that can be absorbed by the chromophore and induces an excited state. Both singlet and triplet excited states have been identified and either state may cause the hydrogen transfer to form the Z-nitronic acid (*aci*-nitro), which is converted to the E-isomeric form (Yip, Sharma et al. 1985; Yip, Wen et al. 1991; 2006). The resulting *aci*-nitro compound is a long-lived intermediate and with several possible isomeric forms, as aforementioned. It is the E,E isomer that spontaneously forms the cyclic benzisoxazole that will ultimately lead to substrate release. This structure is converted to hemi-acetyl intermediate, which is then further hydrolyzed to the 2-nitrosobenzylcarbonyl and the released biomolecule (Walker, Reid et al. 1988; Corrie,

Barth et al. 2003; Il'ichev, Schworer et al. 2004) (Goeldner and Givens 2006). The nitroso byproduct has historically been theorized to be potentially reactive and toxic to biological systems. However, there are only a few incidences of complications related to this byproduct reported in the literature (Kaplan, Forbush et al. 1978; Zhang, Buchet et al. 2004) and subsequent work suggests that the conclusions of these studies were not accurate (Goeldner and Givens 2006).

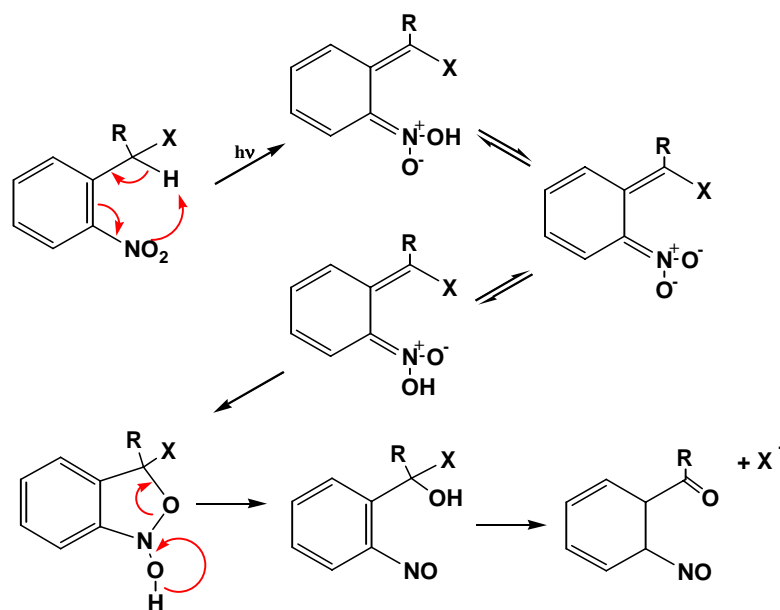


Figure 1.5: Proposed photolytic mechanism of 2-nitrobenzyl

1.3.2.2 *p*-Hydroxyphenacyl Caging Group

The *p*-hydroxyphenacyl group (pHP) is a relatively new category of caging compounds. Although it was first utilized in photo-reactions in 1962 (Anderson and Reese 1962) and identified as a potential photolabile protecting group by releasing glycine in 1973 (Sheehan and Umezawa 1973), it was only about a decade ago that this family of compounds was utilized as a caging group for biomolecules. Much like the original 2-nitrobenzyl caging of ATP by Kaplan, this group was also exploited by

Givens and Park to generate photo-released ATP (Givens and Park 1996; Park and Givens 1997). Despite their recent entry into the caging field, these compounds have been met with enthusiasm and are often included in biocaging review articles (Pelliccioli and Wirz 2002; 2006; Mayer and Heckel 2006).

As dictated in the name, the general structure of the *p*HP group consists a phenyl ring with an acyl attachment chemistry and a hydroxyl in the para-position. The acyl functional group attachment allows for several attachment schemes such as carbonyls, acyl halides, esters, and more. Other substitutions can be made at the meta-positions on the phenyl ring. Electron donating groups at these positions cause a hyperchromatic shift, but they also drastically reduce the quantum yield of the photo-reaction (Conrad, Givens et al. 2000). In contrast, electron-withdrawing ring

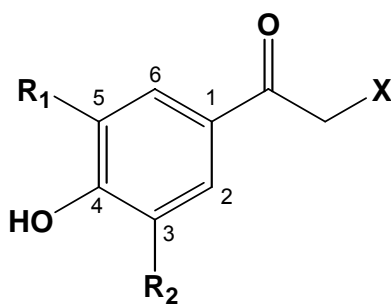


Figure 1.6: *p*-hydroxyphenacyl cage group

substitutions tend to increase the quantum yield (Goeldner and Givens 2006). Interestingly, the withdrawing substitutions have little effect on the absorption spectra. Figure 1.6 illustrates the basic structure of the *p*HP cage group.

The photo-release mechanism of the *p*HP cage is not as well understood as the 2-NB group, but a general proposed chemical pathway has been proposed. The initial photon-induced excitation creates a singlet excited state of the phenolic ring.

This is then converted to a triplet state prior to substrate release (Conrad, Givens et al. 2000). Deprotonation of the excited compounds results in an anion oxide intermediate. The proton transfer from the caged species to the solvent is supported by a strong dependence on solution pH for uncaging (Goeldner and Givens 2006). The anion form of the caged species is believed to undergo substrate release as the rate limiting step as illustrated in figure 1.7 (Goeldner and Givens 2006). However, this process is currently considered to be speculative. The resulting intermediate is believed to undergo hydrolysis and reprotonization to form *p*-hydroxyphenylacetic acid (*p*HPA). Other proposed mechanisms hypothesize direct substrate cleavage from the triplet excited state (not shown) (Goeldner and Givens 2006). These mechanisms would allow for O-methyl or alkylether groups at the para-position, since deprotonization is not required. In addition, the cage intermediate following substrate release may be in equilibrium with an anion oxide isomer. Other exceptions to the proposed mechanism include an example in which caged carboxylic esters photo-released directly from the singlet state (Zhang, Corrie et al. 1999; Zhang and Taylor 1999) and that an attempt to identify the spirodienedione intermediate through TRIR were unsuccessful (Pelliccioli and Wirz 2002).

Substrates caged by *p*HP include but are not limited to ATP (Givens and Park 1996; Park and Givens 1997), phosphates (Park and Givens 1997; Conrad, Givens et al. 2000), and various amino acid based structures (Givens, Jung et al. 1997). These studies indicate that the *p*HP cage group is capable of desirable quantum yields, rapid photo-release, acceptable solubility and stability in aqueous conditions, and non-toxic photo products. In addition to the favorable aspects of these

compounds, several drawbacks were also identified. Most notably, these compounds do not absorb well for wavelengths above 320 nm (Pelliccioli and Wirz 2002). As aforementioned, derivations on the ring structure can improve the absorption properties, but this causes in a drastic decrease in quantum yield.

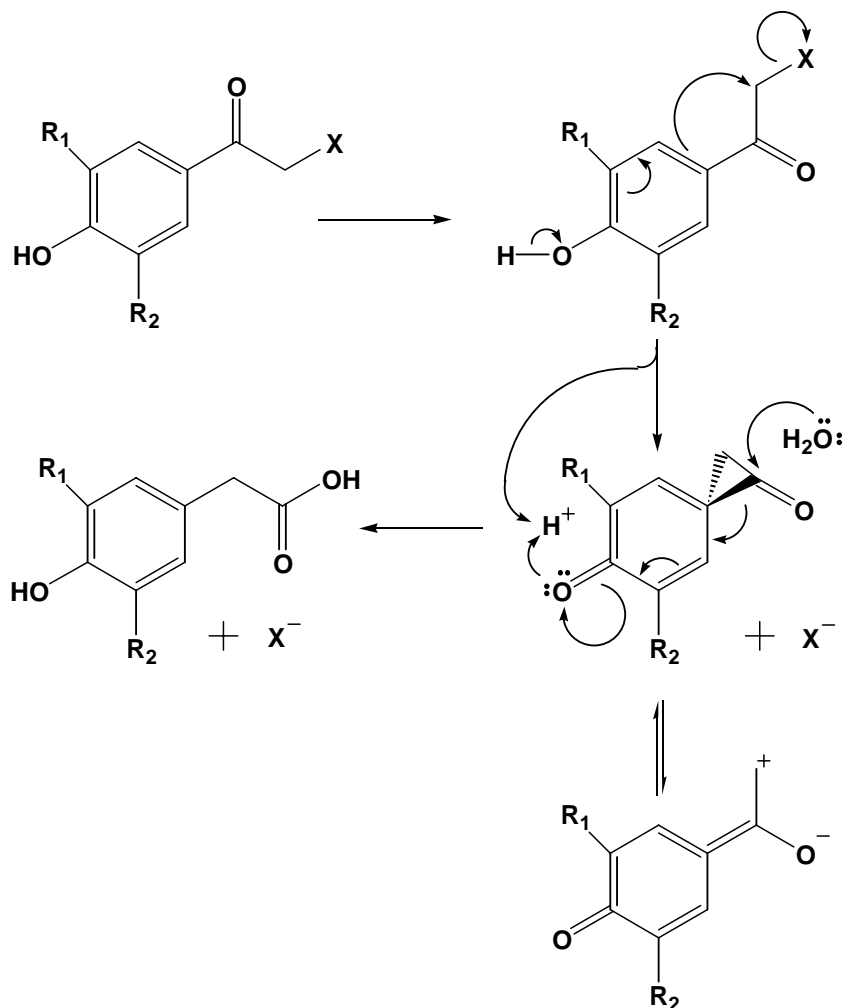


Figure 1.7: *p*-hydroxyphenacyl proposed photolytic mechanism

1.3.2.3 Coumarinyl Caging Group

The coumarinyl group was first recognized as a potential photoprotection group in 1984, when a (coumarin-4-yl)phosphate ester was found to be photosensitive

(Givens and Matuszewski 1984). It was nearly a decade later before this chemical group was evaluated as alternative cage compounds for the 2-NB group (Furuta, Torigai et al. 1993). These compounds typically possess high absorption coefficients, fast photo-release kinetics, and large two-photon excitation cross-sections (Pelliccioli and Wirz 2002; 2006). The strong absorption properties of these compounds (ϵ_{max} typically from 4,000 to 20,000 $\text{M}^{-1}\text{cm}^{-1}$) make up for relatively poor quantum yields of photo-release (Goeldner and Givens 2006). Another property of these cage compounds is a strong fluorescence signal. The emission spectra may overlap with common fluorescent probes, which limits the use of coumarin derivatives in certain biochemical assays. Despite this minor limitation, the coumarinyl group has demonstrated practical photochemical properties along with a wide diversity of derivatization possibilities.

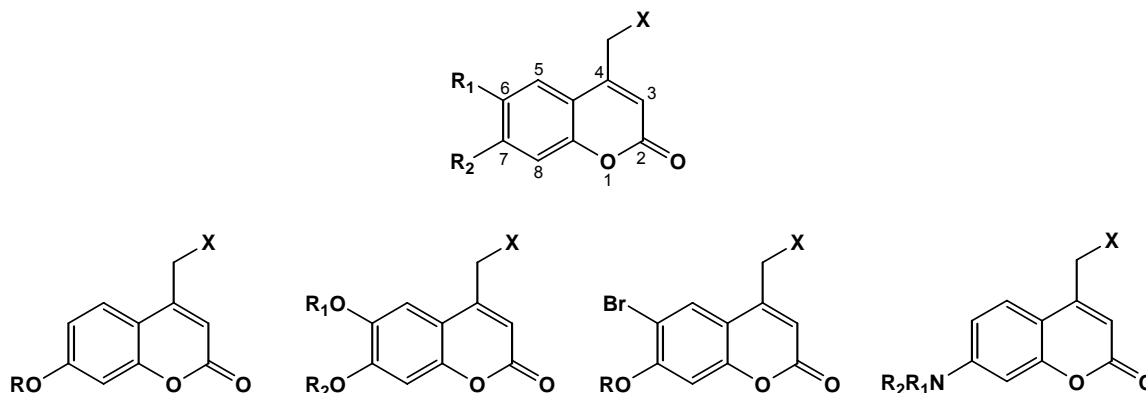


Figure 1.8: The coumarinyl cage group

The base structure of this group is a derivatized coumarin, as the name indicates. Coumarins consist of two fused six-member rings, one of which is an oxygen containing heterocyclic ring with an adjacent carbonyl group (figure 1.8). Attachment is in the meta-position in reference to the ring-bound oxygen. A methyl

functionality lies between the bound substrate and the coumarin. Ring-substitutions at C6 and C7 are commonly used to red-shift the absorption maxima. Ring derivatizations can also be used to improve membrane permeability and water solubility. In addition to these substitutions, the nature of the bound substrate can have a significant effect on the photochemical properties of cage release. The coumarinyl group can be subdivided into several groups consisting of; 7-alkoxy, 6,7-dialkoxy, 6-bromo-7-alkoxy, and 7-dialkylamino (reviewed by (Goeldner and Givens 2006)). Figure 1.8 illustrates these sub-classifications in reference to the base structure.

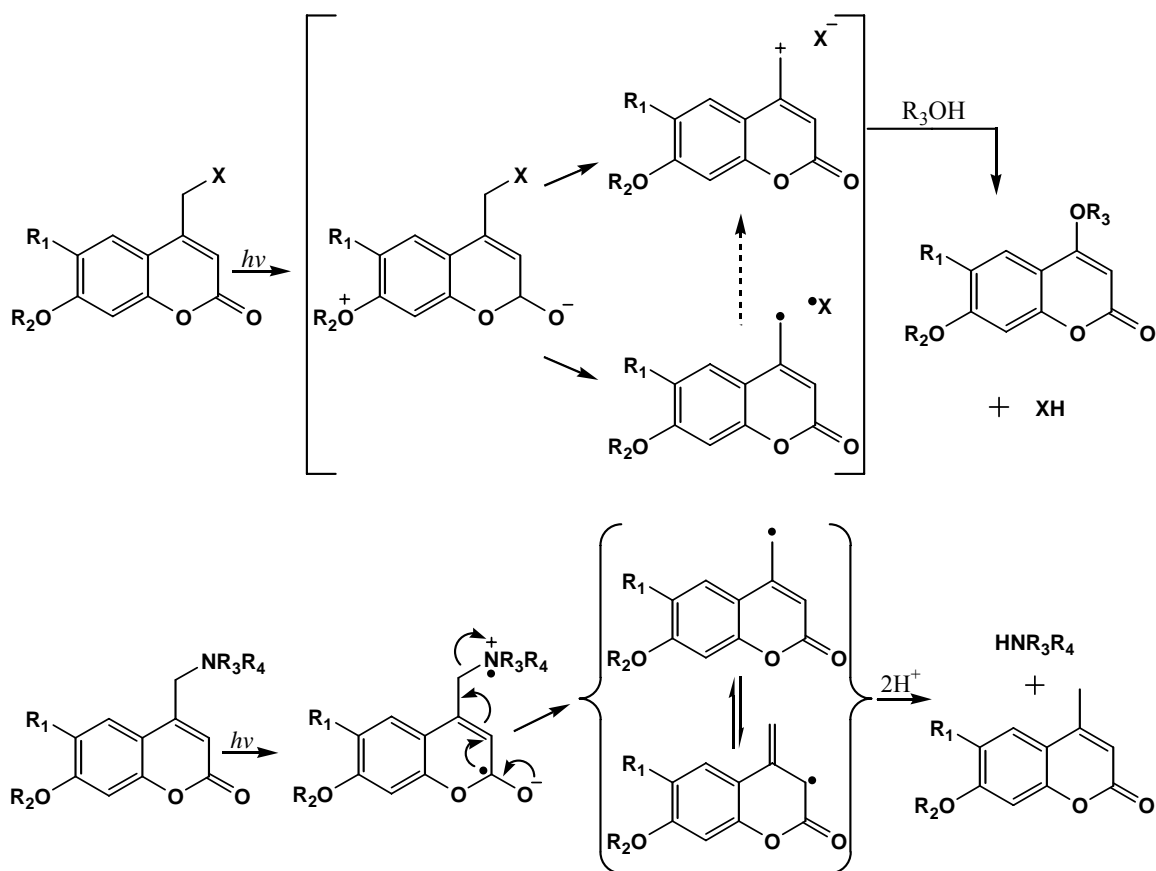


Figure 1.9: Coumarinyl proposed photolytic mechanisms

A photo-release mechanism was proposed from the studies of various coumaryl-caged phosphates (Schade, Hagen et al. 1999; Eckardt, Hagen et al. 2002; Hagen, Frings et al. 2003). In this scheme, photo-activation results in an excited singlet state, followed by heterolysis or homolysis and subsequent electron transfer at the site of substrate attachment. The unstable cationic released cage is then trapped by the solvent. Figure 1.9 demonstrates this mechanism. Alternatively, studies of coumarinyl-caged amines suggested a slightly different mode of photo-release, shown in figure 1.9b (Sarker, Kaneko et al. 1997; Sarker, Kaneko et al. 1998; Schoenleber and Giese 2003). Photo-excitation results in electron-donor dependent homolytic cleavage and the formation of a radical anion intermediate.

The coumarinyl group has successfully been used to cage phosphates, carboxylates, carbonyls, alcohols, amines, and sulfonates (reviewed by (Goeldner and Givens 2006)). Generally, the photo-kinetic properties of these compounds and the flexibility for creating various coumarin derivatives are desirable. Despite the success of this group used for *in vitro* assays, only a few examples in biological systems exist. However, these studies have also yielded positive results. In fact, one of the first examples of a coumarinyl-caged macromolecule used in a biological system was a Bhc-caged mRNA for photo-induction of gene expression (Ando, Furuta et al. 2001; Ando, Furuta et al. 2004).

1.3.2.4 Benzoin Caging Group

The benzoin group was first reported in 1971, where 3',5'-dimethoxybenzoin caged acetate was released upon photoexposure (Sheehan and Umezawa 1973).

This study reported a clean photolysis reaction yielding acetate and dimethoxybenzofuran at an exceptionally high quantum efficiency ($\Phi = 0.64$). Although various other derivatives have been tested, the two most common forms include the unsubstituted and the 3',5'-dimethoxy benzoin (reviewed by (Pelliccioli and Wirz 2002)). The general structure of these compounds is depicted in figure 1.10, along with the general photo-release scheme. A detailed figure on the photo-release mechanism is not shown do to the high degree of disagreement in several proposed mechanisms. It is likely that the nature of the substrate and the attachment chemistry have a profound effect on the mode of photo-release. Several studies demonstrate quenching of photo-release by the addition of piperylene or naphthalene, indicating that photolysis occurs through the excited triplet state (Sheehan and Umezawa 1973; Rajesh, Givens et al. 2000). These quenchers facilitate vibration relaxation of the excited state, and they function through the triplet state since it is less energetic. However, studies of different benzoin-caged substrates demonstrated a lack of susceptibility to quenching (Sheehan and Umezawa 1973; Pirrung and Shuey 1994),

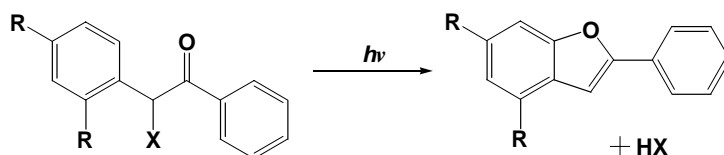


Figure 1.10: The benzoin cage group

suggesting different photolytic pathways. Proposed mechanisms of photolysis include heterolytic dissociation and cation formation through the singlet state (Rajesh, Givens et al. 2000), formation of a strained bicyclic intermediate that breaks down to release the substrate (Sheehan and Umezawa 1973), and triplet state heterolytic cleavage to

form an ion pair followed by elimination through ring closure (Cameron, Willson et al. 1996).

Benzoin cage compounds typically exhibit high quantum yields and fast release kinetics, (Sheehan, Wilson et al. 1971; Corrie and Trentham 1992; Givens, Athey et al. 1993; Pelliccioli and Wirz 2002). However, there are several drawbacks to this cage group. It has a strong absorption coefficient, but this occurs in the 300 nm range (Pelliccioli and Wirz 2002). Radiation of this wavelength is not tolerated by biological systems. Additionally, these compounds exhibit strong fluorescence, limiting their use for some fluorescence-based *in vitro* assays (Pirrung and Shuey 1994). Finally, these compounds are highly hydrophobic and reduce the solubility of the bounds substrate in physiological conditions. An attempt to develop a water soluble derivative using bis(carboxymethoxy) substitutions reduced the photolytic yield (Rock and Chan 1998).

1.3.3 Caging of Nucleic Acids

Examples of caged nucleic acids (NAs) are much less abundant and more recent when compared to other categories of caged compounds, such as small-molecule metabolites and proteins. This is surprising given that the original model for caged biomolecules was based on nucleotides such as caged-ATP (Kaplan, Forbush et al. 1978). Additionally, the potential utility of caging NAs is readily apparent since they participate in a variety of biochemical reactions that are inherently dependent on structure. Although earlier examples of caged NAs exist, the first study in which caged DNA was used in a cellular system did not occur until 1999 (Monroe, McQuain et al.

1999; Monroe, McQuain et al. 1999). In this work, plasmids encoding for GFP or luciferase were caged with DMNPE-groups in bulk based on diazo attachment to nucleotide phosphates. Using this strategy, the authors were able to demonstrate photo-induced transgene expression. Despite this three-decade gap from caged ATP to caged DNA use in biological systems, this study ignited interest in the field by demonstrating the utility of caging NAs.

Prior to the 1999 study by Haselton and colleagues, there were several examples of caged NAs being used for chemical or enzymatic applications *in vitro*. Photoprotection groups offer alternatives for NA synthesis. Caging has been used for microarray oligonucleotide synthesis (McGall, Labadie et al. 1996) and as an alternative nucleobase protection for solid-phase synthesis (Alvarez, Vasseur et al. 1999). This technique has also been used to control the self annealing of a hairpin (Ordoukhanian and Taylor 1995) and the hybridization of an oligonucleotide to its complement (Ghosn, Haselton et al. 2005). Caging compounds have also been employed by Meldrum *et al.* to study DNA repair kinetics (Meldrum, Chittock et al. 1998). This study was an extension of their earlier work in which radiolabeled caged-ATP was used to study the same phenomenon (Meldrum, Shall et al. 1990). The first example of a nucleic acid with a caged compound inserted at a precise location was demonstrated by Chaulk and Macmillan (Chaulk and MacMillan 1998). In this study the authors prepared a 2'-O-caged phosphoramidite for insertion into a full-length RNA oligonucleotide. They prepared a ribozyme target that was caged at the site of catalytic cleavage and demonstrated protection of the RNA substrate until photoexposure. These authors expanded on this original work to disrupt spliceosome

and polymerase activity using the site-specifically caged NA strategy (Chaulk and MacMillan 2001). Responding to requests from the scientific community, Chaulk and MacMillan have recently published detailed protocols for their technique (Chaulk and MacMillan 2007). This 2'-hydroxyl caging strategy was later adopted by Pitsch for the development of alternative conditions for synthesizing RNA (Pitsch, Weiss et al. 1999). In addition to these early studies, there is a large body of literature relating to photo-induction of strand breaks using photosensitive adducts (Reviewed by (Mayer and Heckel 2006)).

Chaulk and MacMillan used a *de novo* synthetic process to cage RNA on the 2'-hydroxyl while Monroe *et al.* used a batch-style reaction to achieve random attachment to the phosphate backbone, or "statistical caging". The latter was also adopted to cage mRNA and plasmid DNA using a derivatized coumarin caging group (Ando, Furuta et al. 2001; Ando and Okamoto 2003). Through this strategy, Ando *et al.* were able to control transcription of the mRNA in a zebrafish model. Interestingly, the caged mRNA appeared to be surprisingly stable. This contrasts with our results, in which caging of double-stranded RNA resulted in fragmentation of the target (see section 1.4), presumably through a 2'-hydroxyl attack at the phosphotriester (Breslow and Xu). The same approach which caused hydrolysis of the dsRNA was used to produce 1-(4,5-dimethoxy-2-nitrophenyl)ether (DMNPE) caged siRNAs (Shah, Rangarajan et al. 2005). In both incidences of statistical RNA backbone caging reported in the literature, the caged RNA effectors demonstrated reduced activity relative to their respective controls, which was partially restored by exposure to 350-365nm light. In an effort to reduce the leak activity, improve the efficiency of photo-

induction, and avoid RNA hydrolysis, two groups have separately expanded on caged siRNA by incorporating a single photolabile group onto the 5' terminal phosphate of the siRNA antisense strand (Nguyen, Chavli et al. 2006; Shah and Friedman 2007). These studies are discussed in further detail in chapter 3. Briefly, Nguyen *et al.* demonstrated that these caged siRNA had very little activity until silencing was efficiently restored with light. Small leak activities were explained by N-1 contaminants from the synthesis process, in which the cage-containing terminal nucleotide was missing. Shah and Friedman disputed this interpretation since their data shows a significant higher leak RNAi activity in the caged state. Their interpretation was that the RISC components have the ability to interact with the remaining non-bridging phosphate-bound oxygen, allowing some RNAi to proceed.

Significant progress has been made in recent years toward site-specific caging of nucleic acids. A review of the studies above suggests that in order to achieve a binary, “on-off behavior”, for caged NAs, control over positioning of the caging group is necessary. The original work by Chaulk and MacMillian was limited to only adenosine residues that are caged on the 2'-hydroxyl. However, the design of a caged NA for various effectors will require more flexibility. Pitsch and colleagues expanded the 2'-O-caging to include the other bases. However, other work has attempted to include the caging species on the nucleobases. The first example of a caged nucleobase appeared in 1992, where a caged adenosine derivative was used for self-replication but was not incorporated into an oligonucleotide (Hong, Feng et al. 1992). The first example of a caged base within an oligonucleotide came in 2004 and was also an adenosine derivative (Ting, Lerner et al. 2004). This study used a non-

traditional photoactive C8 thioether-linkage to control DNAzyme activity. Shortly after this study, the 2-nitrobenzyl caging moiety was used for all bases. A 2-nitrobenzyl group to cage the O4-position of thymine and the resulting NAs were used to disrupt T7 polymerase (Krock and Heckel 2005) and control aptamer activity (Heckel and Mayer 2005). This same team also caged the guanine nucleobase in order to control aptamer activity by controlling G-quadruplex structure formation (Mayer, Krock et al. 2005). At nearly the same time, another group presented NPE caged guanine to study tertiary folding kinetics of RNA (Wenter, Furtig et al. 2005). Almost immediately following these studies, Höbartner and Silverman produced a complete set of NPE base-caged RNA residues (Hobartner and Silverman 2005). This offers a great deal of design flexibility to researched developing caged oligonucleotide effectors. However, these compounds are still significantly limited in two ways. First, generation of the caged precursors requires considerable chemical expertise and is a limiting factor for many biologists. Second, since the caging groups are non-substituted 2-nitrobenzyl cage groups, uncaging requires photoexposure in a range of wavelengths that is damaging to biological systems. One final example of base caging comes from Dmochowski and colleagues. This group has created a 25nt oligonucleotide containing a cytosine with a nitrobenzyl linker that is further conjugated to a fluorescence quencher (Tang and Dmochowski 2005). An adjacent nucleotide contains a fluorophore, which emits a fluorescent signal upon photo-release of the quencher. They used this cage attachment chemistry to control RNase H mediated digestion through hairpin loop caging (Tang and Dmochowski 2006).

1.3.4 Special Considerations

1.3.4.1 Two-Photon Excitation

One of the newest frontiers in caging technology is the application of the two-photon excitation (TPE) strategy, first applied by Webb and colleagues (Denk, Strickler et al. 1990). The time required to produce an excited electron state when a chromophore absorbs a single photon is on the order of 10^{-15} s^{-1} (Ellis-Davies 2007). TPE occurs when two photons of half the necessary energy are absorbed within this time-frame, or “simultaneous” absorption. The probability for the simultaneous absorption of two photons is proportional to the square of the incident light intensity

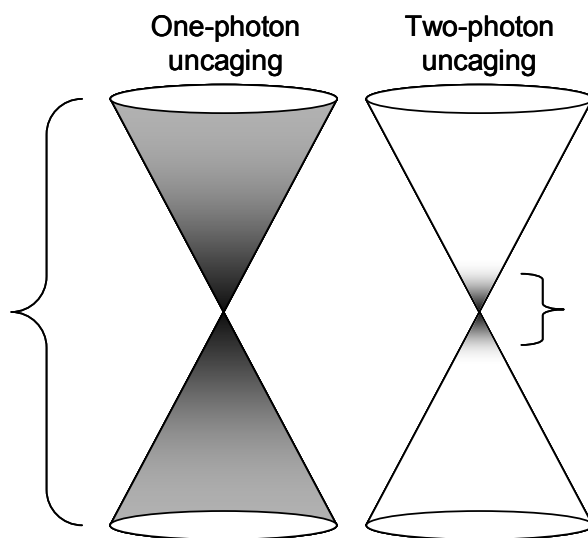


Figure 1.11: One versus two-photon uncaging. Brackets and shading depict the region of efficient uncaging.

and the two-photon absorption cross-section, measured in units of Göppert-Mayer (1 GM = $10^{-50} \text{ cm}^4 \cdot \text{s} \cdot \text{photon}^{-1}$) (Göppert-Mayer 1931; Pelliccioli and Wirz 2002). This strategy has several advantages over single-photon uncaging. Since the excitation is exponentially dependent on the incident light intensity, much greater three-dimensional control over substrate release can be achieved. Figure 1.11 illustrates that TPE is

confined to a very small region near the focal point of the excitation laser. It has been demonstrated that the spatial resolution of TPE can reach sub-femtoliter volumes [Brown, 1999 #334; Brown, 1996 #335]. Another benefit of TPE is that it relies on IR radiation for excitation. Light in this wavelength range is capable of deeper tissue penetration and is less likely to cause damage to biological systems. Nevertheless, photo-toxicity in response to TPE has been observed in biological systems when the power of the incident laser exceeds 5 to 10 mW (Hopt and Neher 2001).

1.3.4.2 Convertible Nucleoside Approach

An alternative to generating phosphoramidites containing photolabile protecting groups on the nucleobase or the ribose 2'-hydroxyl is post-synthesis substitution of the oligonucleotide. For this technique to be effective, the protecting groups used need to be stable under the conditions of RNA solid-phase synthesis, but they must also be susceptible to some form of substitution for post-synthetic placement of the cage compound. In an effort to generate cross-linked nucleic acid duplexes to study DNA-protein interactions, a group led by Verdine developed a method for incorporating reactive nucleotide analogs for post-synthetic substitution of NAs. They named their technique "the convertible nucleotide approach" (Ferentz and Verdine 1992; Ferentz, Keating et al. 1993). Building on the foundation of successful post-synthetic modification, this group developed a complete set of convertible nucleotide analogues for site-specific incorporation into DNA (Macmillan and Verdine 1990; Macmillan and Verdine 1991; Erlanson, Chen et al. 1993; Ferentz, Keating et al. 1993) and RNA (Allerson and Verdine 1995; Allerson 1996; Allerson, Chen et al. 1997). The

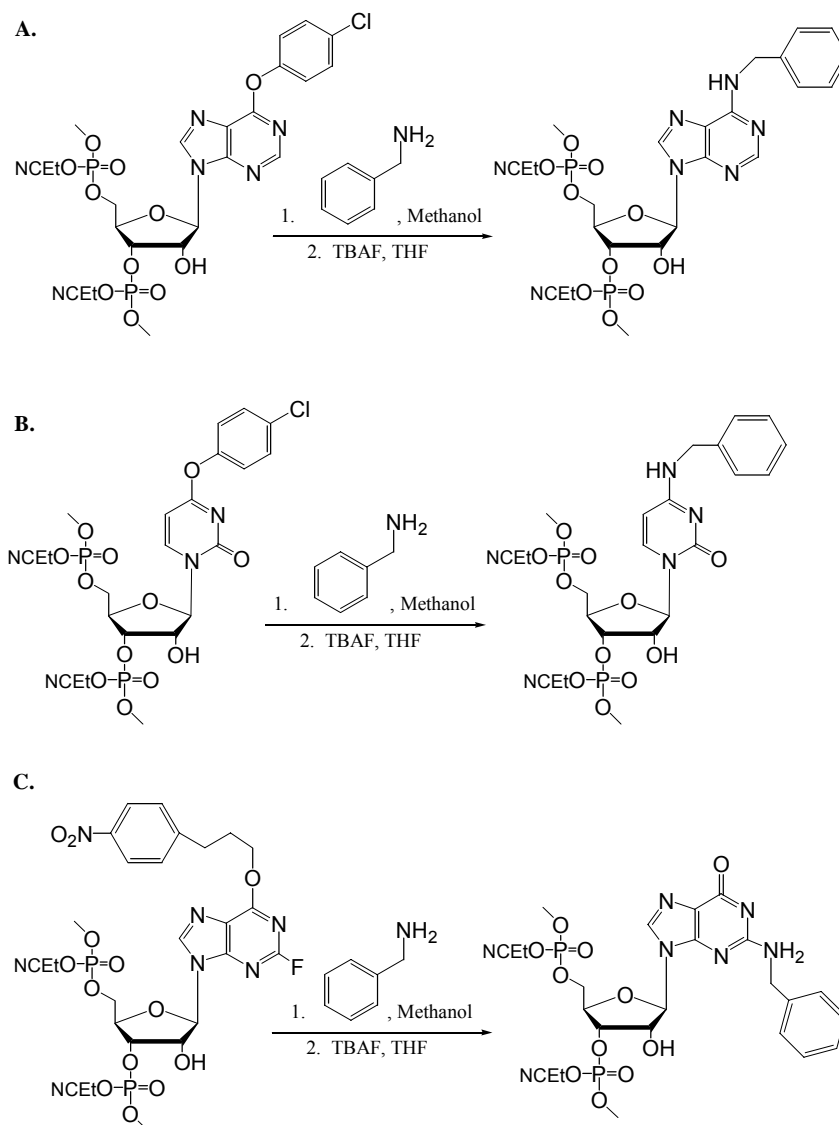


Figure 1.12. Convertible nucleotide approach. Benzylamine used as a model for 2-nitrobenzylamine mediated caging. A = convertible adenosine reaction, B = convertible cytosine reaction, and C = convertible guanine reaction

conversion reaction requires a primary amine that is nucleophilic in nature and is performed following oligonucleotide synthesis. In the case of convertible RNA, this reaction is performed prior to 2'-deprotection. If a suitable cage compound containing a nucleophilic amine is available, this process would be practical for biologists and those in other disciplines whose focus is not on synthetic chemistry techniques.

Although a number of amines were tested by Verdine's group, the attachment of a 2-nitrobenzyl group through the convertible nucleotide approach was not attempted. However this group did successfully demonstrate the conversion reaction using benzyl amine (fig 1.12) (Allerson 1996). Recently, this same chemistry was used to generate site-specifically modified siRNAs by reacting benzyl amine with an internal convertible G (Puthenveetil, Whitby et al. 2006). Although the authors of the latter study were using this technique to probe the cytokine response induced by small RNA duplexes, this serves as a foundation for the use of this approach for site-specifically modified siRNAs. This work demonstrates the use of this approach to generate an internally N6-caged adenosine using 2-nitrobenzyl amine and a novel 4,5-dimethoxy-2-nitobenzyl amine.

CHAPTER 2

Initial Feasibility Studies for Caging RNA

2.1 Determination of Caging Efficiency

Before experimental conditions of cage attachment to oligonucleotides could be varied for optimization (described below), it was necessary to determine spectral properties of the dimethoxy-2-nitrobenzyl product. The hypothesized position of cage attachment for the reactive diazo-intermediate is on the negatively charged phosphate of the NA. This theory is based on common use of diazo chemistry to alkylate phosphate groups in addition to previous caged nucleic acid examples (reviewed by (Monroe and Haselton 2004)). Therefore, the expected product would be a phosphate, which would likely have little effect on the absorbance spectrum of the NA. A simple experiment was performed to determine the spectral properties of DMNPE-phosphate.

2-nitrobenzyl hydrazone cage precursor (5 mg) was activated in DMF (1 mL) and filtered according to the protocol discussed below. A control was simultaneously processed without the addition of the 2-nitrobenzyl hydrazone. Both the activated diazo cage and process control (0.1 mL) were added to an excess of concentrated phosphoric acid (15 mL). The process control was used to obtain baseline spectra at various dilutions in deionized water. Absorbance spectra for several dilutions of reacted cage were obtained in triplicate, and extinction coefficients were determined for A₂₆₀, A₃₅₅, and A₅₀₀. The results ($\epsilon_{260} = 3064$, $\epsilon_{355} = 4512$, $\epsilon_{500} = 0 \text{ M}^{-1}\text{cm}^{-1}$), were in agreement with previous studies (reviewed by (Monroe and Haselton 2004)).

Following a caging reaction, the isolated caged oligonucleotide products were analyzed through spectroscopy to determine caging efficiency. Briefly, the

absorbance spectra of a caged products were measured from 230 to 500 nm. A500 was utilized as a standard to zero each measurement. A355 was used to calculate the molar concentration of attached DMNPE. Once this concentration was known, the absorbance at 260 nm due to this DMNPE was subtracted from the measured value. The corrected A260 was used to calculate the molar concentration of the nucleic acid. The degree of phosphate alkylation is reported as “caging efficiency”. This term is descriptive of the percentage of the phosphate groups has reacted with the diazo 2-nitrobenzyl. For instance, an oligonucleotide with 20 monomers would have 19 phosphate groups, assuming the 5'-end is not phosphorylated. For this sample scenario, a 100% caged product would require a 19:1 molar ratio of oligonucleotide to cage group in solution.

$$\% \text{ Caging Efficiency} = \frac{\frac{100 \cdot (A_{355})}{(\epsilon_{355\text{DMNPE}})}}{\left[\frac{(A_{260}) - \frac{(A_{355})(\epsilon_{260\text{DMNPE}})}{(\epsilon_{355\text{DMNPE}})}}{(\epsilon_{260\text{NA}}) \cdot (\text{phosphates/NA})} \right]}$$

Equation 2.1: Equation used to calculate the caging efficiency following removal of all unreacted diazo cage compound. The numerator is used to determine the molar concentration of attached cage. The denominator is used to calculate the molar concentration of free phosphates using a corrected absorbance.

After UVA light exposure, the quantum yield (Φ) can be calculated for the photolysis event. In this case, Φ refers to the number of photo-release events for each photon absorbed by the cage molecule. Measuring this property requires an additional purification step to remove any photo-released cage from the deprotected NA. With

proper product purification and characterization of the incident light, Φ can be calculated from analysis of the post-UVA light treated caged species and the pre-determine absorbance properties of the cage molecule.

$$\text{Quantum Yield } (\Phi) = \frac{\left(\frac{A_{355\text{Caged}} - A_{355\text{Caged}}}{(\epsilon_{355\text{DMNPE}}) \cdot L} \right)}{\left[\frac{\text{Light Dose (J/cm}^2\text{)}}{\left(\frac{h \cdot C_{(\text{speed of light})}}{\lambda} \right)} \right] \text{Area} \cdot \text{LOG}^{-1}(\epsilon_{355\text{DMNPE}} \cdot C_{\text{DMNPE}} \cdot L)}$$

Equation 2.2: Equation used to calculate Φ following photo-release. The numerator is used to determine the molar amount of DMNPE removed by light treatment. The denominator is used to calculate the number of photons absorbed by the caged species.

2.2 Determination and Optimization of Caging Protocol

The cage attachment procedure was modeled after previous examples in the literature (Monroe, McQuain et al. 1999; Ghosn, Haselton et al. 2005; Shah, Rangarajan et al. 2005). Dimethoxy-2-nitorbenzyl hydrazone (5 mg) was dissolved in an organic solvent and converted to the diazo-form using MnO_2 (50 mg) for 20 minutes at room temperature under agitation. The MnO_2 was pelleted through centrifugation and the supernatant was filtered through a prewetted diatomaceous earth column. The resulting active cage solution was added to an aqueous solution of NA, buffered to a desired pH. The reaction was shielded from light, and typically allowed to react at 4°C for 18 hours. Once complete, the unreacted cage was removed through size exclusion chromatography using solvent resistant LH-20 sephadex (GE Healthcare Bio-Sciences Corp., Piscataway, NJ). The product solution was then dried in vacuo until most of the solvent was removed. Deionized water was used to bring the

concentrated solution to 500 μL . All remaining organic solvents, by products, and unreacted cage molecules were removed through a nitrocellulose spin filter (YM3, Microcon).

Table 1.1 Caging efficiencies of various NA targets.
NA type, base composition and pH are varied.

| Sample Type | pH | Caging Efficiency | |
|---------------------------|-----|-------------------|-------------------|
| | | No UV Exposure | + 365 nm Exposure |
| DNA mixed sequence | 5.5 | 46.7 | 13.4 |
| DNA mixed sequence | 8.0 | 4.0 | 1.6 |
| DNA oligo dT | 5.5 | 41.5 | 9.3 |
| DNA oligo dT | 8.0 | 6.4 | 1.4 |
| FNA mixed sequence | 5.5 | 36.2 | 12.4 |
| Morpholino mixed sequence | 5.5 | 18.3 | 4.3 |
| Morpholino mixed sequence | 8.0 | 7.2 | 4.9 |

In an effort to obtain purified products through a range of caging efficiencies, several variables of the caging reaction were investigated. The following variables were examined to determine their effect on the caging reaction: nucleic acid type (DNA, RNA, PS, 2'-fluoro substituted NAs, morpholino), nucleobase composition, concentration and molar excess of active diazo-cage, reaction duration, reaction temperature, organic solvent, and pH of the aqueous buffer. Variables which affected the efficiency of the cage reaction included pH, relative molar excess of active cage, and type of nucleic acid target. PS NAs experienced the highest alkylation rate among the samples tested. Morpholino oligonucleotides, which lack a phosphate backbone, also showed cage attachment, albeit at a lesser rate. Since these polymers do not contain any phosphates, this suggests that either a minimal degree of nucleobase alkylation is possible or that a more specific reaction is occurring with the specialized

backbone of this NA. Reaction with the backbone morpholinos is unlikely as they are comprised of stable 6-membered morpholino rings bound by phosphorodiamidate linkages. Sugar-modifications seemed to have little effect on the caging process, and therefore DNA, RNA, and FNA all yielded equivalent efficiencies. Reaction temperature and reaction duration also had little effect on the outcome of the reactions. This is likely because these reactions proceeded to completion in the timeframes that were tested, even at 19°C. The organic solvent used to activate the cage hydrazone also had little effect on caging reaction outcome. However, different organic solvents

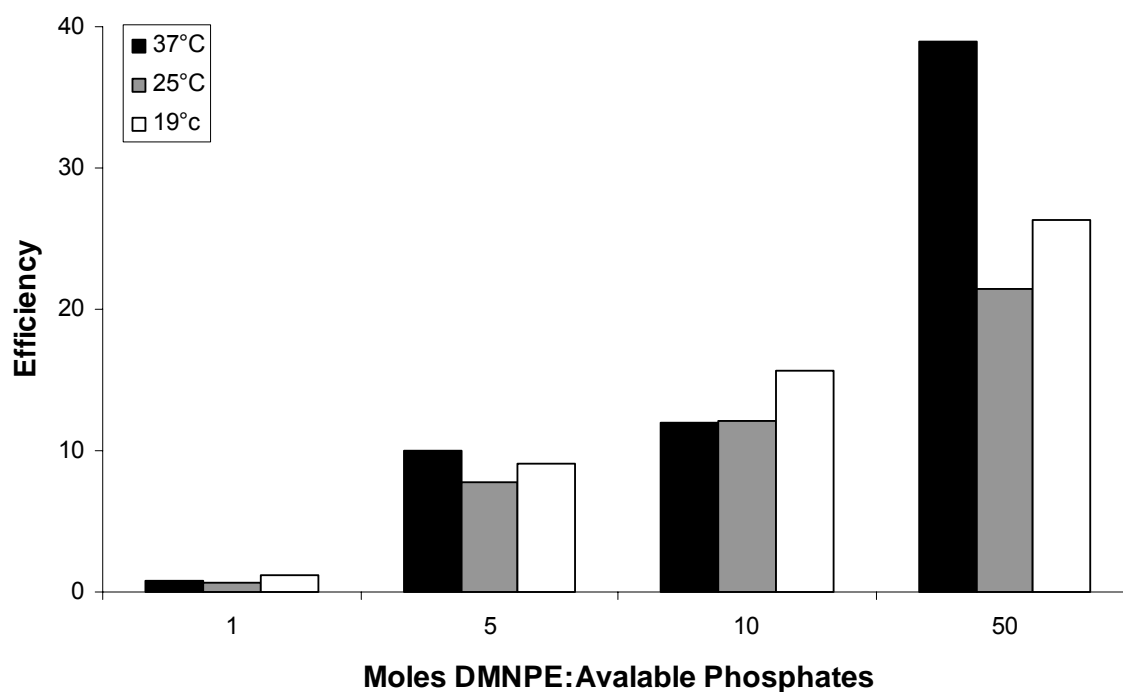


Figure 2.1: Caging efficiency by cage concentration and reaction temperature

required optimization of the purification process to prevent loss of the product and poor reaction yields. Altering base composition yielded somewhat inconsistent results. However, it was evident from these preliminary studies that the sequence of the

nucleic acid may have an unexpectedly robust influence on caging efficiency. Below are results from two sample experiments that tested some of these variables.

In addition to developing a protocol to adjust the caging efficiencies for various NA targets, improvements to caged product purification were also required. Previous studies that utilized this caging technique targeted larger NAs such as plasmid DNA or mRNA (Monroe, McQuain et al. 1999; Ando, Furuta et al. 2001). This required fewer caging molecules to render the biomolecules inert, which allows for the purification through phase separation. For hybridization disruption, oligonucleotides seem to require a higher percentage of caged phosphates, which reduces the hydrophilicity of the molecule and results in inefficient liquid-liquid extraction. Since caging of the oligonucleotides alters the hydrophilicity and eliminates backbone charge, separation based on these principles is challenging. Size-exclusion chromatography and filtration, two techniques based on molecular size, provided the most reasonable alternative. However, organic solvent contamination is often incompatible with the materials used for these separation techniques. Additionally, the crude product can not simply be dried to remove the organic solvents because the unattached caging material will partially precipitate from the remaining aqueous solution. Therefore, a solvent-resistant size-exclusion chromatography material, LH-20 sephadex, was used. The separation capabilities were tested for each organic solvent used in the reaction (DMF, DMSO, acetonitrile). Figure 2.2 illustrates that separation occurs well for solutions containing 30% or less acetonitrile in aqueous buffer. Any new solvent system must be tested in this manner to ensure proper cage removal. Once the solvent conditions were determined for adequate separation from the free

cage, the system was also tested using spin filters at a relative centrifugal force of 500g. Preswollen LH-20 sephadex could be used in either a gravity or spin column, and each technique had benefits and drawbacks. Gravity columns could handle a larger load of material, but the process was slower and generated larger volumes that required longer drying steps. Spin columns were very fast, but only a limited volume could be added to the column bed. Additionally, the fixed angle rotor found in many microtube centrifuges sometimes caused uneven elution of the product solution. Following size-exclusion, the solutions were dried *in vacuo* until less than 25 μL of solvent remained in order to remove most of the organic component. This solution was brought to a volume of 500 μL with deionized water and applied to the cellulose filtration system, YM3 amicon spin filters (Millipore, Billerica, MA). The product was filtered several times by adding water to the filter and spinning to elute the unwanted

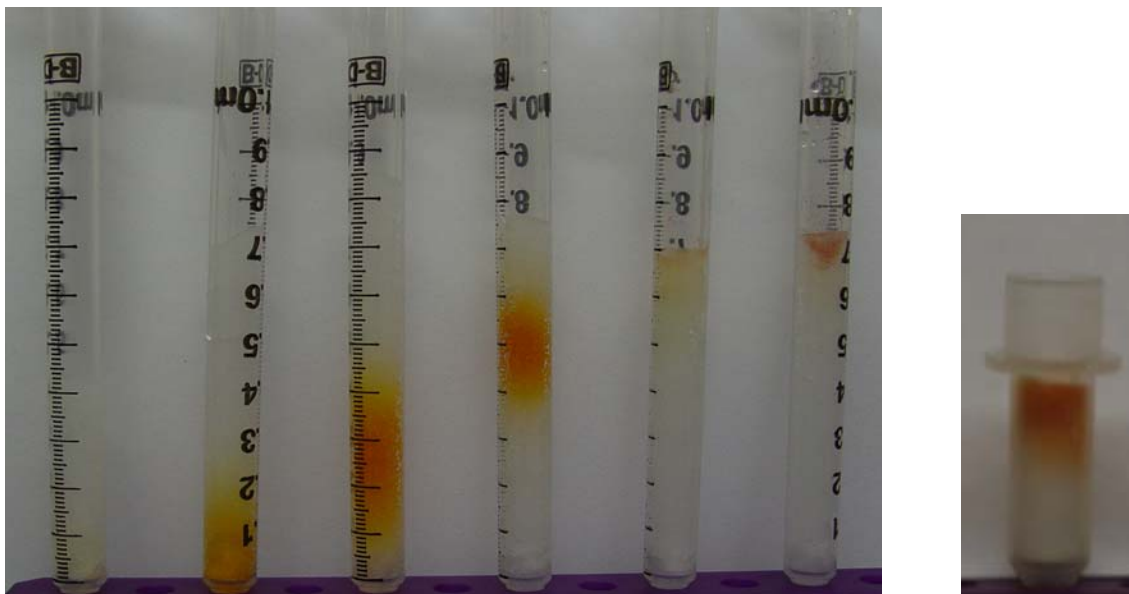


Figure 2.2: LH-20 sephadex resolution. Size-exclusion separation as a function of % organic solvent. From left to right, loaded LH-20 sephadex was washed with 100%, 80%, 60%, 40%, 20%, and 0% organic solvent (acetonitrile). The panel on the right illustrates the resolution of a spin filter eluted at 400Xg at 30% organic solvent.

material. This step removed any remaining organic solvents, removed any remaining free cage contamination, and desalted the product. However, this step was particularly sensitive to organic contamination, and improper handling before this step resulted in poor yields. When performed properly, this cleaning protocol would consistently result in caged NA recovery yields greater than 90%.

The final reaction conditions used to generate caged oligonucleotides that were unmodified on the phosphate or the nucleobase are as follows. Dimethoxy-2-nitorbenzyl hydrazone (5 mg) was dissolved in 1 mL of acetonitrile and activated using MnO_2 (50 mg) for 20 minutes at room temperature. If less efficiently caged products were desired, several dilutions of the active diazo-cage were made following MnO_2 removal. The nucleic acid was diluted to 500 ng/ μL in BisTris buffer (50 mM Bis-Tris-HCl, 1 mM EDTA, pH 5.5), and the active cage was added to achieve a final solution of 2:1 acetonitrile:water. The reaction was agitated at 4°C for 18 hours in the dark. At this time, water was added to the reaction solution to obtain a 3:10 acetonitrile:water concentration. A gravity column was packed with prewetted LH-20 sephadex and washed with three column volumes using the appropriate solvent. The entire reaction was added to the column and the eluent was collected. The column was washed with 3 X 200 μL using deionized water to ensure all nucleic acid was eluted from the column. The collected product was dried in a vacuum centrifuge until less than 25 μL remained. This was added to 500 μL of water in a YM3 amicon spin filter, which was spun at 12,000Xg for 100 minutes. Water was added (500 μL) twice and the spinning elution was repeated each time. All eluents from this step were kept until the product recovery was verified, and then they were discarded. YM3 filtration would typically

yield 50 μ L of an aqueous solution of the purified product. The product was measured by spectroscopy to determine caging efficiency and product yield.

2.3 Caging of 700bp dsRNA

Initially it was proposed that caging of long double-stranded RNA would be a feasible means to control RNAi by light. This has several benefits over caging small RNAs. First, these targets can be generated more easily through *in vitro* enzymatic methods. Secondly, this technique did not require the screening for active siRNA sequences, as Dicer acts to digest these products into a pool of siRNAs. This process can be carried out *in vitro* using a recombinant Dicer enzyme to generate siRNAs for use in mammalian cell culture. Finally, caging at this stage offers another level of control since the processing by Dicer is an additional protein-NA interaction that may be disrupted. However, this preliminary experiment allowed the identification of a major design flaw in the original proposal.

The Dicer siRNA Generation Kit (Genelantis, San Diego, CA) provided all the necessary materials for the initial experiment including: the dicer enzyme, a control GFP reporter plasmid, T7 polymerase, and the appropriate PCR primers. PCR was carried out according to the manufacturer instructions to generate a 700bp RNA transcript. This dsRNA was subjected to the caging reaction using DMF as the organic solvent. The product was analyzed by spectroscopy and DMNPE attachment was verified. These products were further analyzed by capillary electrophoresis using the Agilent 2100 Bioanalyzer lab-on-a-chip platform and the accompanying DNA 1000 reagent system [Agilent, Clara, CA], according to the manufacturer protocol. Figure

2.3 shows the electropherograms of the resulting products as they relate to the 15bp and 1500bp internal standard peaks. The process control RNA is detected at around 90 seconds, which corresponds to the expected migration time for a 700bp NA. However, the caged sample elutes much sooner, at around 50 seconds. This shift direction was unexpected since cage attachment should increase the migration time through standard principles of electrophoresis. Indeed, photoexposure increased the mobility of the caged species, suggesting removal of the cage groups.

These results indicate that caging RNA using phosphate alkylating diazo cage compounds is possible, but it also results in fragmentation. RNA is known to be

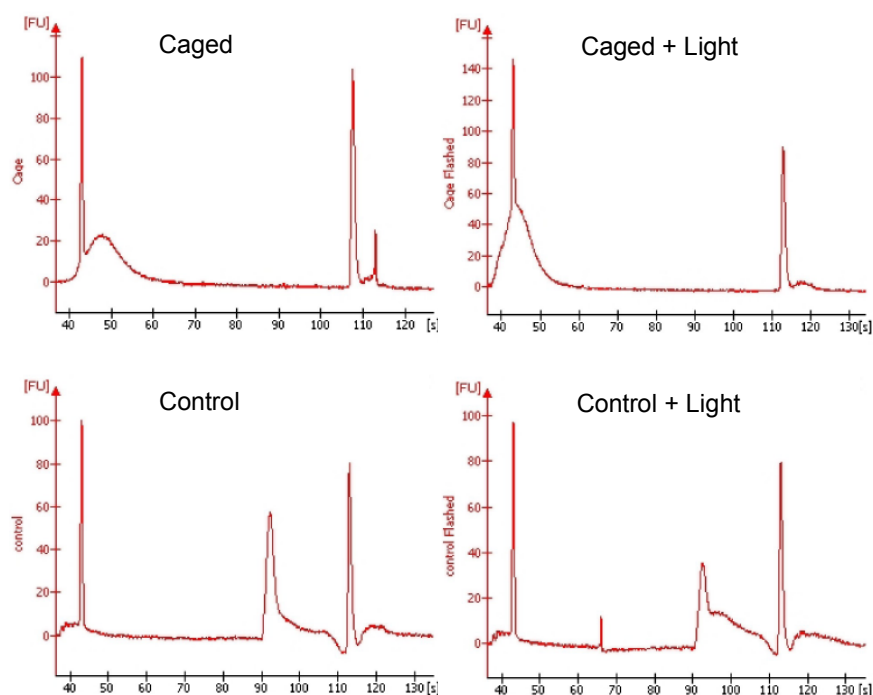


Figure 2.3: Capillary electrophoresis of caged 700bp dsRNA. Faster elution of caged RNA indicated strand cleavage from the caging process.

susceptible to self-hydrolysis due to the presence of the 2'-hydroxyl on the ribose moiety. Additionally, RNA phosphotriesters have been shown to be particularly

unstable in aqueous solutions (Breslow and Xu). This aqueous instability is due to the 2'-hydroxyl attack and cyclization of the 2'-3' positions of the ribose, creating an unstable intermediate. Therefore internally caged nucleotides might be very susceptible to scissile bond cleavage and degradation of the RNA. Alternatively, hydrolytic release of the cage molecule is a possibility. This experiment prompted a search for a chemically stabilized RNA mimic and is the subject of Chapter 3.

2.4 Design of the siRNA for the pAcGFP Reporter System

Established siRNA design requirements were followed, such as maintaining approximately 50% GC content of 21nt sense and antisense strands which hybridize to yield 2nt, 3' overhangs (Elbashir, Lendeckel et al. 2001). The overhangs were designed as UU on both strands, and a sequence was chosen so that the antisense overhang was still homologous to the target gene. Additionally, the first nucleotide of both the sense and the antisense transcripts was guanine since it is typically the first addition by T7 polymerase (Donze and Picard 2002). This required the 19th nucleotide of each transcript to be cytosine. Additionally, several sequence requirements were necessary for endeavors into the site-specific incorporation of a cage species. The most likely base for this site specific incorporation is adenosine because of its stability, history of ATP experiments, possession of an exocyclic primary amine, and previous caging of this nucleotide in the literature. Therefore, one adenosine was placed within the first 5 nucleotides from the 5'-end and one was placed at the 11th nucleotide from this end. These are considered as important sites for RISC recognition and mRNA processed. The sequence of the GFP plasmid, pAcGFP-N1 (Clontech, Carlsbad, CA),

used in knockdown experiments was searched for an appropriate target, which was also subjected to a BLAST search to ensure no cross-reactivity with other known genes.

CHAPTER 3

2'-Fluoro Nucleic Acids Induce RNA Interference

3.1 Introduction

RNA interference refers to a highly specific, very potent, and naturally-occurring post-transcriptional silencing of protein expression initiated by RNA (for review, see (Tomari and Zamore 2005)). Since its discovery in 1998 (Fire, Xu et al. 1998), RNAi has drastically altered our understanding of gene regulation by introducing a plethora of small regulatory RNA molecules. These molecules are termed small-interfering RNAs (siRNAs), small-hairpin RNAs (shRNAs), or microRNAs (miRNAs), depending on their origin and specific structure (Elbashir, Lendeckel et al. 2001; Matzke and Matzke 2003). In addition to these variations, recent works show that single-stranded RNA molecules (antisense siRNA) can elicit RNAi in mammals (Martinez, Patkaniowska et al. 2002; Schwarz, Hutvagner et al. 2002; Amarzguioui, Holen et al. 2003; Holen, Amarzguioui et al. 2003). A collection of proteins known as the RNA-induced silencing compound (RISC) incorporate the siRNAs, which act as a guide for sequence recognition and enzymatic degradation of target mRNAs in the cytoplasm. Some intramolecular RNA structural requirements that are necessary to elicit these various pathways and consequences with respect to siRNA design have been described in recent studies. A common focus of these works is chemical modification of siRNAs to improve pharmacological efficacy. In order to develop useful RNAi drugs, the siRNA must be efficiently delivered systemically, exhibit highly specific knockdown of the target gene, and maximize the duration of silencing. For these reasons, modifications have been made which optimize the lipophilicity of RNA,

increase the stability of the duplex, and impart resistance to RNAses, respectively. The relative successes and failures of these modifications have helped to identify useful alterations that may be well-tolerated by the RNAi pathway.

Phosphate backbone and ribose modifications are widely used to increase resistance of RNA to enzymatic degradation ((Elbashir, Lendeckel et al. 2001; Amarzguioui, Holen et al. 2003; Braasch, Jensen et al. 2003; Chiu and Rana 2003; Czauderna, Fechtner et al. 2003; Harborth, Elbashir et al. 2003; Dowler, Bergeron et al. 2006) reviewed by (Manoharan 2004; Zhang, Du et al. 2006)). In addition to nucleases resistance other such modifications impart other desired characteristics such as preference for a certain helix formation or increased thermal stability (Kurreck 2003; Manoharan 2003; Manoharan 2004). For this reason, many types of modified siRNAs have been evaluated for their ability to elicit target mRNA degradation and subsequent gene knockdown with highly variable results between studies. Other than halide substitutions, modifications at the 2' site have been problematic. O-methyls, locked nucleic acids (LNAs), or other bulky substitutions can be used only sparingly and are thought to protrude into the minor groove and disrupt RISC recognition of the duplex (Braasch, Jensen et al. 2003; Chiu and Rana 2003; Czauderna, Fechtner et al. 2003). Complete 2'-deoxy substitution, results in a conformational change of the duplex to a B-type helix and does not exhibit RNAi activity (Chiu and Rana 2003). 2'-Deoxy-2'-fluoro modifications seem to be the best-tolerated alteration with respect to maintaining silencing activity (Manoharan 2003; Manoharan 2004). Unfortunately, 2'-F substituted purines have been unavailable commercially until recently, so only pyrimidine-modified siRNA mediated gene silencing has been attempted to date.

Several studies have shown similar levels of RNAi elicited between wild-type siRNA and these synthetic counterparts that contain fluorine on every pyrimidine (Braasch, Jensen et al. 2003; Chiu and Rana 2003; Harborth, Elbashir et al. 2003; Manoharan 2003; Layzer, McCaffrey et al. 2004; Manoharan 2004; Soutschek, Akinc et al. 2004). Sullenger and colleagues showed that 2'-F pyrimidine-modified siRNAs and unmodified siRNAs have similar activity over a range of concentrations and silencing durations (Layzer, McCaffrey et al. 2004). Chiu and Rana compared silencing potency of various siRNA modifications and found that siRNA completely modified with 2'-F pyrimidines and 2'-H purines showed only a 50% decrease in knockdown ability relative to an unaltered siRNA counterpart (Chiu and Rana 2003). Interestingly, Bhat and colleagues demonstrated that fully-modified duplexes which included 2'-F pyrimidine nucleotides and 2'-O-methyl purine nucleotides actually increased RNAi efficiency, and in one case they achieved a 500-fold increase in silencing ability (Allerson, Sioufi et al. 2005). The combination of several types of chemical modifications into a single siRNA molecule are becoming increasingly common as illustrated by a recent work by Morrissey and colleagues (Morrissey, Blanchard et al. 2005). Alternatively, 2'-deoxy-2'-fluoro- β -D-arabinonucleic acid modifications, in which the 2'-fluoro is inverted, have been used to partially modify siRNA and successfully induce RNAi (Dowler, Bergeron et al. 2006). The combination of these results suggests that the 2'-OH is not necessary for RNAi, but changes at this location that alter either the global duplex structure or disrupt the minor groove can abolish interference. In addition to improving resistance to enzymatic degradation while maintaining silencing efficiency, 2'-modifications have been shown to reduce off-target

effects normally observed following siRNA delivery (Jackson, Burchard et al. 2006; Cekaite, Furset et al. 2007). Since halide substitutions are thought to maintain the A-type helical structure by enforcing a C3'-endo sugar pucker confirmation (Guschlbauer and Jankowski 1980; Chiu and Rana 2003) and they are not large enough to disrupt the minor groove, siRNAs that contain 2'-F functional groups at every location may still elicit potent RNAi. Although fully 2'-F-modified nucleic acids have been generated and evaluated for several characteristics which are crucial in antisense applications, these compounds have not been evaluated for gene silencing in cells or *in vivo* (Kawasaki, Casper et al. 1993). Replacing the hydroxyl at every location may also provide further resistance to enzymatic degradation by nucleases and eliminate RNA degradation through 2'-OH nucleophilic hydrolysis.

A mutated polymerase, originally developed for the ability to incorporate both rNTPs and deoxy-counterparts, may provide a cost-effective method to generate fully-fluorinated siRNAs. Specifically, T7 with a mutation of tyrosine to phenylalanine at position 639 (Y639F) eliminates discrimination at the 2'-location of the NTP substrate by abolishing hydrogen bonding requirements (Sousa and Padilla 1995). Eliminating the requirement for 2'-recognition might allow the polymerase to incorporate any 2'-functional group that is not limited by steric hindrance. NTPs with small functional group modifications at this location, such as amines and halides, are incorporated into full length transcripts at differing efficiencies dependant on these steric limitations (Padilla and Sousa 1999). Given that this enzyme has been used to incorporate 2'-F modified pyrimidine NTPs at every location in full-length transcripts, its use may be extended to generate a fully-fluorinated product.

The potential benefits of fluorinated RNA with respect to RNAi stability have prompted us to generate fully 2'-deoxy-2'-fluoro substituted nucleic acid (FNA) through solid phase synthetic and *in vitro* transcription methods. Nuclease digestion assays were performed to evaluate resistance to degradation compared to native RNA. We have evaluated the ability of small interfering fluoronucleic acid (siFNA) to initiate knockdown of a target gene in mammalian cell cultures. Additionally, these siFNAs were evaluated for their silencing ability in both their duplex and single-stranded antisense forms.

3.2 Materials and Methods

3.2.1 siRNA Design

Established siRNA design requirements were followed, such as maintaining approximately 50% GC content of 21nt sense and antisense strands which hybridize to yield 2nt, 3' overhangs (Elbashir, Lendeckel et al. 2001). The overhangs were designed as UU on both strands, and a sequence was chosen so that the antisense overhang was still homologous to the target gene. Additionally, the first nucleotide of both the sense and the antisense transcripts was guanine since it is typically the first addition by T7 polymerase (Donze and Picard 2002). This required the 19th nucleotide of each transcript to be cytosine. Using these design criteria, runoff transcription could be used to generate each strand *in vitro*. The sequence of the GFP plasmid, pAcGFP-N1 (Clontech, Carlsbad, CA), used in knockdown experiments was searched for an appropriate target, which was also subjected to a BLAST search to ensure no cross-reactivity with other known genes.

3.2.2 siRNA and siFNA Preparation

RNAs were generated *in vitro* using a T7 polymerase (Donze and Picard 2002) and using partial duplexes designed for run-off transcription. DNA templates (Sense: 5'-AAGCGGATCTTGAAGTTCACCTATAGTGAGTCGTATTA-3', Antisense: 5'-AAGGTGAACTTCAAGATCCGCTATAGTGAGTCGTATTA-3', T7 Primer: 5'-TAATACGACT-CACTATAG-3') were synthesized, desalted, and HPLC purified from Alpha DNA (Montreal, Quebec, Canada). Equal molar ratios (75pMoles/ μ l) of each template and the T7 primer oligonucleotide were annealed by bringing the solution to 95°C and slowly cooling to 4°C over 20 minutes. The RNAMaxx® *in vitro* transcription kit (Stratagene, Cedar Creek, TX) was used according to manufacturer instructions to generate each strand of RNA individually. FNA strands were generated using 2'-NTPs (purines from Trilink Biotechnologies, San Diego, CA, pyrimidines from Epicentre, Madison, WI) and an alternate *in vitro* transcription kit, Durascribe® (Epicentre, Madison, WI), which utilized a Y639F mutant T7 polymerase, R&DNA Polymerase™ (Sousa and Padilla 1995; Padilla and Sousa 1999). Final concentrations of templates and NTPs were 50 ng/ μ l and 5 mM, respectively. Transcription incubation times were extended from 8 hours for native unmodified RNA generation to 48 hours for FNA generation. The transcription mixtures were treated with DNase I at a final concentration of 0.5units/ μ l overnight at 37°C to completely digest the DNA template. The RNA/FNA products were then precipitated with sodium acetate and ethanol, washed three times, and resuspended in nuclease-free water. Additional purification of fluorinated products was carried out using Microcon YM-3 cellulose spin filters (Millipore, Billerica, MA) to remove possible early termination

products under approximately 10nts in length. Product concentrations were determined by UV/VIS absorbance spectroscopy. The 21-nt FNAs were also chemically synthesized by University of Calgary Core DNA & Protein Services (Calgary, AB, Canada). Synthetic FNAs were PAGE purified and verified through matrix-assisted laser desorption/ionization (MALDI) mass spectrometry. Homologous strands at equal molar ratios were annealed as aforementioned to generate duplex siRNA or siFNA.

3.2.3 Hybridization Analysis

Melting curves were measured for FNA duplexes, DNA duplexes, and FNA/DNA hybrids to compare transcribed and synthetic FNA oligonucleotide hybridization to the same target. For each case, complementary strands were brought to equal molar concentrations of 4 μ M in a medium-salt buffer (100 mM NaCl, 10 mM sodium phosphate, 0.1 mM EDTA, pH 7.5). The samples were annealed by heating to 95°C for 5 minutes and cooling to 4°C over 10 minutes, degassed under vacuum, transferred to a quartz cuvette, and covered with 100 μ l of dimethylsiloxane to prevent evaporation. Melting experiments were conducted using an AVIV model 14DS spectrophotometer (Lakewood, NJ). OD₂₆₀ was measured as a function of temperature from 15°C to 90°C with a 2.5°C step. The samples were held at each temperature for 2 minutes before absorbance reading were recorded. Melting temperature (T_m) values were calculated by determining the local maximum of each melting curve's first derivative.

3.2.4 Nuclease Digestions

RNAse One™, an *E. Coli* derived RNAse, and an accompanying buffer (Promega Corporation, Madison, WI) were used to evaluate nuclease resistance to FNAs. Equal molar ratios of single-stranded or duplex RNAs and FNAs were suspended in optimal buffer and pH conditions as described by the manufacturer. RNAse One™ was added to each solution to a final concentration of 0.5 unit/μl. The digestion reactions were incubated overnight at 37°C. The products were evaluated qualitatively by capillary electrophoresis on the Bioanalyzer 2100 Lab-Chip system (Agilent Technologies, Wilmington, DE) using a custom protocol designed to evaluate small oligonucleotides. The manufacturer loading buffer was replaced with a solution of 200 nM N-Tris(hydroxymethyl)methyl-3-aminopropane sulfonic acid (TAPS) and 2 mM EDTA at pH 8.0-8.5 to eliminate the 15bp markers, which have similar mobility to the experimental samples. With the exception of the loading buffer, a DNA 500/1000 electrophoresis chip was loaded according to the manufacturer protocol, but the chip was run under the mRNA Nano programming conditions (provided within the manufacturer's software package) to obtain data within a useful range of short migration times (<40 sec). The intensities for each electropherogram were normalized to baseline fluorescence and are presented as a composite gel image.

3.2.5 Cell Culture and Transfection

BHK-21 (Baby Hamster Kidney) cells were cultured in reduced serum Dulbecco's Modified Eagle's Medium (DMEM-RS) (HyClone, Logan, UT) supplemented with 3% heat inactivated fetal bovine serum (HyClone, Logan, UT) at

37°C under 5% CO₂ in a humidified chamber and regularly passaged at subconfluence. Cells were seeded on 12 well plates (BD Biosciences, Franklin Lakes, NJ) 18 hours prior to transfection at approximately 20K cells/cm². Cotransfections of pAcGFP-N1, and siRNA or siFNA were mediated with lipofectamine (Invitrogen, Carlsbad, CA). Transfection mixtures containing 0.1 µg of pAcGFP-N1, varying amounts of siRNA or siFNA, and lipid (3:1 ratio of lipid with respect to total nucleic acid) were assembled in 100 µl of reduced protein medium (OPTI-MEM[®], Invitrogen, Carlsbad, CA) and incubated at room temperature for 30 minutes. The plated cells were rinsed with OPTI-MEM and 500 µl of OPTI-MEM was added to each well. The transfection mixtures were added to the appropriate wells and the cells were incubated at 37°C under 5% CO₂ for 6 hours. The transfection media was then replaced with cell culture media and the plates were incubated for 48 hours and harvested for expression analysis.

3.2.6 Flow Cytometry RNAi Analysis

Transfected and control cell culture samples were harvested and fixed in PBS suspension with 1% or 0.5% paraformaldehyde prior to GFP expression analysis via flow cytometry. GFP fluorescence was collected at 530±15 nm (FL1), and cellular auto-fluorescence was collected at a wavelength greater than or equal to 650 nm (FL3) on a fluorescence activated cell sorter (FASC-Scan) cytometer (Becton Dickinson, San Jose, CA) equipped with 488 nm excitation. For each sample, a maximum of 30,000 events were collected. Intact cells were gated on a FSC (forward angle light scatter) versus SSC (90 degrees light scatter) dot plot. An FL1 versus an FL3 display of a

GFP-negative control was gated and applied to all samples and analyzed to yield a percentage of cell events in the GFP-positive region. This GFP-positive percentage for each sample was normalized to an average of GFP-positive controls for the specific set of experiments and expressed as a mean value \pm standard error. In addition to gating analysis, the linear mean of GFP fluorescence intensity was calculated using all measured cell events.

3.2.7 Semiquantitative PCR Analysis

BHK-21 cells were co-transfected with 100ng of pAcGFP plasmid and the aforementioned siRNAs or siFNAs as previously described. Each sample type: siRNA (13.3 nM), two concentrations of siFNA (13.3 and 33.3 nM), positive control, and negative control was generated in triplicate. At 48hrs post-transfection, the cells were harvested and washed with PBS. Approximately 100,000 cells were fixed in 0.5% PFA in PBS and evaluated by flow cytometry to determine GFP expression levels. Total RNA was isolated from the remaining cells (approximately 400,000) using TRI Reagent (Sigma, St. Louis, MO). The RNA isolate was treated with Turbo DNA-free (Ambion, Austin, TX) to eliminate genomic and plasmid DNA contamination. The yield of isolated RNA was evaluated by OD260 and purity by OD260/OD280 using a Bio-Tek Synergy HT multi-detection microplate reader (Bio-Tek Instruments, Inc., Winooski, VT). The integrity of the RNA was evaluated by electrophoresis in a denaturing 0.8% agarose slab gel and stained with SYBR GOLD (Invitrogen Molecular Probes, Carlsbad, California). Each RNA isolate (500ng) was reverse transcribed with BD Sprint PowerScript Pre-Primed Random Hexamer primers RT-PCR Kit (BD

Biosciences, Palo Alto, CA), divided into single-use aliquots, and stored at -20°C. Desalted primers for the knockdown target (GFP: forward primer, 5'-TAC AAC TAC AAC GCC CAC AAT GT-3'; reverse primer, 5'-CAC GCT GCC ATC CTC GAT-3') and a control gene (GAPDH, glyceraldehyde-3-phosphate dehydrogenase: forward primer, 5'-TGG CAA AGT GGA TAT TGT CG-3'; reverse primer, 5'-AGA TGG ACT TCC CGT TGA TG-3') were synthesized (Integrated DNA Technologies, Coralville, IA). For real-time PCR, the following components were mixed: 12.5uL iTaq Sybr green supermix with ROX (BioRad, Hercules, CA, USA), 3.5uL of PCR grade water, 2uL of both forward and reverse primers at 10uM and 2.5uM for GAPDH and GFP, respectively, and 5uL template cDNA diluted 100-fold. Non-template controls and a standard curve (beginning with a non-diluted mixture of all cDNAs and including 5-serial 10-fold dilutions of this mixture) were simultaneously run in conjunction with the experimental samples using both primer sets. PCR was carried out using a Chromo4 Real-Time PCR Detection System (Bio-Rad, Hercules, CA, USA). For all samples and primer sets, the following thermal cycling conditions were used: incubation (50°C for 2 mins), denaturation (95°C for 5 mins), 45 cycles of amplification and fluorescence quantification (95°C for 15 secs followed by 60°C for 60 secs), and melting fluorescence quantification (heating from 55°C to 95°C and measuring at 0.2°C step-intervals after holding for 0.02 secs). Both GAPDH message levels and PCR efficiencies (calculated via amplification slopes with Opticon Monitor 3 software) were used to ensure the results for each sample were suitable for analysis. Following amplification, a representative GFP product was sequenced to ensure the correct amplicon was generated.

3.3 Results

3.3.1 FNA Generation

Synthetic sense and antisense FNA oligonucleotides were successfully generated through solid phase synthesis at a 250nMole yield and verified by MALDI and further purified by PAGE separation. Mass spectroscopy of these products prior to PAGE purification gave primary peaks of 6693m/z and 6715m/z for the antisense and sense strands, respectively. These values agree with the expected mass calculated for each product. Extra peaks, which were only slightly discernable above background noise, corresponded to base depurinations that occur as a result of MALDI, or the presence of residual monovalent cations. UV/VIS absorbance spectroscopy was used to determine the total amount of FNA generated for each transcription reaction. An extinction coefficient was calculated for each product based on the sequence and standard absorbance profiles for nucleic acids. Since 2'-Fluoro-2'-deoxy-NTPs have absorbance properties comparable to native NTPs (2'-F-dATP, $\epsilon = 15,400 \text{ M}^{-1}\text{cm}^{-1}$, 2'-F-dGTP, $\epsilon = 13,600 \text{ M}^{-1}\text{cm}^{-1}$, Trilink Biotechnologies), the same extinction coefficients were used for the RNA and FNA products. At 48 hours, an average of $83.9 \pm 7.4 \text{ }\mu\text{g}$ (n=8) of total product was generated in a typical 20 μl reaction volume. This was comparable to manufacturer's estimated yield of unmodified RNA generation using this enzyme, which was 40-60 μg for an equivalent reaction held for 4 hours. PAGE separation of the products followed by nucleic acid staining and comparison to included standards indicated that full-length transcripts were present in addition to some early termination products. An average of $28.7 \pm 8.9\%$ (n=4) sample recovery was obtained from Microcon spin filter purification. PAGE results showed little

difference between single stranded and duplex FNA products (figure 3.2). The average yield of unmodified RNA using the RNAMaxx® *in vitro* transcription was approximately $92 \pm 6.9 \mu\text{g}$ ($n=6$) for an 8 hour reaction of the same volume. This amount was in agreement with the manufacturer's estimated yield.

2.3.2 Hybridization Analysis

Melting curves shown in figure 3.1 were measured to calculate the T_m of various duplexes to assess the purity and accuracy of the transcribed products and synthesized FNA. Synthetic FNAs exhibited the highest melting temperatures, with a

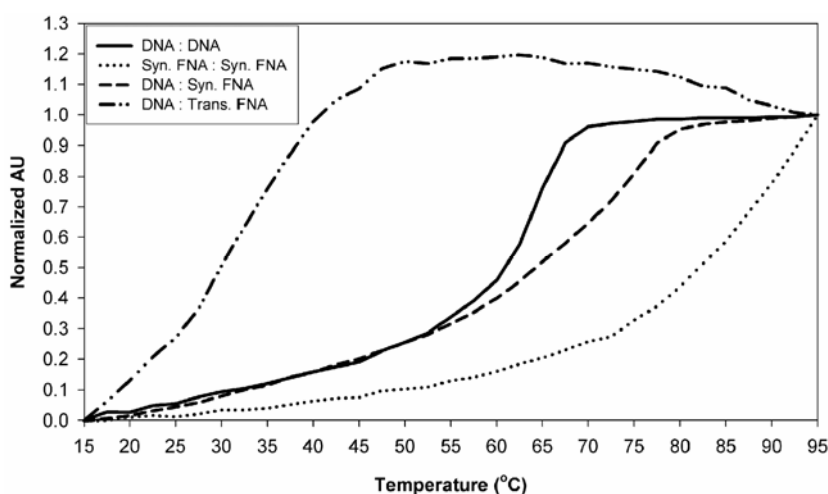


Figure 3.1: Melt-curve analysis of FNA hybridization. Nucleic acid hybridization measured by absorbance as a function of temperature. The black line represents the absorbance measurements at temperatures from 15°C to 95°C normalized to the lowest reading of each sample. The dF/dT of these curves gives a local maximum, representing the T_m of the duplex. The nucleic acid hybridization T_m values are shown as follows: A) DNA/DNA duplex ($T_m = 65^\circ\text{C}$), B) DNA/Synthetic FNA duplex ($T_m = 72.4^\circ\text{C}$), C) Synthetic FNA/Synthetic FNA duplex ($T_m = 89^\circ\text{C}$), and D) DNA/Transcribed FNA duplex ($T_m = 35^\circ\text{C}$).

FNA:FNA duplex T_m of 89°C and a FNA:DNA duplex T_m of 72.4°C . This increase in melting temperature relative to the DNA duplex ($T_m = 65^\circ\text{C}$) agrees with earlier findings

that these modifications act to improve duplex stability (Kawasaki, Casper et al. 1993; Yazbeck, Min et al. 2002). Conversely, when the transcribed FNA is hybridized with its DNA complement, the duplex dissociates at approximately 35°C. This reduction in T_m suggests that transcription products contain base incorporation errors and/or early termination products.

3.3.3 Nuclease Digestions

Products of double-stranded and single-stranded synthetic FNAs following digestion by both DNase I and RNase One® were analyzed by electrophoresis (figure 3.2) to qualitatively evaluate nuclease resistance. Comparison of the digestion products to the associated controls, which were not exposed to RNase One® but

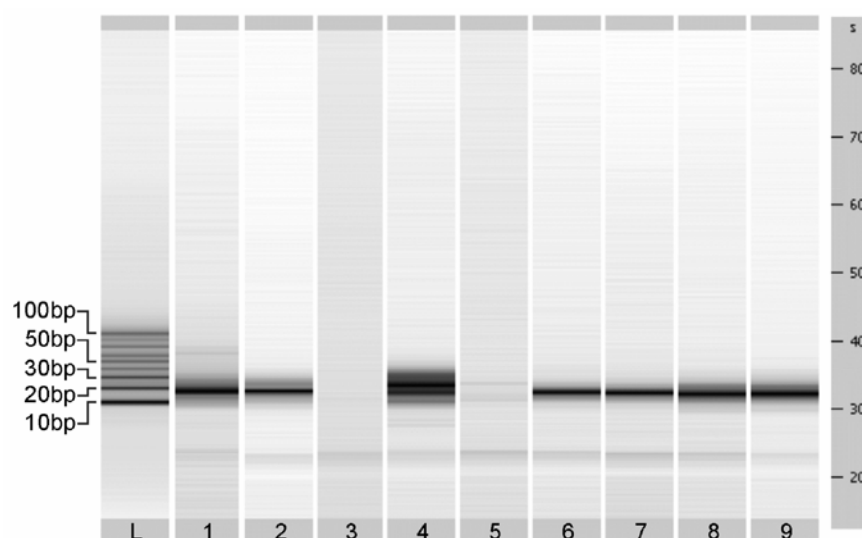


Figure 3.2: Capillary electrophoresis of nuclease treated RNAs and FNAs. All species were originally treated with DNase I following synthesis. Digested products were treated with RNase One® for 18 hours. Control samples were treated to similar buffer and heating conditions in the absence of the ribonuclease. Lane L: 10bp Ladder, Lane 1: single-stranded transcribed FNA, Lane 2: single-stranded RNA control, Lane 3: single-stranded RNA digested, Lane 4: double-stranded RNA control, Lane 5: double-stranded RNA digested, Lane 6: single-stranded FNA control, Lane 7: single-stranded FNA digested, Lane 8: double-stranded FNA control, Lane 9: double-stranded FNA digested

otherwise processed identically to test samples, shows a striking difference between native RNA and fluoro-modified species. Unmodified single-stranded RNAs were completely digested by nuclease treatment. Although duplex RNA is thought to be considerably more resistant to nuclease digestion than single-stranded RNA, these samples show a similar pattern in figure 3.2, which illustrates that siRNA was also completely digested under the aforementioned conditions. Both the single-stranded and the double-stranded digested FNAs were nearly indistinguishable from their processed controls, suggesting that no nuclease degradation occurred.

3.3.4 RNAi of GFP Expression in Cell Cultures

GFP expression levels were normalized to the positive controls in the same experimental plate for both the percent of cells gated and the fluorescence linear mean. The siRNAs designed in this study were effective silencing agents, reducing GFP expression at low concentrations. Native RNA that was synthesized through a similar transcription reaction did not require purification, and knockdown of GFP was evident at the lowest concentration evaluated ($21.8 \pm 3.3\%$ at 3.3 nM siRNA). SiFNAs from custom synthesis were also able to reduce target gene expression at 3.3 nM. Expression of GFP relative to the corresponding positive controls were $35.8 \pm 8.0\%$, $19.9 \pm 3.8\%$, $14.9 \pm 2.8\%$, $11.0 \pm 2.0\%$, and $8.1 \pm 0.8\%$ for 3.3 nM, 13.3 nM, 33.3 nM, 66.7 nM, and 133.3 nM, respectively (figure 3.4 A). These levels were only slightly higher than those for siRNA knockdown, indicating efficient silencing. Preliminary experiments with transcribed siFNAs were used to define a concentration range where treatment effects were responsive to concentration and not due to non-specific toxicity

phenomena. While these initial experiments spanned a concentration range of 3.3 nM to 333.3 nM, the appropriate concentration range for evaluating effective transcribed

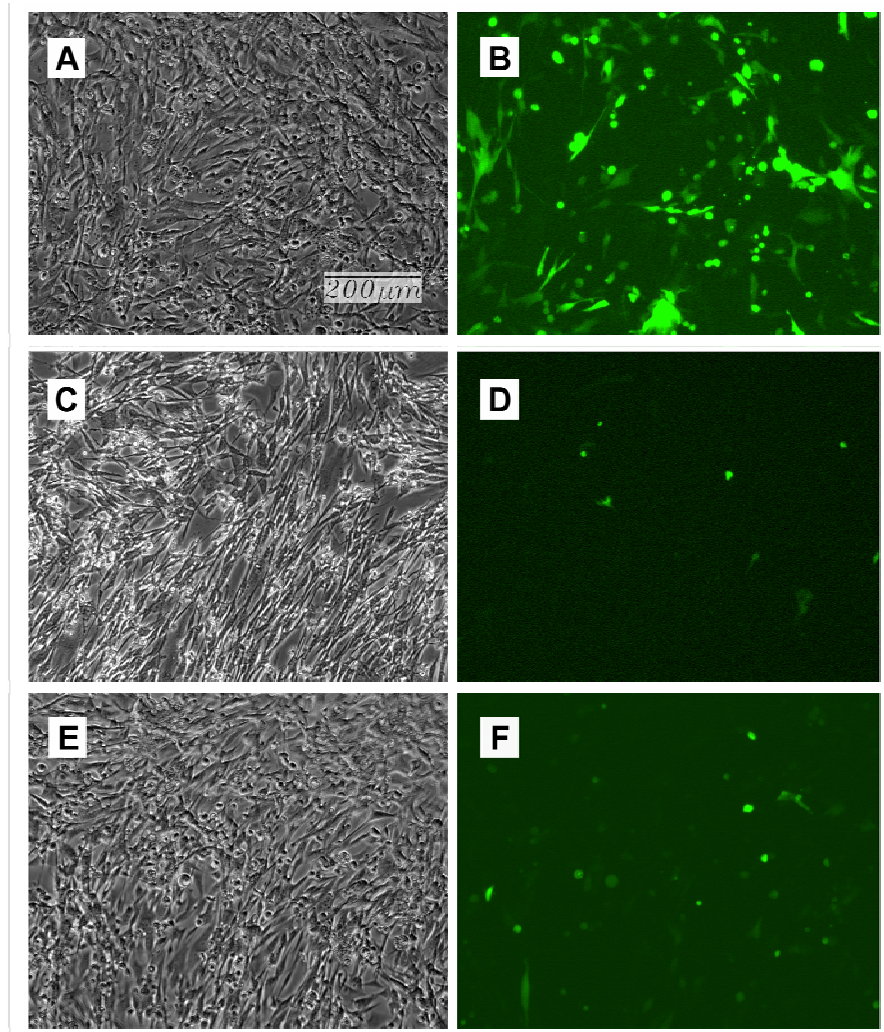


Figure 3.3: Brightfield and fluorescent images microscopy of cell cultures. Transfected BHK-21 cells at 48 hours following transfection: A,B) Positive control, C,D) siRNA knockdown, and E,F) siFNA knockdown.

siFNA mediated GFP suppression was narrowed to 33.3 nM to 133.3 nM. The concentrations in this range were evaluated in triplicate. Since siRNA and synthetic siFNA were effective at lower concentrations, a single set of transcribed siFNA knockdown experiments incorporating the full range from 3.3 nM to 333.3 nM was

included to illustrate trends for comparative analysis. Expression levels relative to positive controls were $70.4 \pm 3.0\%$, $36.2 \pm 2.7\%$, and $24.8 \pm 0.3\%$ following filtered transcribed siFNA knockdown at concentrations of 33.3 nM, 66.7 nM, and 133.3 nM, respectively. The FL1 (530 ± 15 nm) fluorescence linear mean also suggests a reduction in GFP levels following siRNA and siFNA treatment. Figure 3.4B illustrates this reduction and the trend that synthetic siFNA is nearly equivalent to siRNA in reducing total protein content, even at the lowest levels of effector concentration.

Since the enzymatic RNAi pathway can be elicited using single-stranded antisense RNA in mammalian cells (Martinez, Patkaniowska et al. 2002; Schwarz, Hutvagner et al. 2002; Amarzguioui, Holen et al. 2003; Holen, Amarzguioui et al. 2003), antisense FNA was evaluated for its silencing ability in the 33.3 nM to 133.3 nM range. The single-stranded synthetic antisense FNA showed minimal silencing ability, yielding approximately $88.2 \pm 1.3\%$, $81.0 \pm 1.6\%$, and $51.7 \pm 0.8\%$ GFP expression levels for 33.3 nM, 66.7 nM, and 133.3 nM, respectively. The single-stranded transcribed antisense FNA has a similar silencing ability that is indistinguishable from the synthetic FNA, yielding approximately $74.1 \pm 15.7\%$, $84.1 \pm 4.4\%$, and $62.5 \pm 0.7\%$ GFP expression levels for 33.3 nM, 66.7 nM, and 133.3 nM, respectively. In contrast, native antisense RNA exhibited a lower level of GFP activity (approximately 32%) at the lowest concentration studied (3.3nM, not shown) and then maintained between 15-20% expression for the concentrations shown in figure 3.5.

Expression analysis was also supported by decreased mRNA levels following siRNA or siFNA treatment, shown in figure 3.6. The siRNA GFP expression levels

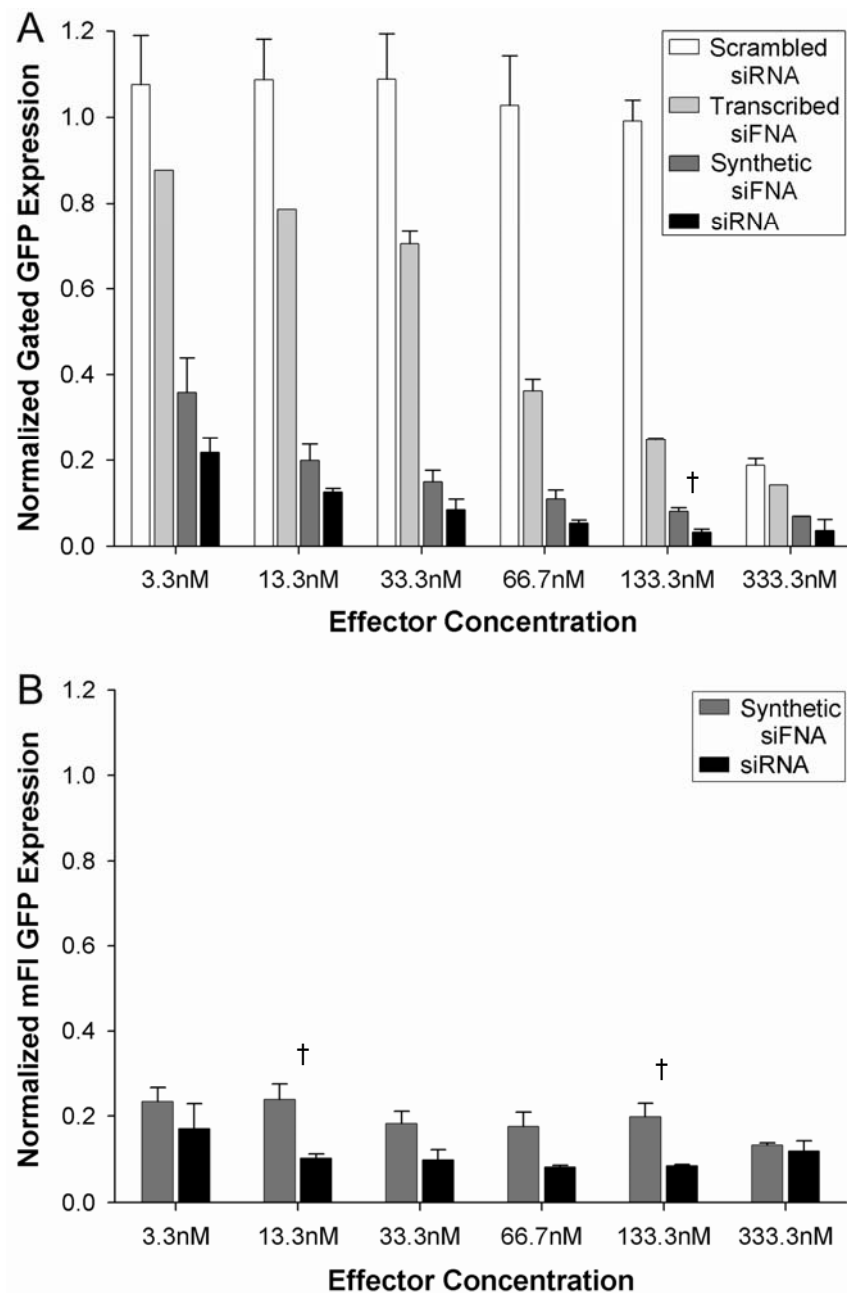


Figure 3.4: RNAi analysis of siRNA and siFNA in cell culture. A: Gated analysis of cell population for GFP expression. Bars from light to dark represent scrambled siRNA, transcribed siFNA, synthetic siFNA, and siRNA. Expression was normalized to the average of GFP-positive controls. B: Cell mFI GFP expression analysis for 30,000 measured events. Grey bars represent synthetic siFNA and black bars represent siRNA. Statistical differences between synthetic siFNA and siRNA for a given concentration are denoted by the symbol † (Student's *t*-test, $p < 0.05$)

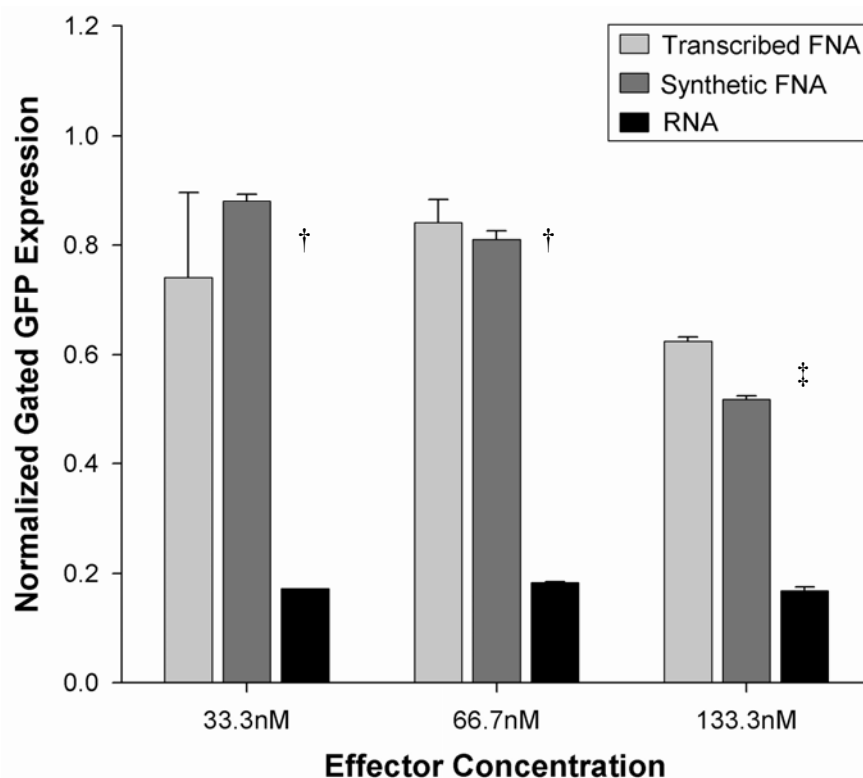


Figure 3.5. RNAi analysis of antisense RNA and FNA in cell culture. FACS fluorescence analysis of GFP expression in cells transfected with antisense siRNA, synthetic antisense siFNA, and transcribed antisense siFNA at various concentrations from light to dark, respectively. Expression was normalized to an average of GFP positive controls. The symbol † denotes a significant differences between antisense FNA and antisense RNA only. The symbol ‡ denotes a significant difference between antisense FNA and antisense RNA and a significant difference between the two antisense FNA populations (Student's *t*-test, $p < 0.05$).

relative to the positive controls measured via flow cytometry were an average of 8.4% for the triplicate samples, while the two siFNA averages were 28.3% and 16.8%. GFP mRNA levels are reported as a ratio to GAPDH message measured in triplicate from the same cDNA sample. The positive control illustrates the variability in transfection efficiency of the pAcGFP, but also that this gene is highly expressed (32.8 ± 18.5

GFP:GAPDH). This ratio is drastically reduced for the siRNA (0.16 ± 0.05 GFP:GAPDH) and siFNA (5.77 ± 1.61 and 3.36 ± 1.77 GFP:GAPDH) samples.

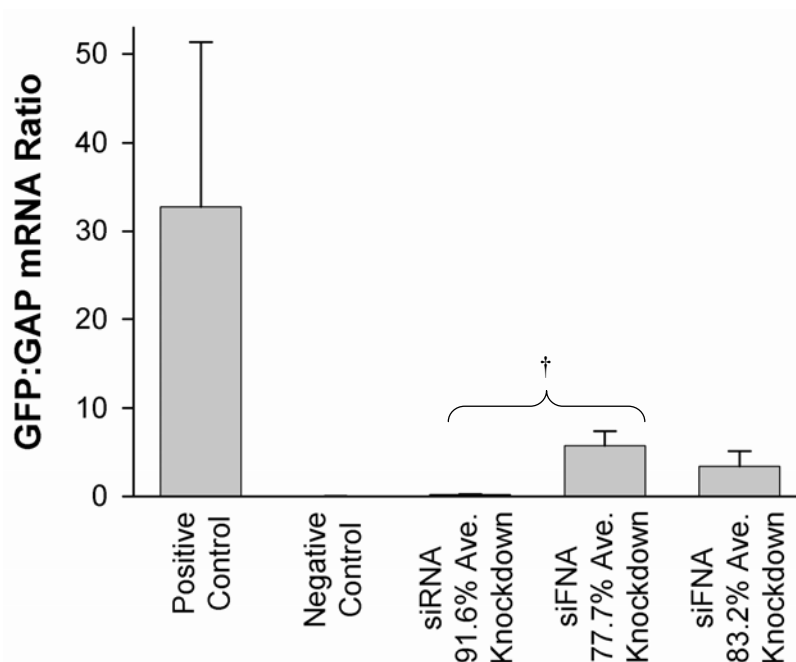


Figure 3.6: Semiquantitative PCR analysis of RNAi knockdown of GFP vs GAPDH. Levels of mRNA are reported as a ratio of GAPDH to GFP. Each category shown as an individual bar represents three separate cellular experiments, which were each measured in triplicate. The siRNA samples achieved an average GFP knockdown of 91.6%. The two concentrations of synthetic siFNAs evaluated reduced GFP expression levels at averages of 77.7% and 83.2%. The symbol † denotes a significant difference between the siRNA and 77.7% siFNA knockdown (Student's *t*-test, $p < 0.05$). No statistical difference was observed between the siRNA and 83.2% siFNA knockdown or between the two siFNA populations.

3.4 Discussion

In this investigation fully-modified 2'-deoxy-2'-fluoro nucleic acids were generated through transcription and solid phase synthesis, evaluated for their nuclease resistance, and tested for knockdown activity in cell culture. FNA effectively induced gene silencing in the duplex siFNA form but is much less effective as an antisense

single-stranded oligonucleotide. The findings presented here are in agreement with earlier works using partially modified nucleic acids. The ability to incorporate these modifications using standard synthesis techniques allows for the additional inclusion of other types of alterations that may aid in drug delivery. The combined results suggest that incorporation of the 2'-fluoro modification may be a useful approach to achieve improved stability of RNAi-based therapeutics without sacrificing potency.

3.4.1 FNA Generation

FNAs for RNAi were successfully generated through both solid phase synthesis and transcription. However, the quality of the product generated from each method is markedly different. Synthetic FNAs were shown to be the proper size through mass spectroscopy and PAGE separation. Elevated melting temperatures of these products illustrated strong association with the target sequence, indicating both that FNAs form more stable duplexes and that base incorporation errors are not likely in the synthetic products. The observed increase in T_m values that occur due to the 2'F substitution are in agreement with previous work that evaluated partially and fully modified oligonucleotides. The transcribed FNAs required further purification using Microcon YM3 spin filters to remove any fragments under 10 nucleotides in length. Approximately 70% of the product was not recovered, which suggests that a large portion of the FNAs were shorter than the desired 21 nucleotides due to early termination. This agrees with early characterizations of the Y639F T7 polymerase regarding the abortive stage of polymerization, where it was found that the wild-type and the mutant polymerase generate a large amount of early termination product in the

2-8nt range (Sousa and Padilla 1995). Despite that the Y639F polymerase is able to initiate DNA and RNA primer extension to a limited extent (Sousa and Padilla 1995), extending the reaction to 48 hours did not yield a higher percentage of full length FNA transcripts. Melting curve data reveals that the synthetic products have very different hybridization behavior than the transcribed FNAs based on the difference in the T_m values. The higher melting temperature of the synthetic FNAs suggests that custom synthesis has a much lower error incorporation rate than the transcription method. While the error incorporation rate of 2-F-NTPs is not known, Y639F T7 polymerase does exhibit miscoding of rNTPs at a similar rate to the wild-type polymerase (Sousa and Padilla 1995). Consequently, transcription base-coupling errors are expected and will have a minimum incorporation rate that is equivalent to the wild-type polymerase. Homopolymer assays to determine the error-rate of the mutant polymerase showed that the incorporation of a complementary NTP was 184-fold greater than that for non-complementary NTPs on a poly(dC) template (Sousa and Padilla 1995). Relative to the poly(dC) template non-complementary base incorporation was approximately 5-fold higher using a poly(dT) template (Sousa and Padilla 1995). Thus errors in base incorporation would be expected at relatively high frequency, even if unmodified nucleotides were used. Despite the higher inaccuracy rate, the transcribed FNAs were still able to elicit RNAi. As a result, the products are still useful and possess appreciable benefits over custom synthesis techniques. Although currently the cost to generate a given amount of FNA product is nearly equivalent for the two techniques, enzymatic generation offers greater flexibility than custom synthesis. Specifically, transcription allows for the generation of several different siFNAs instead of only one

sequence. This provides a technique for siFNA screening, the ability knockdown of an array of targets, or the ability to validate the viability of a siFNA sequence before pursuing custom synthesis.

3.4.2 Digestion Assays

Both the single-stranded and the double-stranded FNAs were resistant to enzymatic digestion using DNase I and RNase One®, while both forms of unmodified RNA were degraded completely under the same conditions. While this does not indicate invulnerability to all enzymatic degradation pathways, it does illustrate improved nuclease resistance over unmodified RNA and DNA. Previous work with pyrimidine 2'-deoxy 2'fluoro modified RNA has also shown improved stability in cell lysate and plasma (Layzer, McCaffrey et al. 2004). However, since pyrimidine only fluoro-modified nucleic acids still contain 2'-hydroxyls, they may still be susceptible to sugar-specific endonuclease digestion. Some evidence of substrate degradation was observed in pyrimidine-only 2'F modified RNA that was incubated for 60 minutes in cell lysate (Chiu and Rana). Additionally, partially-modified siRNAs did not extend target gene knockdown relative to the unmodified species (Layzer, McCaffrey et al. 2004). Incorporating fluorine halides on every nucleotide could eliminate all possibility of 2'-hydroxyl-mediated enzymatic digestion or degradation through spontaneous intramolecular hydrolysis and may further improve the stability of single- and double-stranded siRNAs. The current GFP expression system in BHK cells is not conducive to long-term suppression analysis due to the fact that the effector is diluted in the rapidly proliferating cells. Future studies will explore the silencing duration of siFNAs

using a stably-transfected transient or inducible reporter gene in a system more amenable to long-term gene expression analysis.

3.4.3 RNAi of GFP Expression in Cell Cultures

It was previously shown that RNAi does not require a 2'-hydroxyl to be present in the nucleic acid species, but it requires an unimpeded minor groove and an A-type helical structure (Chiu and Rana 2003). Since fluorine is small enough to fit in the minor groove and the electronegativity of the halide reinforces an A-type helix structure through a preferred sugar pucker conformation (Guschlbauer and Jankowski 1980; Chiu and Rana 2003), fluoro-modifications are particularly well-tolerated by the RNAi pathway. Our results indicate that siFNA can induce RNAi and the silencing efficiency is nearly equivalent to the unmodified siRNA species. In fact, siRNA and siFNA efficacy were only significantly different at the 66.7 nM and 133.3 nM concentrations (Student's *t-test*, $p < 0.05$). These results correlate well with observations regarding RNAi activity of partially or pyrimidine only 2'-F-modified siRNAs, reported elsewhere (Chiu and Rana 2003; Layzer, McCaffrey et al. 2004). One potential reason for the slight decrease in knockdown potency is that FNAs may form more stable duplexes relative to RNAs. This could result in a duplex that is less efficiently unwound by RISC. The melting properties of the synthetic fluorinated oligonucleotide duplexes suggest that this hypothesis may have merit. It is likely that the RNAi pathway is able to overcome this obstacle since the dissociation of siRNA is an ATP-driven process. Additionally, it was observed through the course of this

investigation that minor variations in the initial siFNA hybridization had a noticeable effect on the silencing outcome.

One concern relating to the observed elevated melting temperatures of FNAs is the potential loss of may loose some level of target specificity. Kawasaki and colleagues gave a detailed description of 2'F modifications with respect to increased T_m and base pair specificity (Kawasaki, Casper et al. 1993). In essence, they demonstrate that uniformly- modified NAs maintain base-specificity relative to the perfect complement. Since the 2'F modification results in a large T_m increase, the annealing temperature may still be elevated with a single nucleotide mismatch point-mutation. This could lead to off-target hybridization at physiological temperatures. However it is doubtful that even one or two mismatches in a 21-mer oligonucleotide would result in better complementarity to an off-target mRNA within the transcriptome that has amenable secondary structure for hybridization. Because the RISC machinery must interact with the duplex siRNA and the antisense RNA/mRNA complement along the silencing pathway, RNAi might still be disrupted by a single mismatch within a siFNA molecule. Additionally, the improved duplex stability may also allow the use of small interfering duplexes with a lower GC content to be used for RNAi. In this study, no changes to cellular morphology, growth rate or housekeeping gene expression were observed in response to siFNA treatment. This suggests that if off-target silencing was occurring, the potential effect on the global expression profile was not toxic for the sequence studied. Future endeavors exploring off-target effects could test a series of mismatches at several locations on the sense and antisense strands of the different effector sequences, and include more global measures of gene

expression such as RT-PCR of multiple candidate off-targets or comprehensive microarray analysis (Jackson, Burchard et al. 2006).

Transcribed FNA products displayed the least amount of silencing ability, which is likely due to malformed siFNAs that arise from either early termination products or more likely polymerase base incorporation errors. In the future, it may be possible to improve the transcription efficiency by using a dual-mutated polymerase which has been used to successfully incorporate 2'-O-methyl modified NTPs into full-length transcripts (Padilla and Sousa 2002). Knockdown at higher concentrations of siFNA were not evaluated due to potential transfection lipid toxicities. The upper limit was determined in mock RNAi experiments using scrambled sequences over an extended range of concentrations. At the 333.3 nM concentration, GFP expression was decreased in response to the scrambled siRNAs, indicating nonspecific effects. Additionally, exposing cells to micromolar concentrations of siFNA in the absence of a cationic lipid showed no signs of toxicity nor GFP reduction (data not shown). Therefore, the observed decrease in GFP mRNA and protein expression by siFNA treatment below 333.3 nM is believed to be the result of targeted gene knockdown.

Despite the typically rigid adherence to the characteristic siRNA structure resulting from the processing of dsRNA by Dicer, recent work has demonstrated that RNAi can be elicited by single-stranded antisense siRNAs (Martinez, Patkaniowska et al. 2002; Schwarz, Hutvagner et al. 2002; Amarzguioui, Holen et al. 2003; Holen, Amarzguioui et al. 2003). Although the pathway of RNAi using single-stranded homologues is not well-understood, evidence suggests that at least part of the pathway is conserved among the duplex and antisense siRNAs (Holen, Amarzguioui et

al. 2003). It has also been shown that antisense siRNAs are incorporated into RISC, resulting in targeted RNA cleavage in mammalian cell extracts (Martinez, Patkaniowska et al. 2002; Schwarz, Hutvagner et al. 2002) and in cell culture (Holen, Amarzguioui et al. 2003). In contrast with the apparent similarities, antisense siRNA shows lower activity and reaches peak levels earlier than compared to duplex siRNA (Holen, Amarzguioui et al. 2003). Duplex siRNA requires unwinding while still associated with RISC, which may explain the delayed onset of gene silencing through this RNAi pathway. The transient nature of the single-stranded knockdown could be partially explained by its vulnerability to ribonucleases. Therefore, nuclease-resistant modified antisense siRNA may have potential benefits over native unmodified antisense siRNA. Fully fluorinated nucleic acids were initially thought to have ideal properties to achieve single-stranded knockdown while improving stability of the effector molecule.

Because single-stranded antisense RNA is known to induce RNAi, antisense FNA was also evaluated for its silencing ability. Given that this method does not require delivery of a duplex knockdown agent, the negative affects of early termination are thought to be lessened. Surprisingly, the FNA antisense product shows no significant silencing ability until higher concentration levels are reached, and in contrast to RNA, antisense FNA silencing ability is greatly reduced. Even though misincorporation errors may be present in the transcribed FNAs, antisense products may still hybridize to the target mRNA due to the increases the T_m by the 2'F substitution. This FNA:RNA duplex with potential mismatch bulges may still participate in translational arrest, which could explain the lack of difference observed between the

transcribed and synthetic antisense FNAs shown in figure 3.5. For the siFNA knockdown, these base misincorporation errors may hinder the ability for RISC to recognize the duplex form of the transcribed product duplexes, explaining the larger difference in silencing ability between transcribed and synthetic FNAs shown in figure 3.4. Since it is known that 2'-FNA:RNA duplexes do not induce RNase H1 mediated cleavage of the RNA strand (Yazbeck, Min et al. 2002), the slight reduction in GFP expression caused by the single-stranded antisense products is likely due to minimal levels of antisense translational interruption. 2'-Flouro substitutions in nucleic have been shown to increase the melting temperature when hybridized to either DNA or RNA complements (Kawasaki, Casper et al. 1993; Yazbeck, Min et al. 2002), and in conjunction with improved stability, this supports the idea that some physical disruption of protein synthesis in the cytoplasm may be possible. However, since single-stranded antisense FNAs are inefficient in reducing GFP expression relative to siFNAs, the mechanism of knockdown by duplex siFNAs is not likely to be simple antisense translational arrest or FNA toxicity. Rather, these results, in conjunction with the finding that FNA:RNA duplexes do not act as substrates for RNase H1, suggest that siFNA GFP knockdown is mediated through the RNAi pathway.

3.5 Conclusions and Future Works

RNAi has quickly become one of the primary methods of genetic knockdown and has experienced a rapid expansion in the number of exploited applications and synthetic modifications. In addition to its utility for a wide array of applications conserved over a variety of organisms, the RNAi mechanism has proven to be

remarkably complex. Previous works have illustrated the flexibility of RNAi to tolerate certain chemical modifications into siRNA. By maintaining efficacy while imparting other potentially beneficial properties, such as nuclease resistance and improved cellular delivery, the possibility of using RNAi for therapeutic applications is within reach. In fact, pharmaceutical companies have begun incorporating these types of modifications into potential siRNA drugs, and some of these chemically-modified siRNA therapeutic agents have already reached clinical trials (Sirna Therapeutics, Alnylam, Acuity (Bourzac 2007)). Previous works which have incorporated halides in the 2'-region of nucleic acids were limited due to the scarcity of modified guanine and adenosine residues. Therefore this study investigated the efficacy of RNAi knockdown using fully-fluorinated nucleic acids as small interfering RNAs. Despite the fact that phosphoramidites which contain these modifications are becoming available with increasing frequency, the custom synthesis of fully-fluorinated strands is still cost-prohibitive. For this reason, we also investigated the ability to generate FNAs through transcription using a mutated polymerase. While the transcription technique does not improve the overall cost effectiveness of FNA generation, it adds flexibility to produce many siFNAs of distinctive sequences. The FNAs showed improved enzymatic stability in the presence of nucleases as demonstrated by a digestion assay. It has also been shown here that fully-fluorinated nucleic acids can induce targeted gene knockdown. Since the antisense FNA strand is much less potent than the duplex form, the decreased genetic expression resulting from siFNA introduction is likely due to enzyme mediated RNAi rather than simple translational blockade. Conversely, this result suggests that single-stranded FNAs are not recognized by RISC due to the lack

of antisense silencing. This may provide some insight into the recognition and binding properties associated with RISC. Synthetic siFNAs resulted in more efficient silencing than the corresponding transcribed species. This is likely due to base-coupling inefficiencies during transcription and/or early termination of the desired products. Melting curve analysis supports the suggestion that transcribed FNAs contain errors. It is possible that improvements in the transcription conditions or the use of a less error prone polymerase may improve the efficacy and yield of this method.

CHAPTER 4:

Caging 2'-Fluoro Nucleic Acids for RNAi

4.1 Introduction

RNA interference (RNAi) refers to the post-transcriptional silencing of protein expression that is initiated by specific small regulatory RNA molecules (reviewed by (Tomari and Zamore 2005)). Several forms of these molecules have RNAi activity including small-interfering RNAs (siRNAs), small-hairpin RNAs (shRNAs), or microRNAs (miRNAs), where their classification depends on their origin and specific structure (Elbashir, Lendeckel et al. 2001; Matzke and Matzke 2003). RNAi has gained attention in laboratory and therapeutic settings because siRNAs are generally more potent regulators of gene expression than traditional antisense compounds (Grunweller, Wyszko et al. 2003). Although siRNAs are highly effective, RNA is relatively unstable and susceptible to enzymatic digestion. In order to develop useful RNAi drugs, the siRNA must be efficiently delivered either systemically or directly to the intended tissue, exhibit specific knockdown of the target gene, and maximize the duration of silencing. In the common effort of expanding the utility of siRNAs, many have explored the use of chemical modifications that optimize RNA lipophilicity, increase duplex stability, or impart nuclease resistance to achieve these aims. Although improving pharmacological efficacy through chemical modification is important for the realization of RNAi therapeutics, less progress has been made with respect to spatial and temporal control over gene silencing. One technique to control RNAi is to use a chemically-inducible endogenous expression of hairpin RNA (Gossen and Bujard 1995; Gossen, Freundlieb et al. 1995; No, Yao et al. 1996; Gupta, Schoer

et al. 2004). While this approach does add a level of temporal control, light-based triggers are potentially much faster and may allow for spatial resolution on the nanometer scale (Betzig, Patterson et al. 2006). One way to achieve photo-control is to introduce a temporary chemical modification which blocks silencing activity and can be removed with an external trigger. Two research groups have recently explored using photolabile protection groups in siRNA toward spatial, temporal, and dosing control of gene knockdown using light (Shah, Rangarajan et al. 2005; Nguyen, Chavli et al. 2006; Shah and Friedman 2007). Coupling this light-activation technique with chemically-stabilized siRNAs may allow RNAi spatiotemporal targeting in more complex biological systems.

The use of photolabile protection groups for the light induction of a biological system was first described by Kaplan in 1978 as caging (Kaplan, Forbush et al. 1978). Caged nucleic acids (NAs) have been used for a variety of applications [reviewed by (Monroe and Haselton 2004; Mayer and Heckel 2006; Ellis-Davies 2007; Tang and Dmochowski 2007; Young and Deiters 2007)]. Photo-caged RNA has been used to control ribozyme activity through sugar caging (Chaulk and MacMillan 1998; Chaulk and MacMillan 2007), RNA folding through base caging (Hobartner and Silverman 2005), as well as mRNA translation (Ando, Furuta et al. 2001; Ando, Furuta et al. 2004) and siRNA silencing through phosphate caging (Shah, Rangarajan et al. 2005; Nguyen, Chavli et al. 2006; Shah and Friedman 2007). However, phosphate caging of RNAs may lead to unstable products due to the potential for self-mediated hydrolysis of the phosphotriester by the neighboring 2'-hydroxyl in aqueous solution (Breslow and Xu). Additionally, multiple attachment sites of cage groups to siRNAs may be necessary to achieve full inactivation.

For practical applications of caged RNAi effectors, the combination of chemical-stabilization and photoprotection might be advantageous. Chemical modifications of the sugar-phosphate backbone of RNAi effectors are widely used to increase resistance of the RNA to hydrolytic and enzymatic degradation (reviewed by (Manoharan 2004; Zhang, Du et al. 2006)). In addition to nuclease resistance, some of these modifications maintain or improve other desired characteristics such as preference for a certain helix formation or increased thermal stability (Kurreck 2003; Manoharan 2004). To achieve RNAi that meets all the desired characteristics, many types of modified siRNAs have been evaluated for their ability to elicit target mRNA degradation and subsequent gene knockdown. These studies have yielded highly variable results between different modification types and sometimes even among siRNAs of differing sequence that have the same chemical modification. Of all the modifications tested, 2'-deoxy-2'-fluoro modifications seem to be the best-tolerated alteration for maintaining silencing activity. Partially fluoro-modified siRNA in which the 2'-F substitutions are limited to pyrimidine moieties are common in the literature, so to achieve completely modified siRNAs other chemical substitutions are sometimes used in combination with the 2'-halide (Braasch, Jensen et al. 2003; Chiu and Rana 2003; Harborth, Elbashir et al. 2003; Layzer, McCaffrey et al. 2004; Soutschek, Akinc et al. 2004; Allerson, Sioufi et al. 2005; Morrissey, Blanchard et al.). Recent results from our group indicate that fully 2'-deoxy-2'-fluoro modified siRNA (siFNA) induces RNAi with similar activity to unmodified RNA (chapter 2). Despite the advances made in chemical stability of siRNA, RNAi is still limited with respect to temporal and spatial regulation.

In this study, statistical (non site-specific) caging of the phosphate backbone was performed on a chemically stabilized RNAi effector, using 1-(4,5-dimethoxy-2-nitrophenyl)diazoethane (DMNPE). To allow the random attachment of multiple caging groups to a single siRNA molecule, the following chapter presents a combination of RNA 2'-OH chemical modification with the random attachment of DMNPE to achieve siRNA with multiple sites caged. The nucleic acid has been fully substituted with 2'-deoxy-2'-fluoro modified nucleotides to eliminate the possibility of 2'-OH mediated self hydrolysis of the phosphotriester in aqueous solution. These caged species were evaluated in mammalian cell culture and developing zebrafish embryos for light-induced RNAi activity.

4.2 Materials and Methods

4.2.1 2'-Deoxy-2'-Fluoro Nucleic Acid Synthesis and Caging

Synthetic sense (5'-GGUGAACUUCAAGAUCGCUU-3') and antisense (5'-GCGGAUCAUGAAGUU-CACCUU-3') 2'-deoxy-2'-fluoro nucleic acids were generated through solid phase synthesis as previously described (chapter 3), where the resulting chemically-modified siFNAs effectively silenced GFP transgene expression through RNAi. Each FNA strand was suspended in 100 μ L of 10 mmol Bis-Tris buffer (pH 5.5) at 1 μ g/ μ L, (150 μ M). 4,5-Dimethoxy-2-nitroacetophenone hydrazone precursor (5 mg, 22 μ mol) (Molecular Probes, Inc., Eugene, OR) was oxidized with MnO₂ (50 mg, 557 μ mol) in 1.0 mL acetonitrile at room temperature under agitation for 20 minutes. MnO₂ was removed by filtration through an acetonitrile-wetted Celite (Sigma Aldrich, St. Louis, MO) syringe filter. The activated diazo-cage solution was mixed with the FNA solution to achieve a 2:1 acetonitrile:aqueous buffer and 300 molar equivalents of the

active diazo compound. A process control sample without nucleic acid and a process control sample without active caging compound were simultaneously run with experimental samples in order to rule out downstream effects resulting from caging reaction processing. The reaction solutions were agitated at 4°C for 18 hours. Excess cage compound was removed by size exclusion chromatography through a gravity column of preswollen (1:2 acetonitrile:water) solvent-resistant LH-20 sephadex (GE Healthcare Bio-Sciences Corp., Piscataway, NJ). The product was further purified by 4 X 500 µL washes through a YM-3 nitrocellulose spin filter (Millipore, Billerica, MA) to remove any residual cage compound, buffer, and organic solvent. The products were dried, and resuspended in TE buffer (10 mM Tris, 1mM EDTA, pH 8.0) or nuclease free water. All products were stored at 4°C and protected from light.

4.2.2 Evaluation of Caged Nucleic Acids *In Vitro*

FNA concentration and degree of cage attachment was determined through spectrophotometric analysis. Absorbance spectra of the caged products were measured from 230 nm to 500 nm. The molar concentrations of the covalently bound cage sample and nucleic acid were calculated from the absorbance of incident light at 260 nm and 355 nm. Reverse phase high performance liquid chromatography (RP-HPLC) was used to evaluate the control, caged, and photo-released FNAs. Each sample type was injected (1.25 µg, 25 µL) in HPLC-grade water into a C18 analytical column, ODS2 spherisorb 5 µm (Waters Corporation, Milford, MA). Separation was obtained using a gradient of 1% TEAA in HPLC water to 1% TEAA in 80% acetonitrile over 20 minutes.

4.2.3 Nuclease Digestions

Bal-31 nuclease (Promega Corporation, Madison, WI) was used to evaluate nuclease resistance of control and caged FNAs. Final digestion conditions were as follows: 2.5 units Bal-31 nuclease, 2 µg 21mer FNA samples, 20 mM Tris-HCl (pH 8.1), 12.5 mM CaCl₂, 12.5 mM MgCl₂, 600 mM NaCl, 6.25 mM EDTA, 0.625% (v/v) glycerol, 50 µL total reaction volume at 30°C. At various time intervals, 5 µL volumes were removed and were heated to 80°C for 10mins to halt digestion and immediately frozen at -20°C for subsequent analysis. These fractions were collected and inactivated at 0, 5, 10, 20, 40, 80, and 160 minute discrete time intervals. Digestion of each FNA sample was evaluated via PAGE using 15% polyacrylamide precast gel (BioRad, Hercules, CA, USA) stained with Sybr Gold (Molecular Probes, Inc., Eugene, OR). Band densitometry analysis was performed using Metaview software (Universal Imaging Corporation, West Chester, PA). Briefly, regions of equal size were drawn around each band and band density was recorded as intensity integration over the area. In the cases where no bands were visible, regions were drawn over the expected location of the bands. Background intensities of each gel were measured and subtracted from the band measurements and each lane was then normalized to the undigested product.

4.2.4 Photoexposure

A GreenSpot photocuring system (American Ultraviolet, Lebanon, IN) was used for exposing nucleic acids, cell cultures, and zebrafish embryos to UVA light doses. Light was delivered through an inverted liquid-filled light guide for bottom-up

exposure of cell-culture wells or microcentrifuge tubes. Infrared, UVC, and UVB light was filtered out using a short bandpass filter (SWP-2502U-400) and an IR-filter (KG-2-IR) (Lambda Research Optics, Costa Mesa, CA). Delivered light had a maximum output at 365 ± 8 nm with a fluence rate of 0.705 W/cm^2 at 4.5 cm or 0.950 W/cm^2 at 3.2 cm (Forman, Dietrich et al. 2007). Total light delivered was 40 J/cm^2 for cell cultures and zebrafish and 200 J/cm^2 for nucleic acid solutions. Adjacent wells in a BD Falcon™ 12-well tissue culture plate (BD Bioscience, Franklin Lakes, NJ) were protected from light by using an aluminum mask with a 2.25 cm diameter opening.

4.2.5 Cell Culture and Transfection

BHK-21 (Baby Hamster Kidney) cells were cultured in reduced serum Dulbecco's Modified Eagle's Medium (DMEM-RS) (HyClone, Logan, UT) supplemented with 3% heat inactivated fetal bovine serum (HyClone, Logan, UT) at 37°C under 5% CO_2 in a humidified chamber and regularly passaged at subconfluence. Cells were seeded on 12-well plates 18 hours prior to transfection at approximately 20K cells/cm^2 . Cotransfections of pAcGFP-N1 (Clontech, Carlsbad, CA) and process control or caged siFNAs were mediated with lipofectamine (Invitrogen, Carlsbad, CA). Transfection mixtures containing $0.1 \mu\text{g}$ of pAcGFP-N1, 3 pmol siFNA sample, and lipid (3:1 ratio of lipid to total nucleic acid) were complexed in $100 \mu\text{L}$ of reduced protein medium (OPTI-MEM®, Invitrogen, Carlsbad, CA) and incubated at room temperature for 30 minutes. Cells were rinsed with $500 \mu\text{L}$ of OPTI-MEM prior to transfection, and the transfection mixtures diluted in $500 \mu\text{L}$ of OPTI-MEM giving final siFNA concentrations of 5 nM in $600 \mu\text{L}$ and were added to the appropriate wells. The

cells were incubated at 37°C under 5% CO₂ for 6 hours, followed by return to normal growth media. For light exposure of cell cultures, media was replaced with OPTI-MEM and cells were photoexposed at 4 hours after the end of the transfection period. To ensure that photoexposure did not have an effect on GFP expression in cell culture, GFP positive controls and siFNA knockdown controls were exposed 5, 10, 20, 40, 60, 80 J/cm² to determine thresholds to UVA light. After exposure, OPTIMEM was replaced with cell culture media and cells harvested at 48 hour post-transfection for expression analysis.

4.2.6 Flow Cytometry RNAi Analysis

Transfected and control cell culture samples were harvested and fixed in PBS suspension with 0.5% paraformaldehyde prior to GFP expression analysis via flow cytometry. GFP fluorescence was collected at 530±15 nm (FL1), and cellular auto-fluorescence was collected at a wavelength greater than or equal to 650 nm (FL3) on a fluorescence activated cell sorter (FASC-Scan) cytometer (Becton Dickinson, San Jose, CA) equipped with 488 nm excitation light source. For each culture sample, a maximum of 30,000 cellular events were collected. Intact cells were gated on a FSC (forward angle light scatter) versus SSC (90 degrees light scatter) dot plot. An FL1 versus an FL3 display of a GFP-negative control was gated and applied to all samples and analyzed to yield a percentage of cell events in the GFP-positive region. This GFP-positive percentage for each sample was normalized to an average of GFP-positive controls for the specific set of experiments and expressed as a mean value ± standard error

4.2.7 Zebrafish Embryo RNAi

Wild-type zebrafish purchased from EkkWill Waterlife Resources were kept at standard laboratory conditions (28°C on a 14 hr light: 10 hr dark photo-period in a recirculating system). Embryos were collected from group spawns, and rinsed several times in embryo medium (Westerfield 2000) prior to microinjection procedures. Microinjection of zebrafish embryos was carried out as previously described (Westerfield 2000) to deliver plasmid and control or caged siFNAs. Injection needles were pulled on a Flaming/Brown P-97 micropipette puller using fire-polished borosilicate glass capillaries with filament (Sutter Instrument Co., Novato, CA). Briefly, a volume of 1-3 nL of a solution containing GFP plasmids (125 ng/μL), process control or caged siFNAs (250 ng/μL), Alexa Fluor 546-conjugated 10,000 MW dextran tracking dye (Molecular Probes, Eugene, OR), and 0.1% phenol red was injected into the embryo by forcing the pipette through the chorion and the yolk cell and then injected into the yolk stream at the 1- to 4-cell stage. After injection, embryos were isolated in a transgenic containment facility and incubated at 28°C until photoactivated at 6-7 hpf. Embryos were exposed to UVA in 35-mm cell culture dishes containing 1 mL of embryo medium. Previous UVA dose-response curves (LD50 of UVA in zebrafish ~800 J/cm²) in zebrafish embryos indicate their very high tolerance to UVA exposure, indicating the safety of these photo-activating light regimens (Dong, Svoboda et al. 2007). After the photoactivation, the embryos were raised to 27-30 hpf and further analyzed at the behavioral level. Prior to 27 hpf, mortality and malformation identifications were used as initial evaluation criteria for UV or siFNA induced toxicity. At 27 hpf, the touch response behavior of each embryo was assayed. Those exhibiting

a normal touch response were fixed in 4% paraformaldehyde for three hours at room temperature.

After fixation, individual embryos were placed in a single drop of PBST on 1-mm-thick slides, coverslipped, and viewed with a Zeiss MOT II inverted microscope with a 20X objective equipped with GFP and rhodamine filter cubes. Embryos were first viewed in bright-field with DIC optics to get a clear view of the trunk region or brain region. Once a crisp view was obtained with DIC optics, the brain region, as well as rostral and caudal spinal cords were imaged under epi-fluorescence utilizing the GFP filter set. Images of the GFP expression were acquired using an ORCA-ER digital camera (Hamamatsu Inc, Japan). For each experiment, a minimum exposure setting required to obtain a non-saturating image of GFP expression in control embryos was first determined. For every experiment, after the control images were acquired, images of all the subsequent experimental embryos were acquired using the very same exposure times as controls. To confirm that the embryos were indeed successfully injected with the various plasmids and molecular reagents, the distribution of the 10,000 MW dextran was visualized. Control embryos and experimental embryos that did not exhibit even dextran distribution within the embryo were excluded from analysis.

4.3 Results

4.3.1 Spectrophotometric Evaluation of Caged FNA

Absorbance spectroscopy was used to determine level of cage attachment to oligonucleotides. Extinction coefficients for attached cage compounds (1-(4,5-

dimethoxy-2-nitrophenyl)ethyl phosphoesters) were determined for 260nm ($\epsilon_{260} = 3064 \text{ M}^{-1}\text{cm}^{-1}$) and 355nm ($\epsilon_{355} = 4512 \text{ M}^{-1}\text{cm}^{-1}$) and were consistent with previously reported values (Walker, Reid et al. 1988; Ghosn, Haselton et al. 2005). These values, accompanied with the known spectral properties of nucleic acids, enabled the determination of molar concentrations of the cage compound and nucleic acid in a sample to give a measure of cage attachment. A representative spectrum for a caged 2'-fluoro-substituted nucleic acid is shown in Figure 4.1. Caged FNAs exhibit a

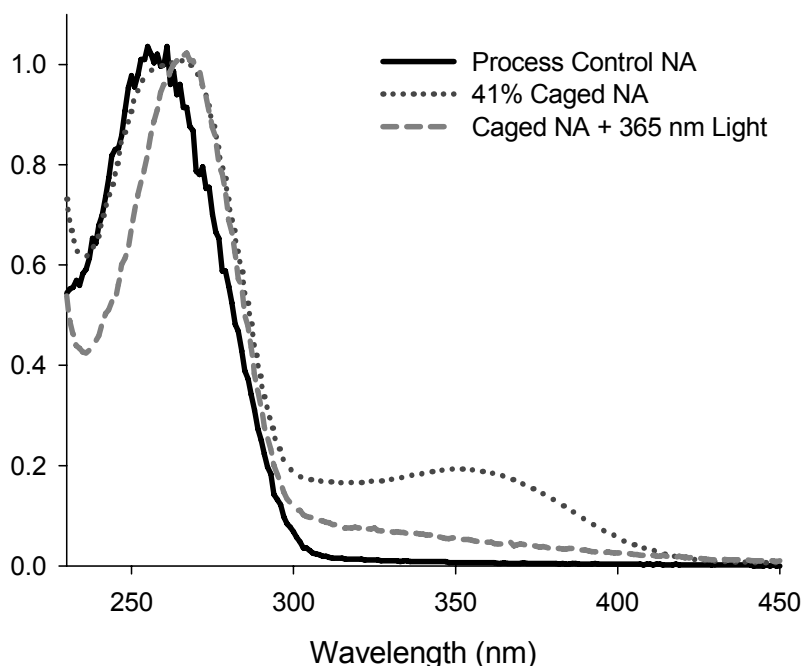


Figure 4.1: Spectrophotometric analysis of FNAs. Processed control (—), caged (— -), and photoexposed caged (.....) NAs are overlaid. All samples were processed in parallel. Following photoexposure, released cage was removed from the solution via filtration.

characteristic absorbance plateau at 355 nm in addition to an absorbance peak at 260 nm. Following UVA light exposure and purification, the photocleaved product resembles the control (non-caged) FNA. The level of cage attachment could be altered by adjusting the concentration of the diazo-reactant relative to the nucleic acid or increasing the reaction duration. Oligonucleotide products with an average number

of cage groups of approximately 1, 3, 4, and 8 to 9 were generated reproducibly by varying cage reaction stoichiometry. For all assays reported, a single caging reaction was utilized and the level of cage attachment for each strand was an average of 7.9 and 9.0 cage groups per 21mer oligonucleotide strand for the sense and antisense FNA strands, respectively.

4.3.2 HPLC Separation of Caged FNAs.

Single stranded 21nt FNAs were characterized using RP-HPLC. A representative HPLC plot is shown in Figure 4.2. FNA control samples eluted quickly with a sharp peak elution profile. Caged FNAs were retained longer than their process

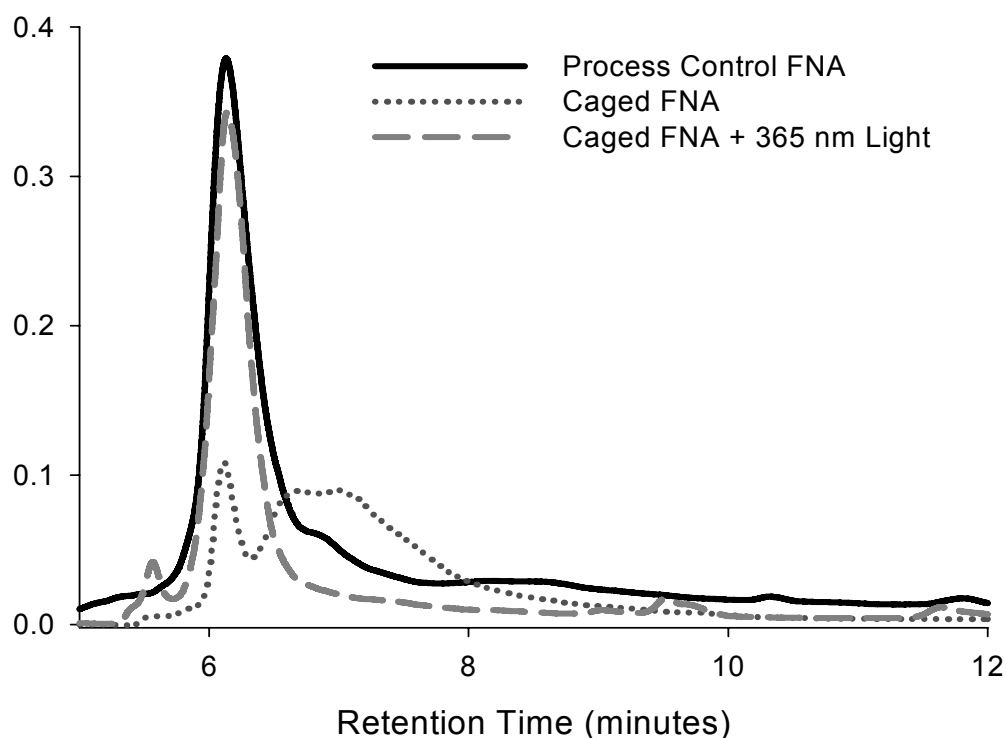


Figure 4.2: HPLC separation of caged FNAs. Elution profiles for processed control (—), caged (---), and photoexposed caged (.....) FNAs are shown. Peak broadening of caged sample is indicative of a heterogeneous product mixture of various degrees of caging. Photoexposure restores mobility to resemble the process control products.

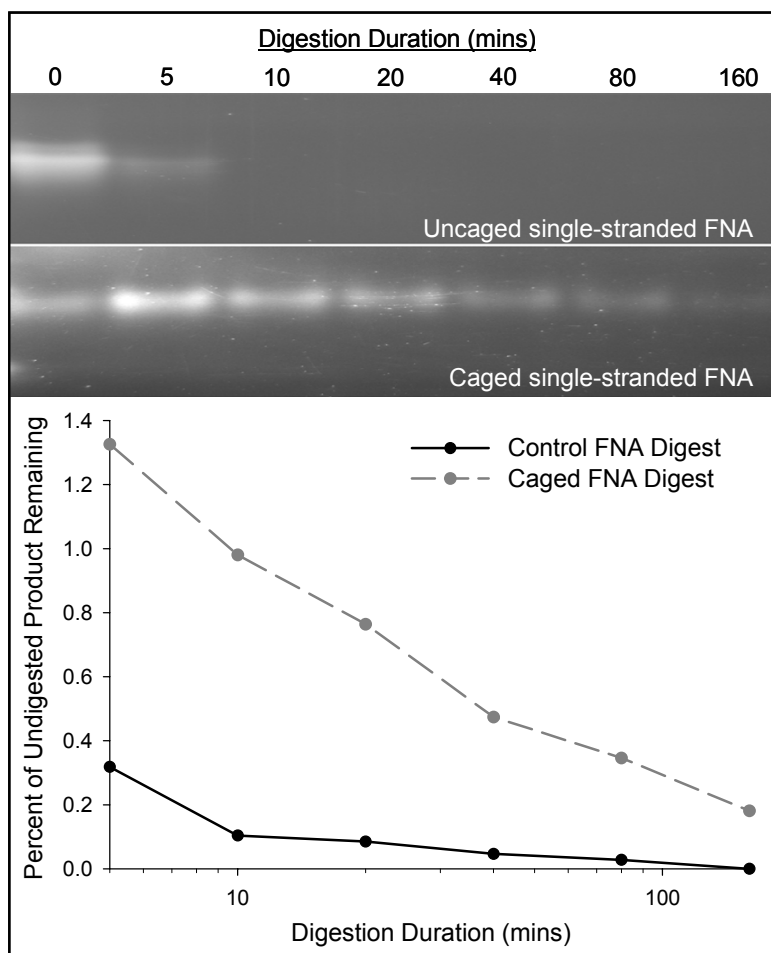


Figure 4.3: Nuclease digestion (BAL-31) of control and caged FNAs. Top panel: PAGE results show that caged FNAs are much more resistant to sugar non-specific nuclease than control FNA. Bottom panel: graphical representation of band-densitometry normalized to band intensity at time = 0 minutes.

control (non-caged reaction, see methods and Fig. 4.1 results) counterparts and exhibited a broadened elution profile. Upon exposure to 200 J/cm² of 365 nm light, the elution profile of the photo-released species resembled the control FNA elution profile, suggesting removal of the cage moieties.

4.3.3 Nuclease Digestions of Caged FNAs.

Although FNAs have previously been shown to exhibit nuclease resistance to sugar specific nucleases (chapter 3) and possess enhanced serum stability (Chiu and

Rana 2003; Layzer, McCaffrey et al. 2004), here we show that BAL-31 nuclease can digest the modified oligonucleotides *in vitro*. This enzyme is a bidirectional exonuclease that is able to hydrolyze RNA and DNA (Wei, Alianell et al. 1983). Time course experiments show improved resistance of caged FNA to BAL-31 nuclease as illustrated in Figure 4.3. The uncaged, process control FNA products were not visible after 10 minutes of digestion. The caged products are still detectable at 160 minutes, indicating that the presence of the cage group acts to slow digestion of the nucleic acids.

4.3.4 Control of RNAi in Cell Culture with Caged FNAs.

Sense and antisense FNA strands were caged in parallel reactions. A process control, in which the caging compound was not added to the reaction with the FNA, was also prepared simultaneously for each strand. These products were matched to provide four siFNA caging schemes; 1) non-caged, 2) only antisense strand caged, 3) only sense strand caged, and 4) both strands caged. In all cases, the attachment of DMNPE decreased the observed RNAi silencing when compared to the activity of the process controls (Fig. 4.4). Exposure of transfected cell cultures to 365 nm light partially restored the RNAi activity for all caged samples. Figure 4.4 illustrates that the RNAi is more sensitive to the caged antisense strand than the caged sense strand. Knockdown activities of caged and photoexposed siFNAs were compared to process control siFNAs. The latter represent fully active RNAi effectors, which were able to eliminate GFP transgene expression in nearly 90% of the cells at a 5nM dose. SiFNAs with a caged antisense strand silenced GFP expression in only $15.3 \pm 13.7\%$ of the cell population, whereas sense strand caged siFNAs silenced GFP in $41.9 \pm$

14.7 % of cells. A further reduction in RNAi activity to 9.7 ± 1.4 % was observed when both strands were caged. All caged siFNA species had significantly reduced silencing activity compared to controls ($p \leq 0.05$). Following photoexposure, each of these

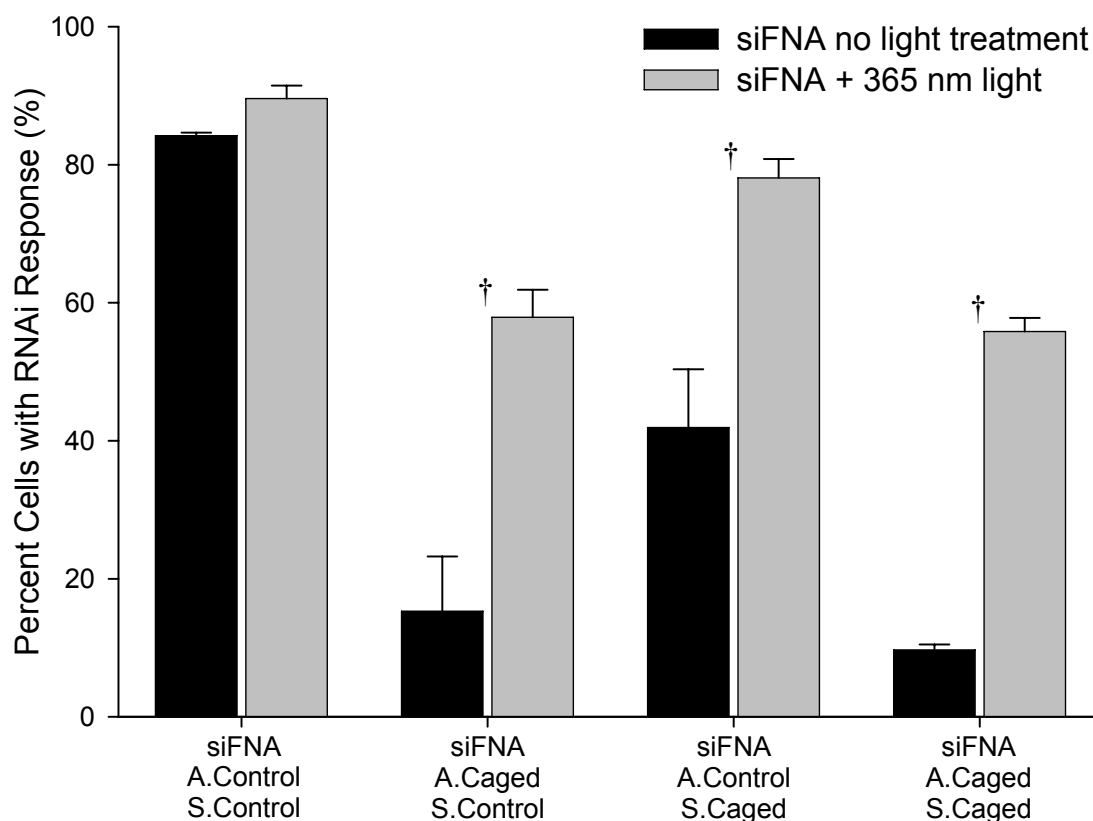


Figure 4.4: RNAi using caged siFNAs in cell culture. ■ Bars represent treatments that were protected from light. □ Bars represent equivalent treatments as the paired black bar followed by delivery of 40 J/cm^2 365 nm light. A significant difference exists between all photoexposed and non-photoexposed caged samples (denoted by †, $p < 0.05$). No statistical difference was seen for the control siFNA (left).

caged siFNA samples exhibited an increase in the percentage of GFP negative cells to 57.9 ± 6.9 %, 78.1 ± 4.7 %, and 55.8 ± 3.4 % for the antisense caged, sense caged, and dual strand caged siFNAs, respectively. While these photoactivated expression increases are significantly different from the corresponding caged samples ($p \leq 0.05$), they are also significantly different from the controls, indicating incomplete restoration

of siFNA activity. GFP positive controls were subjected to various doses of 365 nm light to ensure that photo-treatment did not have a negative impact on transgene expression. No negative affects on cellular morphology or growth rates were observed until light doses reached 80 J/cm². Figure 4.5 shows that percent of GFP-positive cells

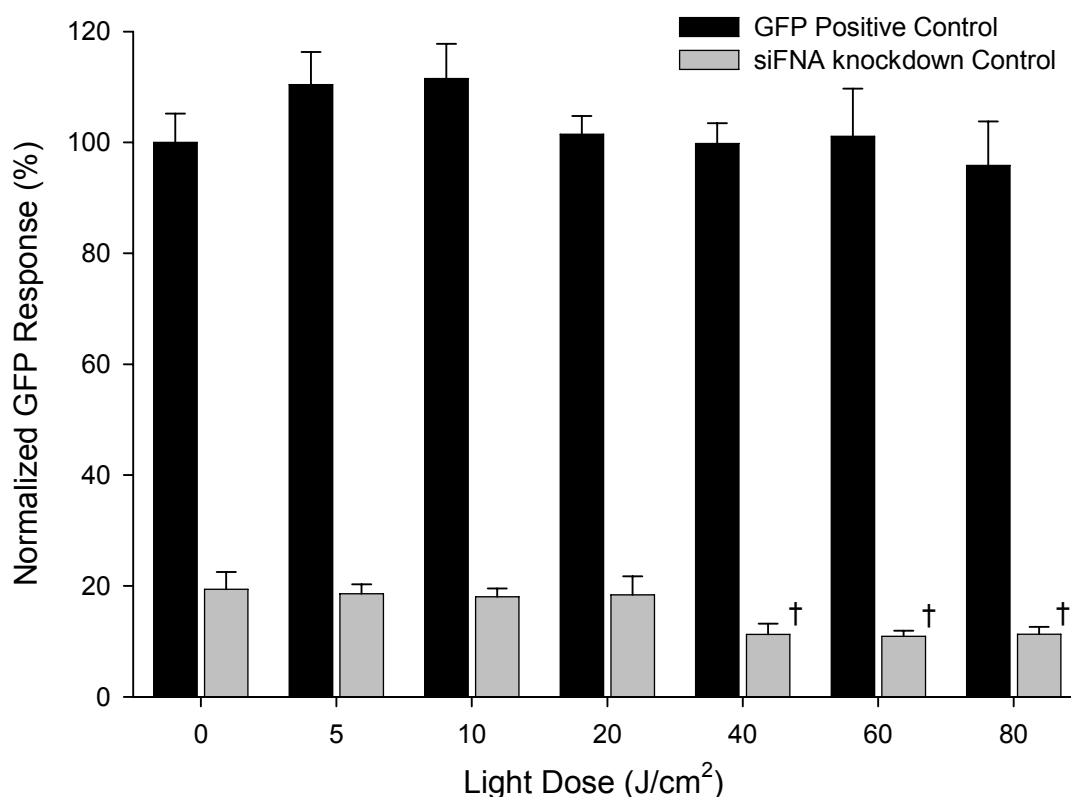


Figure 4.5: Response of cells to various doses of 365 nm light. ■ Represents GFP positive controls at various light doses. □ Represents siFNA knockdown cultures exposed to various light doses. No statistical difference could be found by photoexposing positive controls up to 80 J/cm² ($p < 0.05$). A small decrease in GFP expression was significant (denoted with †, $p < 0.05$) at light doses ≥ 40 J/cm² relative to non-photoexposed cultures, but this was the opposite effect observed from photolysis of caged siFNA treatments. These results indicate that light dosing in this range does not have noteworthy effect on GFP expression or silencing activity.

in samples treated with only plasmid or by plasmid and siFNA remained nearly unchanged through a 80 J/cm² dose of UVA photoexposure, relative to the corresponding non-photo-treated cultures.

4.3.5 *In Vivo* Control of RNAi in Zebrafish Embryos.

All treatment reagents were co-injected into the yolk stream of zebrafish embryos in the 1 to 4-cell stage, and a fluorescently labeled dextran tracking dye allowed for the selection of successful injections and delivery to the cells, as illustrated Figure 4.6. Adequate injections exhibited a uniform red-fluorescence signal. No differences in mortality or malformation were observed in response to the dextran tracking dye or the GFP plasmid at the concentrations tested.

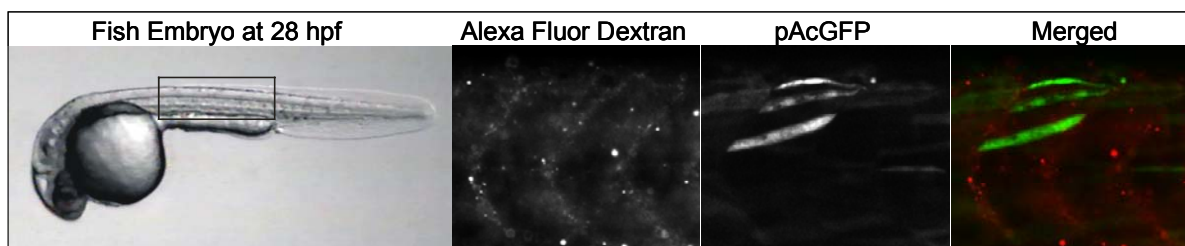


Figure 4.6: Zebrafish injection analysis. Fish embryo at 28 hpf development depicts the region in which image analysis was performed. Left: Dextran tracking dye (red) was observed throughout the region for successful injections. Middle: GFP positive cells resulted in mosaic expression (green). Right: Overlaid of the signals from the labeled dextran and GFP expression in the same fish. This pattern was typically observed in our injection paradigms and indicates uniform delivery and a mosaic expression pattern.

Gene knockdown activity of control and caged siFNAs, prior to and after light exposure, are illustrated in Figures 4.7 and 4.8 with representative fluorescent images. Co-injections of process control siFNA and GFP plasmid exhibited less green fluorescence signal than embryos only injected with GFP plasmid, performed in parallel. This pattern held true at all concentrations of plasmid and siFNA investigated. GFP expression levels in embryos injected with caged siFNAs were similar to those with injections of only GFP plasmid. GFP expression decreased in embryos injected with caged siFNAs and exposed to UVA light at 7 hpf. Doses utilized (40 J/cm^2) had no effect on zebrafish morphology, plasmid expression, or control siFNA silencing.

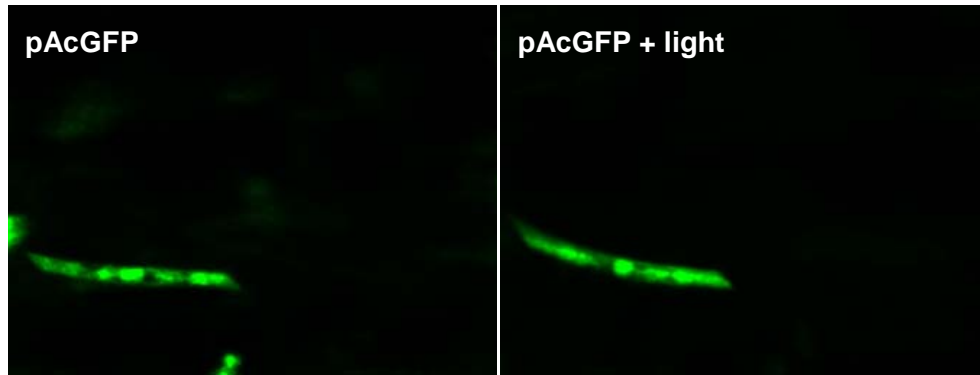


Figure 4.7: GFP expression is unaffected by UVA light exposure (40 J/cm²)

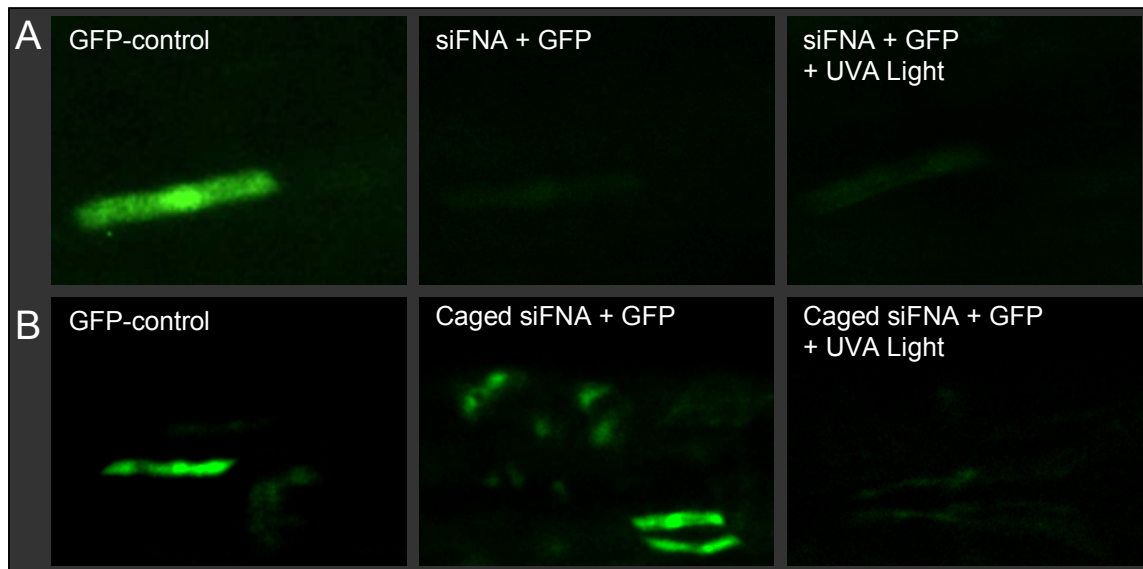


Figure 4.8: RNAi of caged versus control siFNA in zebrafish. Each row represents a complete experimental set of treatments for embryos injected on the same day. Exposure to 40 J/cm² UVA light was performed at 7 hpf. A: Uncaged siFNAs reduce GFP expression relative to controls, and light exposure has no observable effect on GFP expression. B: Caged siFNA resemble GFP control injections, but light exposure reduces GFP expression.

The appropriate concentration of siFNAs used for zebrafish injections was determined through titration assays to determine subtoxic treatment levels. Injections with siFNA concentrations of 500 ng/μL or greater resulted in an increased incidence of mortality and noticeable delays in embryonic development. The severity of this

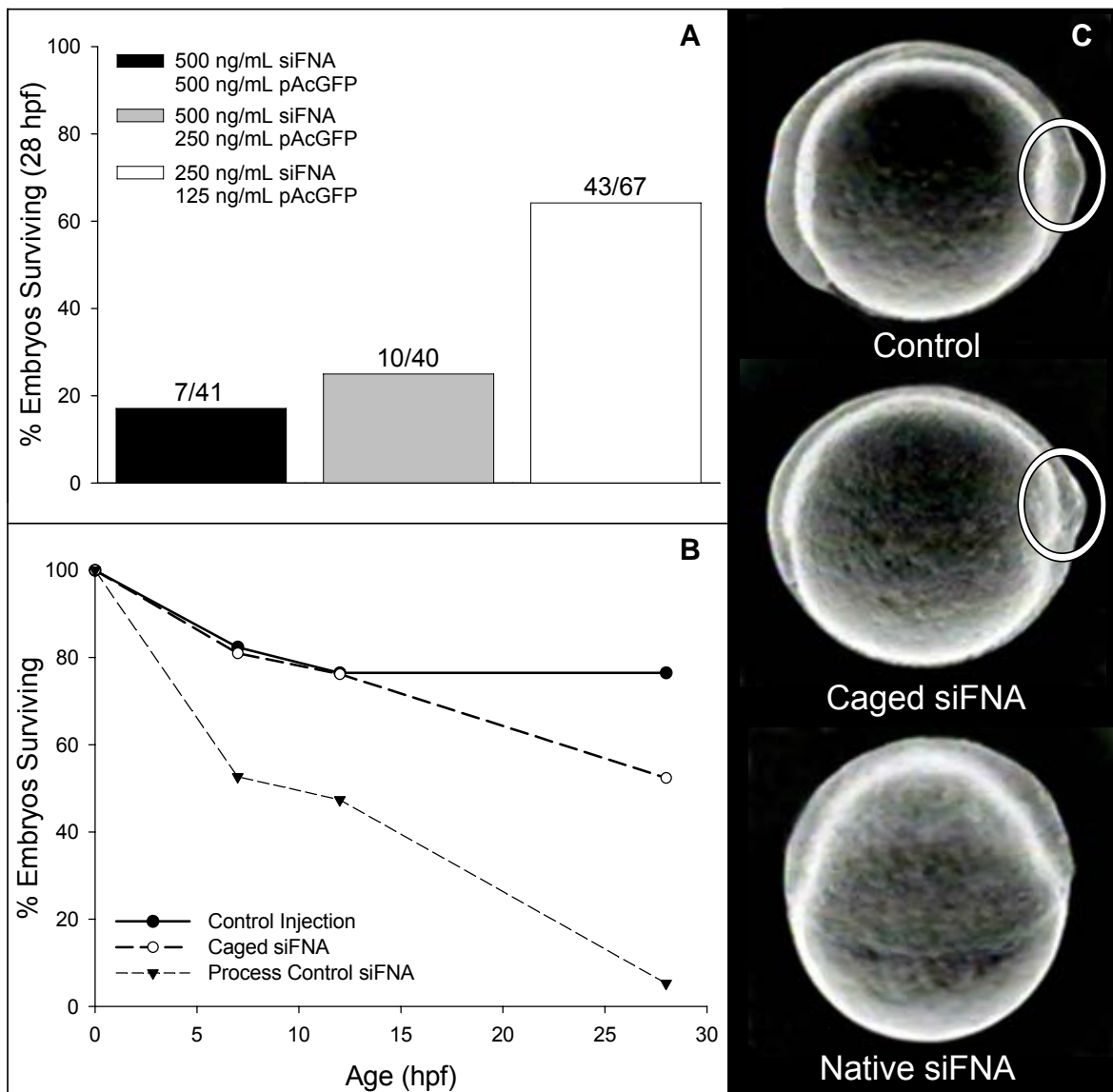


Fig. 4.9: Toxicity evaluation of control versus caged siFNAs. Panel A: siFNA concentrations above 250 ng/ μ L resulted in an increase in mortality. Panel B: Caging of siFNAs protects the developing embryo from the siFNA induced toxicity. Panel C: Illustrates a developmental delay at 12 hpf in response to siFNA toxicity at a concentration of 500 ng/ μ L. Control (no siFNA) and caged siFNA injected embryos exhibit a developing tail bud, denoted by white circles. At the same age, the embryos injected with process control siFNA are several hours behind in development, and they have not transitioned from gastrulation to the tailbud stage.

developmental delay was proportional to the concentration of siFNA delivered to the embryo. Treatment with single-stranded antisense FNA of the same sequence (500

ng/ μ L) did not result in a noticeable developmental delay or increased mortality rate (data not shown). Interestingly, caging the siFNA reduced both the motility rate and observed delay (Fig. 4.9).

4.4 Discussion

RNAi is a widely utilized mechanism for gene silencing, but despite being highly active and stable in cell culture, challenges still exist for effective silencing *in vivo*. These challenges include improving nuclease stability and siRNA half-life, designing thermodynamically stable effectors with improved target binding affinity, achieving efficient biodistribution through idealized pharmacokinetic properties, and targeting of diseased tissue. Most attempts to achieve these goals focus on permanent chemical modification, resulting in a siRNA mimic. These types of siRNA manipulation have provided much information regarding structural requirements for RNAi and what types of alterations can be made without disrupting gene silencing. For instance, a review of 2'-modified siRNAs suggests that the 2'-OH is not necessary for RNAi, but changes at this location that alter either the global duplex structure or disrupt the minor groove can abolish interference (Manoharan 2004; Zhang, Du et al. 2006). Since halide and o-methyl substitutions maintain A-type helical structure by enforcing a C3'-endo sugar pucker conformation (Guschlbauer and Jankowski 1980; Chiu and Rana 2003), and are not large enough to disrupt the major groove, these modifications have been extensively utilized for RNAi. In addition, these substitutions improve resistance to sugar-specific enzymatic degradation and have been shown to reduce off-target effects normally observed following siRNA delivery (Jackson, Burchard et al.

2006; Cekaite, Furset et al. 2007). Despite the advances in siRNA stability through permanent chemical modification, these effectors still lack improved biodistribution and tissue specific targeting capabilities.

One strategy to achieve tissue specific targeting of RNAi is to utilize synthetic siRNAs that can be activated by an external inducing agent. This strategy would utilize the trigger to activate at select sites and times. This has been attempted by several groups with photo-caging RNA in order to silence gene expression using controlled light exposure. The first incidence of RNA caging was accomplished by the incorporation of a 2'-OH photolabile protecting group into RNA for disruption of the hammerhead ribozyme activity (Chaulk and MacMillan 1998). This system efficiently provided light-reversible protection of the substrate RNA. Although highly efficient, this technique required extensive synthetic procedures to produce the protected oligonucleotide. An alternative approach to caging RNA was demonstrated with the random attachment of 6-bromo-7-hydroxycourmanrin-4-ylmethyl (Bhc) cage compound to exogenous mRNA through a reactive diazo-intermediate (Ando, Furuta et al. 2001). This approach was adopted using a similar attachment chemistry to produce 1-(4,5-dimethoxy-2-nitrophenyl)ether (DMNPE) caged siRNAs (Shah, Rangarajan et al. 2005). In both incidences the caged RNA effectors demonstrated reduced activity relative to their respective controls, which was partially restored by exposure to 350-365 nm light. Although not proven, it is presumed that caging of nucleic acids with diazo-intermediates results in phosphate attachment. Therefore, a potential drawback of these studies was the potential for phosphotriester-mediated hydrolysis of caged species. RNA phosphotriesters have been shown to be unstable in aqueous solutions

where the 2'-OH may play a role in hydrolysis (Breslow and Xu). Therefore internally caged nucleotides might be very susceptible to hydrolytic release of the cage molecule itself or scissile bond cleavage and degradation of the RNA. Our early attempts to cage 700bp dsRNA using reactive diazo compounds resulted in fragmentation of the RNA in aqueous buffer (Chapter 2).

In an effort to reduce the leak activity, improve the efficiency of photo-induction, and avoid RNA hydrolysis, two groups have separately expanded on caged siRNA by incorporating a single photolabile group onto the 5'-terminal phosphate of the siRNA antisense strand (Nguyen, Chavli et al. 2006; Shah and Friedman 2007). Each exploited a commercially-available NPE-derived linker on the 5'-terminal nucleotide during 3' to 5' RNA solid phase synthesis. Based on previous work, this phosphate is thought to be critical for siRNA incorporation into RISC (Chiu and Rana 2003; Czauderna, Fechtner et al. 2003; Ma, Yuan et al. 2005). However, the results of these studies were mixed. Nguyen et al. demonstrated that these caged siRNA had very little activity and that silencing was efficiently restored with light doses that were required to remove all cage linkers, which was determined *in vitro*. Observations of minute leak activities were explained by N-1 contaminants from RNA synthesis that had silencing activity due to the absence of the final caged linker. Shah and Friedman disputed this interpretation since their data shows significant leak RNAi activity in the caged un-induced state. Additionally Friedman and colleagues tested highly purified antisense RNA strands with non-photolabile linkers at the 5'-phosphate to verify their results. Their interpretation was that the RISC components have the ability to interact with the remaining non-bridging oxygen, allowing some RNAi to proceed. Although the

5'-phosphate on the antisense strand is known to be required for RNAi activity (Nykanen, Haley et al. 2001; Martinez, Patkaniowska et al. 2002; Schwarz, Hutvagner et al. 2002), it has also been shown that various linker modifications to this terminal location are tolerated if the 5'-phosphoester bond is intact (Schwarz, Hutvagner et al. 2002; Harborth, Elbashir et al. 2003). To avoid this residual activity, light-activated RNAi might require an alternate site of cage attachment or caging on multiple sites for each siRNA. Recently the site-specific strategy of caging siRNAs was expanded to include internally-caged nucleobases with impressive results (Mikat and Heckel 2007). While photo-caging of siRNAs has demonstrated promise in spatially and temporally controlling RNAi, this technique does not address some of the other desired characteristics for improving pharmacological efficiency of RNAi. Results shown here combine the benefits of 2'-F modified siRNAs with DMNPE caging in order to achieve stable, light-inducible, RNAi.

Fully modified 2'-F RNA was generated through solid-phase synthesis and caged using a diazonium nitrobenzyl derivative in a batch-style reaction. While conditions of this reaction could be altered to produce varying degrees of cage attachment, the more heavily caged products were used in the model biological systems to reduce leak RNAi activity. Evaluation of the caged products in several *in vitro* characterization assays allowed for qualitative analysis of cage attachment and photo-release. PAGE separation of caged products was carried out as previously described (Ghosn, Haselton et al. 2005) and indicated cage attachment (data not shown). In this assay a high incidence of cage attachment markedly diminishes visualization using ethidium-like stains. This phenomenon could be caused by a

reduction in the association between the stain and nucleic acid, quenching of the fluorescent signal, or a combination of the two factors. In addition to gel shift assays, the products were also evaluated by RP-HPLC, where direct absorbance detection does not rely on fluorescent staining. The chromatography results (Fig. 4.2) clearly show separation between the uncaged and caged species. Differences in affinity for the non-polar stationary phase are believed to arise from the elimination of a negative charge on the backbone as well as the addition of the non-polar cage moiety. The observed peak broadening of the caged NAs indicates that the solution was a heterogeneous mixture of products ranging in the degree of cage attachment. Therefore, even in samples that are heavily caged, some strands of nucleic acid may still have a limited number of cage compounds attached. For all assays tested, UVA photoexposure restored the NA properties to resemble the process control samples.

It has previously been suggested that photo-release of a caged-species with n multiple adducts requires an irradiation dose that scales to the n^{th} power for equivalent uncaging (Tang and Dmochowski 2007). However, the observed quantum yield of DMNPE-caged FNA ($n=9$) does not support this hypothesis. For instance, DMNPE-caged ATP quantum yield reported in the literature is between 0.1 and 0.05 (Goeldner and Givens 2006; Ellis-Davies 2007). Assuming similar quantum yields for DMNPE phosphoesters on FNA, complete photocleavage would require several orders of magnitude greater light exposure than we observed was necessary for complete photocleavage (Fig. 4.2).

Caging also provides resistance to enzymatic digestion. Fully modified FNAs were previously shown to be impervious to several sugar-specific nucleases

(chapter 2). However, these NAs are still susceptible to certain sugar-nonspecific nucleases, such as BAL-31. Figure 4.3 illustrates that single-stranded FNAs were rapidly processed by this enzyme at the concentrations tested. However, the attachment of DMNPE drastically decreased the BAL-31 degradation of FNA. Since BAL-31 acts primarily as a bidirectional, single-strand specific, exonuclease (Wei, Alianell et al. 1983), the enzyme might be able to easily process uncaged end nucleotides. Once reaching one or multiple adjoining caging sites within the nucleic acid, the enzyme might be interrupted from its digestive process, similar to the disruption of Bam H1 digestion of DMNPE-caged plasmid DNA (Monroe and Haselton 2004). It has previously been demonstrated that the 2'F modification increases siRNA stability in serum and plasma but this does not translate to longer silencing *in vivo* (Layzer, McCaffrey et al.). Therefore, intracellular digestion of these modified NAs might be more efficient than under *in vitro* conditions. The combination sugar modification and backbone caging may provide enough enzymatic resistance to increase lifetimes of FNA and the duration of RNAi-mediated gene knockdown. Unfortunately, cell culture assays are not amenable to extended time course experiments since the RNAi effectors are quickly diluted through cellular proliferation. Additionally, delayed activation of the caged siFNA could not be tested in these systems since the fluorescent protein is stable, resulting in a persistent signal. Future studies utilizing a destabilized or more transient reporter gene *in vivo* would be useful in exploring prolonged RNAi lifetimes through cage attachment.

It has been shown above that DMPNE attachment to FNA can affect NA:NA as well as NA:enzyme interactions. Therefore, caging of siFNAs may have the potential

to disrupt RNAi in various ways such as: disruption of RISC recognition, helicase unwinding of the duplex, mRNA target recognition, ejection of the digested target for RISC recycling, localization of RISC to specialized organelles, and downstream processing such as chromatin remodeling. Figure 4.4 demonstrates that caging of either strand in a siFNA reduces RNAi activity. However, the caged antisense strand results in greater disruption of RNAi activity even though both strands were evaluated with similar degrees of cage attachment. This is not unexpected since the sense FNA strand is discarded early in the RNAi pathway. Reduction of sense strand caged RNAi is likely caused by improper siFNA formation, reduced delivery of the caged species through lipid mediated transfection, disruption of RISC recognition, disruption of helicase removal of the sense strand, or a combination of these factors. A parallel study carried out by our research group has demonstrated that caging of a fluorophore-labeled phosphorothioate oligonucleotide resulted in no observable difference in lipid-mediated cellular delivery (Fabion, in preparation). Additionally, it is unlikely that cellular delivery is drastically reduced due the attachment of DMNPE since photoexposure of sense-caged siFNA treated cells restores RNAi activity to levels that are nearly equivalent to the uncaged-control effectors. This observation also suggests that when only one strand is caged, FNA duplexes are stable prior to delivery. Caging of the antisense strand had the benefit of significantly less leak in RNAi activity. However, only partial restoration using 365 nm light was achieved. HPLC evaluation of these products suggests that the caged FNAs may consist of a heterogeneous mixture of products that vary in the degree of DMNPE attachment. More lightly caged species may allow for residual RNAi activity, while DMNPE might

not be fully removed upon photoexposure for heavily caged species. Compounding the issue of varying amounts of the cage molecule, the location of attachment is likely variable. Disruption of RNAi might be highly dependant on the location of the cage species. Since it is carried through the entire RNAi pathway, it is more likely that the antisense strand has multiple RISC interaction and critical processing locations along its length and, therefore, it is more likely for a randomly attached cage group to disrupt silencing. Several potential critical locations for effective RNAi have been identified through siRNA chemical modification studies as well as structural evaluation of RISC protein components (Song, Liu et al. 2003; Manoharan 2004; Parker, Roe et al. 2004; Zhang, Du et al. 2006). Together, these investigations support the observation that the antisense strand is more sensitive to modification or cage attachment.

Zebrafish embryos were used as an *in vivo* model to test photo-induced silencing with caged siFNA to support the cell culture results. The mosaic expression pattern of the GFP reporter transgene prevented quantitative analysis. This mosaic expression pattern has been previously reported in other studies (Ando, Furuta et al. 2001). The red-fluorescence signal from injected labeled dextran indicates uniform delivery by microinjection (Fig. 4.6). Nevertheless, qualitative observations strongly suggested that caging reduces the silencing activity of these molecules and that this activity can be restored by photoactivation. The reduction in GFP expression is not likely due to photoexposure, as the GFP controls are unaffected with similar light doses. Additionally, the LD50 of UVA in zebrafish ($\sim 800 \text{ J/cm}^2$) is several orders of magnitude larger than we have observed in cell cultures (Matsuura, Dong et al. 2005;

Forman, Dietrich et al. 2007). Thus zebrafish are a particularly appropriate model for photoactivated gene expression studies.

Another observed benefit of caging these RNAi effectors is protection from toxicity associated with siFNAs. Several potential causes of this toxicity include off-target RNAi gene silencing, innate toxicity of siFNAs and their metabolites, or overwhelming of the RNAi machinery with siRNA substrates. It has been previously reported that RNAi in zebrafish has a particularly high incidence of off target effects (Oates, Bruce et al. 2000; Zhao, Cao et al. 2001; Giraldez, Mishima et al. 2006). Therefore, it is likely that the observed increase in mortality rate and developmental delay are related to an RNAi phenomenon, rather than toxicity of breakdown products of FNAs. Additionally, single stranded FNAs injected at high concentrations did not result in observable toxicity (data not shown). RNAi toxicity might be more dramatic in a developing system, since endogenous microRNAs are theorized to play a major role in genetic regulation (Matzke and Matzke 2003). This further supports the conclusion that caging of the RNAi effector prevents them from entering the RNAi pathway. If this is true, then the fact that these molecules were activated at 7 hpf demonstrated intracellular stability of the caged species. Therefore caging of RNAi effectors would allow delivery to the biological system at concentrations that would otherwise be toxic, followed by photo-induction of gene silencing at a specific stage of development in a manner that could be used to control dosing to sub-toxic levels.

Chemically stabilized siFNA was successfully controlled through transient chemical modifications which can be disassociated with light. The use of 2'-fluoro modification throughout the NA eliminated the possibility of unstable phosphotriester

formation. This allowed for multiple attachments of the photolabile compound to the phosphate backbone of each siRNA strand. These caged species exhibit increased resistance to nuclease digestion and reduced RNAi silencing, and these effects were partially reversible with the application of 365 nm light. Although this strategy was successful in achieving photo-induced RNAi with chemically stabilized effectors, the external trigger was not 100% efficient. In order to approach this level of efficiency, cage groups would likely need to be placed at desired locations, which would need to be directed through synthetic methods as opposed to random attachment through co-incubation with a reactive intermediate. Despite necessary future improvements, the results presented here suggest that caging can be used in conjunction with other siRNA chemical modifications to achieve controllable RNAi with improved pharmacological properties.

CHAPTER 5:

Base-Caged ATP: an Alternative to γ -Phosphate Caged ATP

5.1 Introduction

The first example of applying photochemistry to control biological activity of a substrate was caged ATP [Kaplan, 1978 #60]. In this study, 2-nitrobenzyl and 1-(2-nitrophenyl)ethyl groups were attached to the gamma phosphate of ATP to cage its biological activity. These caged ATPs were used to control the activity of a Na:K ATPase ion pump. Since this time, ATP has remained the most frequently caged biomolecule, and is often used a model for different photolabile protecting groups [Reviewed by Givens review]. For instance, the first biological use of the *p*-hydroxyphenacyl demonstrated photo-release of ATP (Givens and Park 1996). Similarly, the coumarin-derived family of caging compounds was first used to cage phosphates (Givens and Matuszewski 1984). Nearly a decade later it was used for caging cAMP in a simulated physiological environment (Furuta, Torigai et al.) and later was used for ATP caging. Caged-ATP is an excellent model due to the myriad of biological processes that are dependant on ATP for energy.

Although alkylation of the ATP γ -phosphate restricts kinase activity, this scheme still has one major flaw. Most applications of caged ATP require an enzyme interaction to process the substrate ATP. Caging at the phosphate prevents dephosphorylation of the ATP, but this does not necessarily prevent protein-ATP recognition. In many cases, caged ATP substrates have been shown to inhibit the target systems being studied, as first described by Forbush (Forbush 1984). Other examples of the gamma-phosphate caged ATP inhibition include actomyosin (Thirlwell,

Corrie et al. 1995], mitochondrial ADP/ATP carrier protein (Broustovetsky 1997), kinesin and microtubules (Higuchi 1997), and the classical Na:K ATPase pump (Geibel, Barth et al.). In the case of actomyosin, the competitive inhibition caused by the presence of caged ATP slowed the shortening kinetics of muscle fibers. This is particularly unfavorable since caged-ATP was classically used to measure the kinetics of this system using a pulse trigger (McCray, Herbette et al.). Since many of these processes are specific to the adenosine nucleotide triphosphate, another potential approach would be to cage the nucleobase. This may eliminate competitive binding and still render the caged ATP biologically inert. Despite the recent advances in nucleobase caging of oligonucleotides (Hobartner and Silverman), synthesis and utilization of base-caged ATP has not been reported to date.

One reason why the generation of base-caged ATP might not have been attempted is that techniques for caging of a nucleobase often require difficult synthetic methods. A potential solution to this problem is to utilize a reactive base-modified NTP as the substrate for caging. This allows for the direct caging of the adenosine through direct attachment schemes. To avoid the requirement for series of protection and deprotection steps, the cage intermediate should not be reactive with the phosphates or the hydroxyl groups on the ribose. A mildly nucleophilic primary amine meets these requirements. Additionally this attachment chemistry should be reactive with the modified nucleobase, such as 6-chloropurine riboside. Here, we show 2-nitrobenzylamine and a custom 4,5-dimethoxy-2-nitrobenzyl amine can be used to cage 6-chloropurine riboside and 6-chloropurine riboside triphosphate to produce base-caged ATP.

5.2 Materials and Methods

Ammonia gas was condensed (60 mL) in a pressure vessel cooled in a dry ice propanol bath to -80°C . Meanwhile, 4,5-dimethoxy-2-nitrobenzyl bromide (DMNBB) (2.5 gr, 9.06 mMol) was dissolved in acetonitrile (ACN) (24 mL) under continuous agitation. The DMNBB solution was added dropwise over 10 minutes to the condensed ammonia liquid with constant stirring. The pressure vessel was sealed, shielded from light, and allowed to equilibrate to room temperature. The reaction proceeded under constant stirring for 69 hours. The vessel was then re-cooled to -80°C and opened after equalization to atmospheric pressure. All ammonia was evaporated and the product was solubilized in 100mL of dichloromethane (DCM). A 10% w/v sodium carbonate aqueous solution was added to the DCM for phase extraction to separate the nitrobenzylamine product from the ammonium bromide salt. The aqueous phase was washed 2 more times with DCM. The collected DCM layers were dried over potassium hydroxide and filtered through Whittman paper funnel. The product was further purified via silica gel chromatography (1:9 methanol:DCM, $R_f = 0.05$). The product containing fractions were dried *in vacuo*, leaving a reddish brown solid. 4,5-dimethoxy-2-nitrobenzylamine (DMNB-NH₂) was verified through NMR, ESI-MS, and FTIR spectroscopy.

For nucleoside model studies, chloropurine riboside (CPR) was purchased from TriLink BioTechnologies (San Diego, CA) and 2-nitrobenzylamine (NB-NH₂) was purchased from Sigma Aldrich (St. Louis, MO). NB-NH₂ or DMNB-NH₂ (200 μmol) was dissolved in 1-propanol or methanol (58.2 μL) and triethylamine (41.8 μL). CPR (25 μmol) was added to the solution and the reaction was gently agitated at 42°C for 18 hours. Fractions were taken at various time intervals to monitor the reaction progress

via reversed phase HPLC on a C18 column (spherisorb ODS2 5 μ m bead Waters Corp., Milford, MA). Separation via HPLC was carried out at a flow rate of 0.5 mL/min under the following solvent conditions: 90:100 to 50:100 A:B linear gradient over 30 minutes, linear increase to 100% B over 20 minutes, and 5 minute hold at 100% B, where A is 0.1% triethylammonium acetate (TEAA) in water and B is acetonitrile. HPLC was also used to purify products for ESI-MS analysis.

For ATP caging, a chloropurine riboside triphosphate (CPR-TP) solution (100 mM) was purchased from TriLink BioTechnologies. NB-NH₂ or DMNB-NH₂ (260 μ mol) was dissolved in methanol (150 μ L) by heating to 60°C in a water bath. Triethylamine (50 μ L) and 16.6 μ L of a 100mM CPR-TP aqueous solution (1.66 μ mol) were added to the solution, and the reaction was rocked at 42°C for 18 hours. Once complete, DCM (500 μ L) and deionized water (500 μ L) were added to the solution and phases were mixed by shaking. The aqueous layer was collected and washed twice more with 500 μ L of DCM. The aqueous layer was passed through an DEAE sepharose fast-flow anion exchange column (GE Healthcare), which was prewashed with 1 M NaCl solution and copious amounts of water. The product was eluted using step increases in concentration of NaCl solutions up to 1 M. The resulting fractions were dried *in vacuo*, reconstituted in deionized water, and stored at 4°C and protected from light for analysis.

A luciferin-luciferase ATP reporter kit was purchased for analysis of the base caged ATPs (Enliten®, Promega Corp., Madison, WI). Additionally γ -phosphate caged ATPs (NPE and DMNPE) were purchased for comparative analysis (Molecular Probes, Eugene, OR). The luciferin-luciferase reagents were reconstituted using the kit buffer according the manufacturer specifications. These enzyme buffer was further diluted

(1:5 or 1:10) with HEPES (20mM, pH 7.5). Various concentrations of ATP samples or mixtures (5 μ L total) were added to a 96-well plate. Photoexposures were performed directly in the plate, before adding the luciferase reagent. The diluted reagent was added (45 μ L per well, 90% of final volume) to the plate immediately before measuring luminescence on a Fluorstar plate reader. All plates contained several ATP and water standards for experiment equilibration.

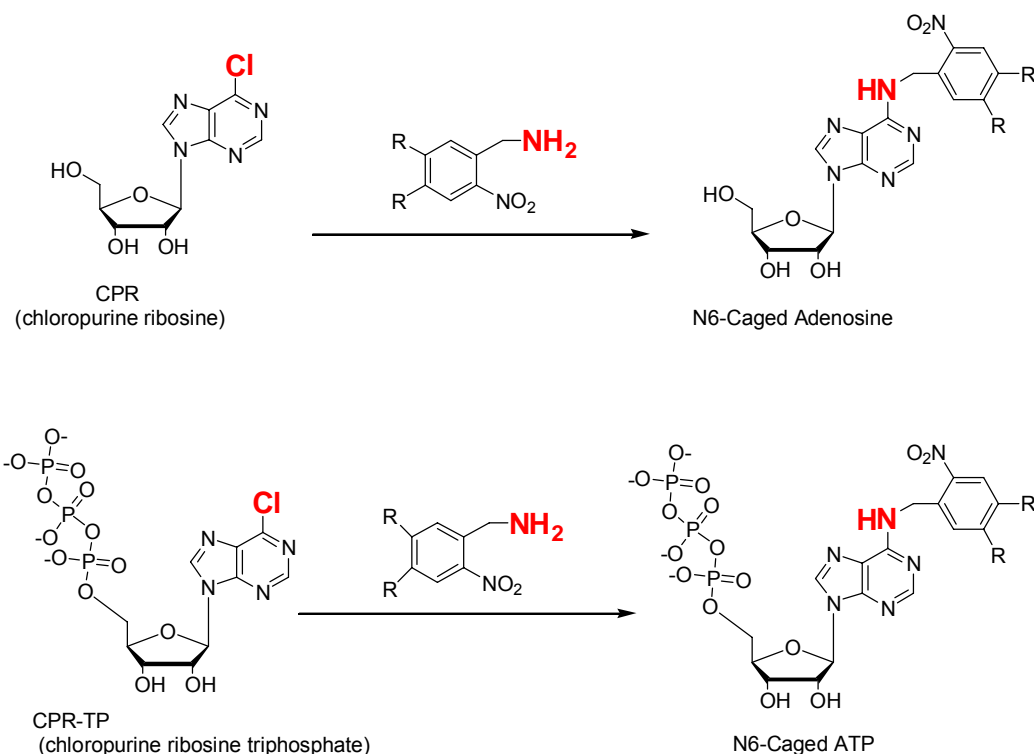


Figure 5.1: Base-caged adenosine scheme. ATP reaction reaction with 2-nitrobenzyl amine caging groups (R = H, n-nitrobenzyl amine, R= OCH₃, 4,5-dimethoxy-2-nitrobenzyl amine)

Photoexposures were performed using either a transilluminator (TFM-20, UVP Inc., Upland, CA) (λ = 308 nm, 6.5 mW/cm²) or a GreenSpot Photocuring System (λ = 365 nm, 0.95 W/cm²) (American Ultraviolet, Lebanon, IN). Light was delivered to the samples through a bottom-up method using the transilluminator or an inverted

liquid-filled light guide for the GreenSpot system. Infrared, UVC, and UVB light was filtered out from the GreenSpot light source using a short bandpass filter (SWP-2502U-400) and an IR-filter (KG-2-IR) (Lambda Research Optics, Costa Mesa, CA). Total light delivered was 60 J/cm². Non-photoexposed samples were added to the appropriate wells following light treatments.

5.3 Results

2-nitrobenzylamine was purchased from Sigma Aldrich (St. Louis, MO), however the dimethoxy-analogue was synthesized to have a cage suitable for use in cells and tissues. The amination of DMNBB was separated on thin layer chromatography (R_f = 0.15 in 1:4 methanol:DCM or R_f = 0.05 in 1:9 methanol:DCM)

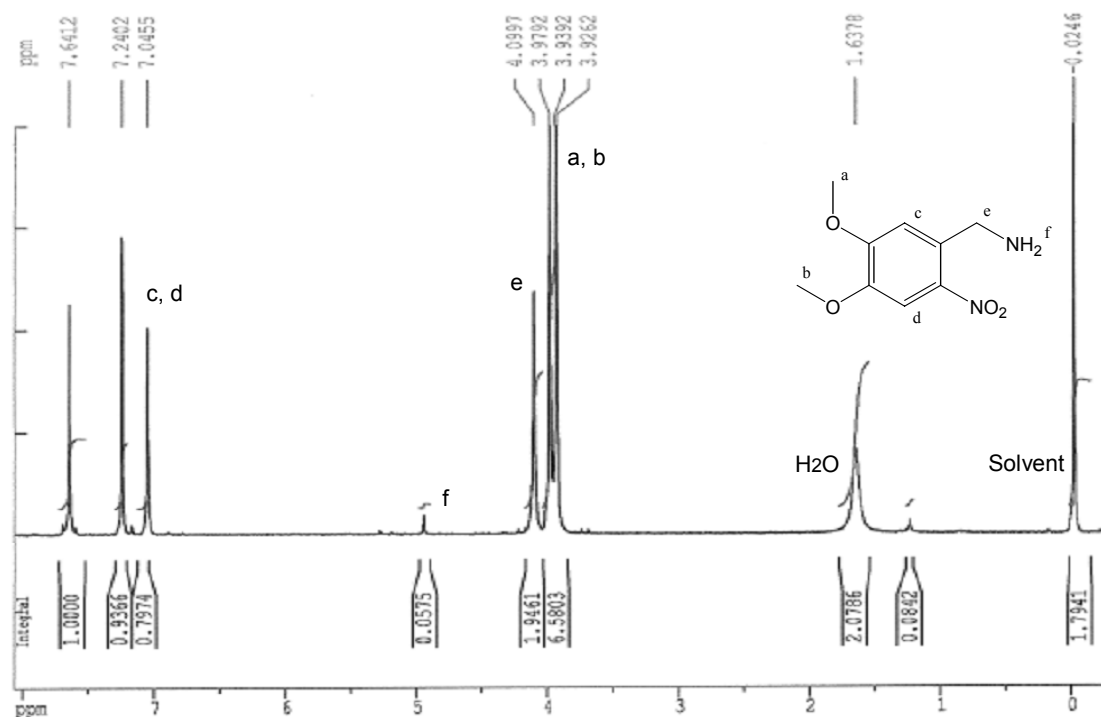


Figure 5.2: NMR of DMNBNH₂. A labeled chemical structure of the product correspond to peak labels for H-peak identification.

and stained using ninhydrin plus heat for detection of amines (data not shown). Although ammonia was used in vast molar excess, formation of a secondary amine was detected. Column silica chromatography yielded a pure product with mass spectroscopy showing a molecular weight of 213, corresponding to $\text{DMNB-NH}_2 + \text{H}^+$. The primary amine was difficult to observe using $^1\text{H-NMR}$ due to proton exchange with the solvent (fig. 5.2, peak f). However, the presence of the amine resulted in a signal shift for the two hydrogen atoms associated with exocyclic carbon (fig.5.2, peak e). FTIR was used in conjunction with $^1\text{H-NMR}$ and ninhydrin staining to verify the presence of the primary amine.

Both 2-nitrobenzylamine compounds were tested for the ability to convert 6-chloropurine riboside to caged amine via substitution of the chloro-modification. Reactions were carried out separately so that crude fractions could be removed and

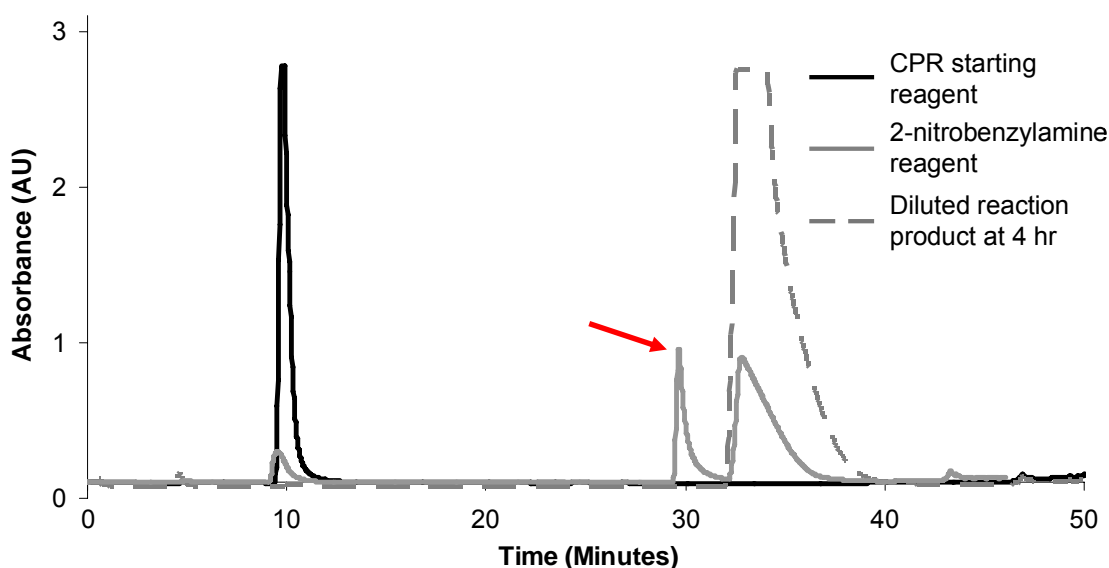


Figure 5.3: HPLC monitoring of CPR and NB-NH_2 cage reaction. Overlaid elution profiles of NB-NH_2 cage reaction with starting reagents. Red arrow indicates product formation at 4 hours into reaction. ESI-MS of the product peak correlated to 2-nitrobenzylamine caged adenosine (MW: 403.3).

evaluated by RP-HPLC at hourly intervals. Caging reactions using NB-NH₂ gave a clean product that eluted between the two starting reagents. Figure 5.3 demonstrates product formation at 1 hour and the elution of the product relative to the starting reagents. The product peak was collected and verified by ESI-MS (MW = 403.3). The reaction using DMNB-NH₂ resulted in the formation of several side products (Fig 5.4).

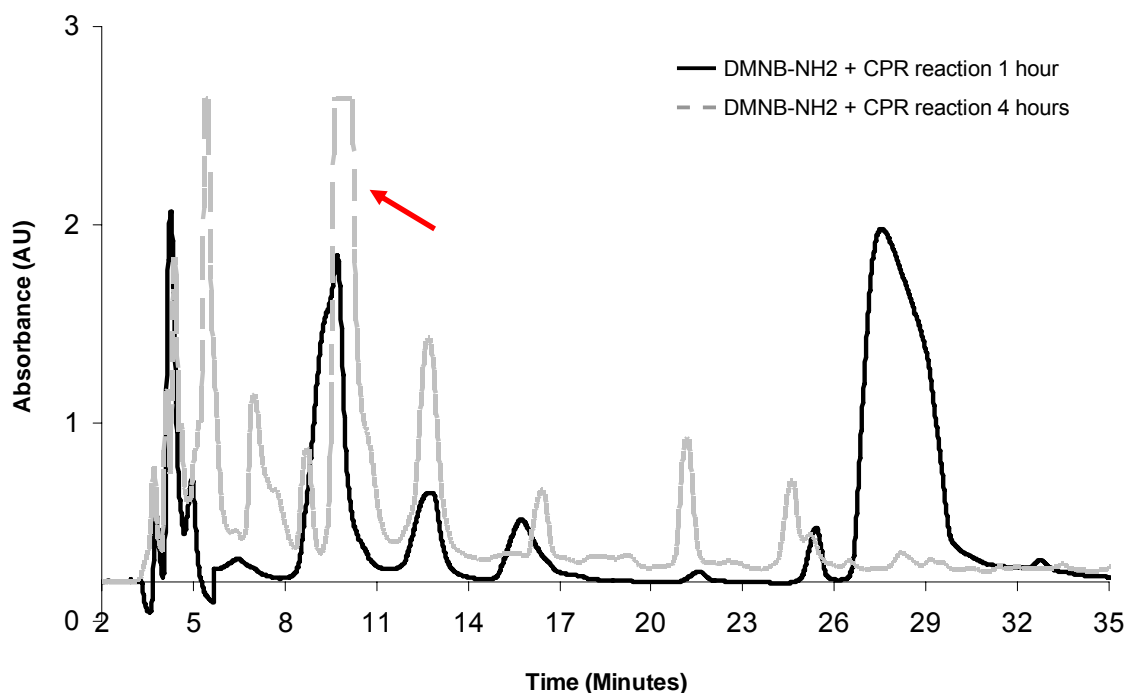


Figure 5.4: HPLC monitoring of CPR and DMNB-NH₂ cage reaction. Overlaid elution profiles of DMNB-NH₂ cage reaction with starting reagents. Red arrow indicates product formation of interest, but a significant number of side-product contaminants are present. ESI-MS of the product peak correlated to 2-nitrobenzylamine caged adenosine (MW: 463.1).

In this reaction, the cage reagent appears to react with the solvent system (methanol and triethyl amine) or simply breaks down. This results in precipitate formation and a loss of signal relating to DMNB-NH₂ by 4 hours reaction time. However, the product of interest was generated, collected, and verified by MS (MW = 463.1).

Once the caging reactions with the CPR nucleoside model were verified, the same process was used to generate caged ATP from 6-chloropurine riboside triphosphate. After the 18 hour reaction, a liquid-liquid extraction was used to separate the unreacted cage from the nucleoside triphosphate products. Similar to the nucleoside model studies, a precipitate formed in the reactions and this effect was more pronounced in the DMNB-NH₂ reaction. Additionally, the resulting DMNB-NH₂ aqueous phase contained chromophores causing the solution to appear dark blue. Prior to ion exchange chromatography, the aqueous phase for both products underwent a colorimetric change during the drying process, suggesting further reactions by remaining contaminants. During anion exchange, a yellow and green band eluted at low salt concentrations. However, the fraction corresponding to nucleotide triphosphate elution retained a dark blue appearance. Alternatively, the NB-NH₂ caged yielded in a clear eluent. The collected fractions were evaluated via absorbance spectroscopy to determine caged-ATP yield. Yields of nucleotide triphosphate crude products were 90% and 62.7% for NB-NH₂ and DMNB-NH₂, respectively.

Since 6-chloropurine riboside triphosphate has negligible activity in the luciferase reporter assay (table 5.1), the crude caged-ATP products could be used without further purification. Luminescence was recorded prior to and following photoexposure using ATP, NPE and DMNPE γ -phosphate caged ATPs, and NB-NH₂ and DMNB-NH₂ base-caged ATPs. The results using a final ATP concentration of 10 μ M, corresponding to the predetermined mid-concentration in the linear range of the assay (data not shown), are summarized in table 5.1. All caged ATP analogues demonstrated photo-activation ability. DMNB-NH₂ and γ -phosphate NPE caged ATPs

exhibited some leak activity. This leak activity approached 10% for γ -phosphate NPE caged ATP 100 μ M and 1 mM concentrations. Alternatively the DMNB-NH₂ caged ATP did not exhibit an increase in leak activity with elevated concentrations, suggesting this product was free of ATP contamination and/or DMNPE may be more effective at reducing leak-activity than NPE.

Table 5.1 Luciferase ATP assay with caged effectors

| Sample | Before UVA light exposure | After UVA light exposure |
|-----------------------------------|---------------------------|--------------------------|
| ATP | 7852 \pm 438 | N/A |
| γ NPE-caged ATP | 295 \pm 13 | 5623 \pm 394 |
| NBNH ₂ base-caged ATP | 1 \pm 1.3 | 4958 \pm 266 |
| γ DMNPE-caged ATP | 0 \pm 0 | 10,939 \pm 582 |
| DMNBH ₂ base-caged ATP | 273 \pm 70 | 3453 \pm 178 |
| Unreacted CPR-TP | 6 \pm 10.9 | N/A |

Table 5.2 % of RLU from ATP co-incubated with caged effectors

| Sample | 2-nitrobenzyl | 4,5-dimethoxy 2-nitrobenzyl |
|---|----------------------|-----------------------------|
| ATP alone [10 μ M] | 100.0% \pm 32.0% | 100.0% \pm 12.0% |
| ATP [10 μ M] + γ -phosphate caged ATP [10 μ M] | † 23.0% \pm 9.0% | † 51.0% \pm 6.1% |
| ATP [10 μ M] + base-caged ATP [10 μ M] | ‡ 128.1% \pm 12.6% | ‡ 86.7% \pm 6.4% |

Symbol † denotes statistical difference between caged-ATP and ATP standard
Symbol ‡ denotes statistical difference between γ -phosphate and base caged ATP
(Student's *t*-test $p < 0.05$)

Co-incubation of standard ATP and caged ATP analogues (10 μ M final concentrations, 50 μ L) were performed to assess the competitive inhibition properties of the caged species. Table 3.2 summarizes the percentage of ATP activity of the co-incubations, relative to an ATP standard plus buffer that was run in parallel. Both γ -

phosphate caged ATPs reduced the observed luminescent signal. No statistical difference could be drawn between the ATP standard and the co-incubation of ATP with either base-caged ATP.

5.4 Discussion

This work demonstrates the facile synthesis of base-caged ATP analogues without requiring multiple protection and deprotection steps (Pitsch, Weiss et al. 1999; Hobartner and Silverman 2005). These products are attractive alternatives to classic examples of caged ATPs, which are caged on the γ -phosphate and act by preventing enzymatic dephosphorylation (Kaplan, Forbush et al. 1978; McCray, Herbette et al. 1980; Walker, Reid et al. 1988). Phosphate caged ATP has consistently demonstrated competitive inhibition, which may alter the ATP response of the system being studied (Forbush 1984). For instance, the presence of caged ATP following flash-photolysis slows the contraction rate of muscle fibers by transiently blocking the actomyosin interaction (Thirlwell, Corrie et al.). Based-caged ATPs show very little activity prior to photo-activation, suggesting that caging on the nucleobase prevents enzyme recognition since the phosphates are free for kinase processing.

Nucleoside models were initially performed to access the feasibility for caging CPR on the nucleobase. This system allows for simple reaction analysis and purification by reverse phase HPLC. For both NB-NH₂ and DMNB-NH₂, the generation of base-caged adenosine was observed. Since the caged product appears to be relatively stable, the formation of several side products in the DMNB-NH₂ caging reaction is likely the result of interactions between the cage compound and the solvent/buffer environment. However, side-products resulting from depurination,

phosphate hydrolysis, and ring opening can not be ruled out. The conditions of the substitution reactions were mildly basic to avoid these phenomena. Colorimetric changes following caged ATP reconstitution in water from a methanolic solution, suggests reactivity between 2-nitrobenzylamines and water. Additionally, breakdown products could be more readily formed in a slightly acidic aqueous solution than in basic methanol. Differences between the NB-NH₂ and DMNB-NH₂ groups were likely caused by the electron donating properties of the O-methyl ring substitutions.

CHAPTER 6: Conclusions and Future Directions

6.1 Conclusions

The primary goal of this work was to demonstrate photo-induced RNAi by caging the effector compounds. Originally it was hypothesized that statistical phosphate backbone caging of a long dsRNA transcript would be an ideal means to control RNAi activity. However, *in vitro* analysis of these caged products indicated that the formation of a phosphotriester from the caging process resulted in strand breakage. This suggests that internal phosphate caging of an otherwise unmodified RNA is not a suitable technique for use in aqueous systems. Despite our results, diazo-mediated cage attachment to RNA has since been used to control mRNA expression (Ando, Furuta et al. 2001; Ando, Furuta et al. 2004) and siRNA-mediated gene silencing (Shah, Rangarajan et al. 2005). In the latter case, it is possible that a significant fraction of the siRNAs were caged on the terminal phosphates only. These positions may be more readily caged as they have an additional anionic non-bridging oxygen. In an effort to circumvent the issue of phosphotriester RNA hydrolysis, a uniform chemically modified RNA mimic was tested to RNAi activity.

Fully 2'-deoxy-2'-fluoro modified NA (FNA) was generated for testing of RNAi silencing activity. Eliminating all 2'-hydroxyls greatly reduces the probability of spontaneous intramolecular hydrolysis and protects against 2'-hydroxyl-mediated enzymatic digestion. This modification removes this hydroxyl and allows the NA duplex to form the A-type helical structure through a preferred C3-endo sugar pucker confirmation without disrupting the major or minor grooves. Among all the 2'-

substitutions reported in the literature, the 2'-F modification gives the most consistent results of unaffected RNAi ability {reviewed by [(Manoharan 2004; Zhang, Du et al. 2006)]}. Fully-modified siFNAs were generated through synthetic methods and by *in vitro* transcription. Transcription gave a crude product contaminated with early termination products and full length strands with base incorporation errors. Therefore this technique is somewhat impractical unless considerable improvements are made to reduce polymerase miscoding. The synthetic technique worked well using the corresponding phosphoramidites, which until recently were commercially unavailable for the purines. These products were verified through mass spectrometry and PAGE separation. FNAs demonstrated remarkable resistance to enzymatic digestion by sugar-specific nucleases. However, these products could be digested by BAL-31 nuclease, which proceeds through a sugar-nonspecific mechanism. Additionally, NAs with this substitution exhibited much stronger hybridization properties, as measured by a dramatic increase in thermal stability.

The observed RNAi ability of siFNA was nearly indistinguishable from unmodified siRNAs of the same sequence. It was found throughout the course of the initial cell culture RNAi assay that the hybridization protocol had a significant impact on the ability to knockdown the reporter gene. Since the melting temperature for the FNA duplex approached 95°C, it is possible that slightly misaligned siFNAs could be generated if annealing was rushed or performed at a lower temperature. Extended annealing times at high temperatures prior to cellular transfection improved the silencing ability of the siFNAs. However, this phenomenon was not observed using unmodified siRNAs. In addition to duplex silencing activity, single-stranded antisense FNAs were tested for their ability to reduce target gene expression. It has previously

been shown that antisense RNA that is the proper size for RISC association can enter the RNAi pathway (Martinez, Patkaniowska et al. 2002; Schwarz, Hutvagner et al. 2002; Amarzguioui, Holen et al. 2003; Holen, Amarzguioui et al. 2003). However, the silencing activity of antisense FNA was much less potent than either duplex siFNA or single-stranded antisense RNA. This suggests that antisense FNA is not recognized by RISC, and conversely that duplex siFNA silencing occurs through an enzyme mediated process rather than simple translational arrest.

Once the RNAi activity of siFNA was verified, the ability to cage these effectors was revisited. An activated 4,5-dimethoxy-2-nitrophenyl diazonium cage compound could be used to alkylate the phosphate backbone of each FNA strand individually. This reaction could easily be adjusted to obtain products with varying degrees of alkylation. All caged samples, prior to and following photoexposure, were evaluated using spectroscopy, electrophoresis, and HPLC. Caging also provided additional nuclease stability to the FNAs. FNA samples that were not caged were susceptible to the sugar non-specific nuclease, BAL-31. However, the attachment of DMNPE drastically decreased the ability of BAL-31 to degrade the FNA. It is likely that once this bidirectional exonuclease reaches one or multiple adjoining caging sites, the enzyme might be interrupted from its digestion process. It has previously been shown that an increase in serum and plasma stability due to partial 2'-F modification does not correlate to prolonged RNAi *in vivo* (Layzer, McCaffrey et al. 2004). It is possible that these modified nucleic acids are processed either by RNA endonuclease activity or sugar-nonspecific nucleases. Full modification and caging appears to protect against both of these possibilities.

The ability to trigger RNAi activity using caged siFNA was evaluated in cell culture and a zebrafish *in vivo* model. Taking into account that caging of NAs has been shown to affect hybridization ability (Ordoukhanian and Taylor 1995; Ghosn, Haselton et al. 2005) and that it can aide against enzymatic digestion, DMPNE attachment to FNA should be able to affect NA:NA as well as NA:enzyme interactions. Therefore, caging of siFNAs has the potential to disrupt RNAi in various ways such as: disruption of RISC recognition, helicase unwinding of the duplex, mRNA target recognition, ejection of the digested target for RISC recycling, localization of RISC to specialized organelles, and downstream processing such as chromatin remodeling. It was demonstrated that caging of either strand in a siFNA reduces RNAi activity, however, the caged antisense strand results in a more deleterious effect on RNAi activity. This is not unexpected since the sense FNA is discarded early in the RNAi pathway. Reduction of sense strand caged RNAi is likely caused by improper siFNA formation, reduced delivery of the caged species through lipid mediated transfection, disruption of RISC recognition, disruption of helicase removal of the sense strand, or a combination of these factors. A parallel study carried out by our research group has demonstrated that caging of a fluorophore labeled PS oligonucleotide resulted in no observable difference in lipid-mediated transfection (Fabion, in preparation). Additionally, it is unlikely that cellular delivery is drastically reduced due the attachment of DMNPE since photo-exposure of these treatments restores RNAi activity to levels that are nearly equivalent to the uncaged-control effectors. This observation also suggests that caged FNA duplexes are stable prior to delivery. Caging of the antisense strand had the benefit of significantly less leak RNAi activity. However, only partial restoration using 365 nm light was achieved. HPLC evaluation of these

products suggests that the caged FNAs may consist of a heterogeneous mixture of products that vary in the degree of DMNPE attachment. More lightly caged species may allow for residual RNAi activity, while DMNPE might not be fully removed upon photo exposure for heavily caged species. Compounding the issue of varying amounts of the cage molecule, the location of attachment is random and variable. Disruption of RNAi might be highly dependant on the location of the cage species. Since it is carried through the entire RNAi pathway, it is more likely that the antisense strand has multiple RISC interactions and critical processing locations along its length, and therefore it is more likely for a randomly attached cage group to disrupt silencing.

Zebrafish embryos were used as an *in vivo* model to test the photoinduced silencing ability caged siFNA in support of the cell culture results. The mosaic expression pattern of the GFP reporter transgene prevented quantitative analysis. Nevertheless, qualitative observations strongly suggested that caging reduces the silencing activity of these molecules and that this activity can be restored by photo-activation. Caging of these effectors also protects the embryo from toxicity associated with siFNAs. It has been previously reported that RNAi in zebrafish has a particularly high incidence of off target effects (Oates, Bruce et al. 2000; Zhao, Cao et al. 2001; Giraldez, Mishima et al. 2006). Several potential causes of the observed toxicity include off-target RNAi gene silencing, innate toxicity of siFNAs and their metabolites, or overwhelming of the RNAi machinery. Since normal RNAi results in toxicity, it is likely that the observed increase in mortality rate and developmental delay are related to an RNAi phenomenon, rather than toxicity of breakdown products of FNAs. Injection of single-stranded FNAs did not result in equivalent toxicity, suggesting that breakdown products of FNA digestion are not the cause of the observed

developmental delay. Overwhelming of the RNAi machinery would more critical for a developing system, since endogenous microRNAs are theorized to play a major role in genetic regulation (Matzke and Matzke 2003). This further supports the conclusion that caging of the RNAi effector prevents them from entering the RNAi pathway. If this is true, then the fact that these molecules were activated at 7 hpf demonstrated remarkable intracellular stability of the caged species. Therefore caging of RNAi effectors would allow delivery to a biological system at concentrations that would otherwise be toxic, followed by photo-induction of gene silencing at a specific stage of development in a manner that could control dosing to sub-toxic levels.

In an effort to progress toward site-specifically caged RNAi effectors, we have generated a scheme to incorporate a single cage molecule within a full length RNA oligonucleotide using the convertible nucleoside approach. This requires the generation and testing of cage precursor containing a primary amine at the site of attachment for nucleophilic substitution of the internal convertible base placed during custom synthesis. 4,5-dimethoxy(2-nitrobenzyl)bromide was reacted in pure condensed ammonia to produce the 4,5-dimethoxy ring substituted 2-nitrobenzylamine in sufficient yield and purity. Additionally, an unsubstituted 2-nitrobenzylamine was purchased from a commercial source. These compounds have been tested for the ability to generate a photolabile N6-caged adenosine derivative. Nucleoside model studies were carried out by reacting 6-chloropurine ribose with each amine-containing cage compound. The products were successfully isolated on HPLC and verified by MS. Building on the success of these models, chloropurine riboside triphosphate was caged on the nucleobase to generate base-caged ATP. All previous examples of caged ATP have attached the chromophore the γ -phosphate to prevent

dephosphorylation. However, this attachment site does not prevent a NA-protein association for many of the systems being studied. Therefore γ -phosphate caged ATP often acts as a competitive inhibitor for uncaged ATP. Our results demonstrate this competitive inhibition using a luciferase ATP reporter system *in vitro*. Alternatively, the base-caged ATP analogs do not appear to act as competitive inhibitors. These compounds are also effectively activated by photoexposure. One last additional benefit of this system is that the chloropurine riboside reagent is inactive as an ATP in this reporter system. Therefore, contamination from the caging reaction does not cause leak ATP activity, which is a major problem when using γ -phosphate caged ATP. This is even true when the caged ATP is purchased from a commercial source.

6.2 Future Directions

This work successfully demonstrates using chemically modified NAs that have been caged to control RNAi-mediated gene silencing. Also demonstrated is the ability to cage ATP on the nucleobase through nucleophilic substitution. Within each of these categories, further chemical and photochemical evaluation would strengthen the foundation built in this work. Additionally, each of these techniques has opened the possibility for application based investigations. Finally, the study of base-caged ATP provides a platform toward post-synthetic site-specific caging of oligonucleotides for use in RNAi or other nucleic acid applications.

This work could readily be extended toward the goal of site-specifically caged siRNAs. As aforementioned, the ATP study presented here demonstrates the incorporation of a cage molecule at the N6-position of adenosine. The mechanism of substitution should be amenable toward caging through the convertible nucleotide

approach. In this strategy, a full-length RNA oligonucleotide is synthesized with one or multiple convertible-base modifications inserted during solid phase synthesis. While still resin bound and protected, the convertible nucleotide is incubated with a nitrobenzylamine derivative (or another aminated cage compound) for substitution of the leaving group with the cage compound. If the primary amine is nucleophilic enough, this step should also cleave the RNA from its solid support and deprotect the other nucleobases. However, treatment with concentrated methanolic ammonia following the conversion reaction is an alternative to completely cleave the support. The caged RNA is then 2'-deprotected per normal protocols. One of the initial hurdles of this study will likely be the removal of unbound cage and side products of the conversion reaction prior to 2'-deprotection. Our initial attempts of RNA conversion using NB-NH₂ have been unable to circumvent this issue without sacrificing RNA yield. Additionally, characterization of the caged RNAi product might be difficult if the conversion reaction is of low yield. Separation techniques will likely be needed to isolate the properly caged RNAs.

Assuming that site-specific caging of RNA is successful, there are several immediate phenomena to evaluate. Clearly, an analysis of RNAi with point cage insertions should be initiated. This will allow probing into the siRNA to determine the optimal site(s) for photocaging. Ideally a single cage compound could be inserted into an siRNA molecule to completely ablate gene silencing activity. Under these conditions, caged RNA photoactivation will likely be marked more efficient. Our ATP studies suggest that some degree of uncaging occurs using a NPE nitrobenzyl with an intense 365 nm light. If only a single cage compound is inserted per siRNA, the unsubstituted nitrobenzyl group may be adequately uncaged for photoinduced RNAi

using this light that is less harmful to biological systems than 308 nm light typically used to photolyze NPE-caged compounds. The siRNA used in the study was originally designed for the purpose of site-specific caging. The 11th nucleotide from the 5'-end of the antisense strand is an adenosine. This was chosen so that a “convertible A” could be incorporated and post-synthetically caged. Chapter 1 illustrates that this site is sensitive to base and sugar modifications, and therefore is hypothesized that this is an ideal site for cage incorporation to disrupt RNAi.

Site-specific caging may also make 2-photon excitation (TPE) of RNAi effectors more feasible. Currently these compounds require a large number of siRNA/siFNA alkylation to prevent significant leak activity. However, TPE requires a very high intensity of incident light for uncaging. Concentrating the number a chromophores in this region by attaching multiple cages per oligonucleotide may push the required light intensity for uncaging to unsafe limits. A comparison of two-photon uncaging with discrete increases in the number of attached cage molecules (1, 2, 3, etc.) will be a worthwhile endeavor to determine the relationship between required light energy and the number of bound cage compounds. Additionally, the distance between two cage molecules within a single strand may also affect the efficiency of TPE. Chromophores in close proximity may be able to interact with the excited electron state of a neighboring cage compound.

Another application for site-specifically caged RNAs is to improve upon nuclease resistance assays. By incorporating a cage compound at a specific location, the interruption of catalytic activity can be investigated for various nucleases that act through different mechanisms. For example, caging at the 5'-terminus may protect

exonucleases that digest in the 5' to 3' direction. However this may be ineffectual against 3' to 5' exonucleases or endonucleases.

One of the more recent observations uncovered in this study was the developmental delay caused by high concentrations of siFNA and the associated reversal of this phenomenon by effector caging. The cause of this delay is currently unknown, but it likely occurs through either RNAi off-target gene silencing or overwhelming the RNAi machinery. Positional caging may provide a means to explore this effect. For instance, caging at site 11 may inhibit target recognition and degradation but still allow for RISC assembly. If the developmental delay is caused by overloading the RISC machinery, caging at this site might result in observed toxicity but little reporter-gene silencing. This would allow for modeling of the optimal locations for disrupting hybridization and/or target recognition versus the disruption of RISC assembly. Additionally, this might reveal how many cage molecules are needed to disrupt all RNAi processes.

Protection from siFNA-induced delayed development in zebrafish highlights an important potential application for caging. Since the degree of uncaging can be controlled by adjusting total exposure, dosing of an RNAi effector or some other therapeutic agent can be modulated with light. This is a promising tool for determining safe dosing of therapeutic agents. Initially, this phenomenon could be investigated by caging compounds with known upper limits of toxicity and introducing the caged analogues in excess of this dose. If the quantum yield is adequately determined, light dosing could be calculated for corresponding therapeutic doses and this could be tested against traditional toxicity experiments that can be clouded by transport and breakdown of the therapeutic agent.

REFERENCES

- Allerson, C. R. (1996). Synthesis of structurally constrained and functionally tethered RNAs using convertible ribonucleosides. Chemistry. Cambridge, MA, Harvard University: 151.
- Allerson, C. R., S. L. Chen, et al. (1997). "A chemical method for site-specific modification of RNA: The convertible nucleoside approach." Journal of the American Chemical Society **119**(32): 7423-7433.
- Allerson, C. R., N. Sioufi, et al. (2005). "Fully 2'-modified oligonucleotide duplexes with improved in vitro potency and stability compared to unmodified small interfering RNA." Journal of Medicinal Chemistry **48**(4): 901-4.
- Allerson, C. R., N. Sioufi, et al. (2005). "Fully 2'-modified oligonucleotide duplexes with improved in vitro potency and stability compared to unmodified small interfering RNA." Journal of Medicinal Chemistry **48**(4): 901-904.
- Allerson, C. R. and G. L. Verdine (1995). "Synthesis and biochemical evaluation of RNA containing an intrahelical disulfide crosslink." Chemical Biology **2**(10): 667-75.
- Alvarez, K., J. J. Vasseur, et al. (1999). "Photocleavable protecting groups as nucleobase protections allowed the solid-phase synthesis of base-sensitive SATE- prooligonucleotides." Journal of Organic Chemistry **64**(17): 6319-6328.
- Amarzguioui, M., T. Holen, et al. (2003). "Tolerance for mutations and chemical modifications in a siRNA." Nucleic Acids Research **31**(2): 589-95.
- Anderson, J. C. and C. B. Reese (1962). "A photo-induced rearrangement involving aryl participation." Tetrahedron Letters **1**: 1-4.
- Ando, H., T. Furuta, et al. (2004). "Photo-mediated gene activation by using caged mRNA in zebrafish embryos." Methods Cell Biology **77**: 159-71.
- Ando, H., T. Furuta, et al. (2001). "Photo-mediated gene activation using caged RNA/DNA in zebrafish embryos." Nature Genetics **28**(4): 317-325.

- Aufsatz, W., M. F. Mette, et al. (2002). "RNA-directed DNA methylation in Arabidopsis." Proceedings of the National Academy of Sciences of the United States of America **99 Suppl 4**: 16499-506.
- Aujard, I., C. Benbrahim, et al. (2006). "o-nitrobenzyl photolabile protecting groups with red-shifted absorption: syntheses and uncaging cross-sections for one- and two-photon excitation." Chemistry **12**(26): 6865-79.
- Bagga, S., J. Bracht, et al. (2005). "Regulation by let-7 and lin-4 miRNAs results in target mRNA degradation." Cell **122**(4): 553-63.
- Baumberger, N. and D. C. Baulcombe (2005). "Arabidopsis ARGONAUTE1 is an RNA Slicer that selectively recruits microRNAs and short interfering RNAs." Proceedings of the National Academy of Sciences of the United States of America **102**(33): 11928-33.
- Bayne, E. H. and R. C. Allshire (2005). "RNA-directed transcriptional gene silencing in mammals." Trends in Genetics **21**(7): 370-3.
- Bernstein, E., A. A. Caudy, et al. (2001). "Role for a bidentate ribonuclease in the initiation step of RNA interference." Nature **409**(6818): 363-366.
- Betzig, E., G. H. Patterson, et al. (2006). "Imaging intracellular fluorescent proteins at nanometer resolution." Science **313**(5793): 1642-1645.
- Bourzac, K. (2007). "RNAi's drugs." Technology Review **110**(1): 16-16.
- Boutla, A., C. Delidakis, et al. (2001). "Short 5'-phosphorylated double-stranded RNAs induce RNA interference in Drosophila." Current Biology **11**(22): 1776-80.
- Braasch, D. A., S. Jensen, et al. (2003). "RNA interference in mammalian cells by chemically-modified RNA." Biochemistry **42**(26): 7967-7975.
- Breslow, R. and R. Xu (1993). "Recognition and catalysis in nucleic acid chemistry." Proceedings of the National Academy of Sciences of the United States of America **90**(4): 1201-7.

- Broustovetsky, N., E. Bamberg, et al. (1997). "Biochemical and physical parameters of the electrical currents measured with the ADP/ATP carrier by photolysis of caged ADP and ATP." Biochemistry **36**(45): 13865-13872.
- Brown, E. B., J. B. Shear, et al. (1999). "Photolysis of caged calcium in femtoliter volumes using two-photon excitation." Biophysical Journal **76**(1 Pt 1): 489-99.
- Brown, R. H. and J. B. Miller (1996). "Progress, problems, and prospects for gene therapy in muscle." Current Opinion in Rheumatology **8**(6): 539-43.
- Cameron, J. F., C. G. Willson, et al. (1996). "Photogeneration of amines from alpha-keto carbamates: Photochemical studies." Journal of the American Chemical Society **118**(51): 12925-12937.
- Cekaite, L., G. Furset, et al. (2007). "Gene expression analysis in blood cells in response to unmodified and 2'-modified siRNAs reveals TLR-dependent and independent effects." Journal of Molecular Biology **365**(1): 90-108.
- Chaulk, S. G. and A. M. MacMillan (1998). "Caged RNA: photo-control of a ribozyme reaction." Nucleic Acids Research **26**(13): 3173-8.
- Chaulk, S. G. and A. M. MacMillan (2001). "Separation of Spliceosome Assembly from Catalysis with Caged pre-mRNA Substrates A.M.M. acknowledges support from the Natural Sciences and Engineering Research Council of Canada and the Alberta Heritage Foundation for Medical Research." Angewandte Chemie-International Edition **40**(11): 2149-2152.
- Chaulk, S. G. and A. M. MacMillan (2007). "Synthesis of oligo-RNAs with photocaged adenosine 2'-hydroxyls." Nature Protocols **2**(5): 1052-8.
- Chendrimada, T. P., R. I. Gregory, et al. (2005). "TRBP recruits the Dicer complex to Ago2 for microRNA processing and gene silencing." Nature **436**(7051): 740-4.
- Chiu, Y. L. and T. M. Rana (2002). "RNAi in human cells: Basic structural and functional features of small interfering RNA." Molecular Cell **10**(3): 549-561.
- Chiu, Y. L. and T. M. Rana (2003). "siRNA function in RNAi: a chemical modification analysis." RNA-a Publication of the RNA Society **9**(9): 1034-48.

- Chiu, Y. L. and T. M. Rana (2003). "siRNA function in RNAi: A chemical modification analysis." RNA-a Publication of the RNA Society **9**(9): 1034-1048.
- Conrad, P. G., 2nd, R. S. Givens, et al. (2000). "New phototriggers: extending the p-hydroxyphenacyl pi-pi absorption range." Organic Letters **2**(11): 1545-7.
- Cook, H. A., B. S. Koppetsch, et al. (2004). "The Drosophila SDE3 homolog armitage is required for oskar mRNA silencing and embryonic axis specification." Cell **116**(6): 817-29.
- Corrie, J. E. T., A. Barth, et al. (2003). "Photolytic cleavage of 1-(2-nitrophenyl)ethyl ethers involves two parallel pathways and product release is rate-limited by decomposition of a common hemiacetal intermediate." Journal of the American Chemical Society **125**(28): 8546-8554.
- Corrie, J. E. T. and D. R. Trentham (1992). "Synthetic, mechanistic and photochemical studies of phosphate esters of substituted benzoin." Journal of the Chemical Society, Perkins Transactions 1 **18**: 2409-2417.
- Czaderna, F., M. Fechtner, et al. (2003). "Structural variations and stabilising modifications of synthetic siRNAs in mammalian cells." Nucleic Acids Research **31**(11): 2705-2716.
- Dalmay, T., R. Horsefield, et al. (2001). "SDE3 encodes an RNA helicase required for post-transcriptional gene silencing in Arabidopsis." EMBO Journal **20**(8): 2069-78.
- Davidson, T. J., S. Harel, et al. (2004). "Highly efficient small interfering RNA delivery to primary mammalian neurons induces MicroRNA-like effects before mRNA degradation." Journal of Neuroscience **24**(45): 10040-6.
- Denk, W., J. H. Strickler, et al. (1990). "Two-photon laser scanning fluorescence microscopy." Science **248**(4951): 73-6.
- Ding, L., A. Spencer, et al. (2005). "The developmental timing regulator AIN-1 interacts with miRISCs and may target the argonaute protein ALG-1 to cytoplasmic P bodies in C. elegans." Molecular Cell **19**(4): 437-47.

- Dong, Q., K. Svoboda, et al. (2007). "Photobiological effects of UVA and UVB light in zebrafish embryos: Evidence for a competent photorepair system." Journal of Photochemistry and Photobiology B **88**(2-3): 137-146.
- Donze, O. and D. Picard (2002). "RNA interference in mammalian cells using siRNAs synthesized with T7 RNA polymerase." Nucleic Acids Research **30**(10): -.
- Dorsett, Y. and T. Tuschl (2004). "siRNAs: applications in functional genomics and potential as therapeutics." Nature Reviews Drug Discovery **3**(4): 318-29.
- Dowler, T., D. Bergeron, et al. (2006). "Improvements in siRNA properties mediated by 2'-deoxy-2'-fluoro-beta-D-arabinonucleic acid (FANA)." Nucleic Acids Research **34**(6): 1669-75.
- Du, Q., H. Thonberg, et al. (2005). "A systematic analysis of the silencing effects of an active siRNA at all single-nucleotide mismatched target sites." Nucleic Acids Research **33**(5): 1671-7.
- Eckardt, T., V. Hagen, et al. (2002). "Deactivation behavior and excited-state properties of (coumarin-4-yl)methyl derivatives. 2. Photocleavage of selected (coumarin-4-yl)methyl-caged adenosine cyclic 3',5'-monophosphates with fluorescence enhancement." Journal of Organic Chemistry **67**(3): 703-10.
- Elbashir, S. M., J. Harborth, et al. (2001). "Duplexes of 21-nucleotide RNAs mediate RNA interference in cultured mammalian cells." Nature **411**(6836): 494-498.
- Elbashir, S. M., W. Lendeckel, et al. (2001). "RNA interference is mediated by 21- and 22-nucleotide RNAs." Genes & Development **15**(2): 188-200.
- Elbashir, S. M., J. Martinez, et al. (2001). "Functional anatomy of siRNAs for mediating efficient RNAi in *Drosophila melanogaster* embryo lysate." EMBO Journal **20**(23): 6877-88.
- Ellis-Davies, G. C. (2007). "Caged compounds: photorelease technology for control of cellular chemistry and physiology." Nature Methods **4**(8): 619-28.
- Elmen, J., H. Thonberg, et al. (2005). "Locked nucleic acid (LNA) mediated improvements in siRNA stability and functionality." Nucleic Acids Research **33**(1): 439-47.

- Erlanson, D. A., L. Chen, et al. (1993). "DNA Methylation through a Locally Unpaired Intermediate." Journal of the American Chemical Society **115**(26): 12583-12584.
- Ferentz, A. E., T. A. Keating, et al. (1993). "Synthesis and Characterization of Disulfide Cross-Linked Oligonucleotides." Journal of the American Chemical Society **115**(20): 9006-9014.
- Ferentz, A. E. and G. L. Verdine (1992). "Aminolysis of 2'-Deoxyinosine Aryl Ethers - Nucleoside Model Studies for the Synthesis of Functionally Tethered Oligonucleotides." Nucleosides & Nucleotides **11**(10): 1749-1763.
- Fillman, C. and J. Lykke-Andersen (2005). "RNA decapping inside and outside of processing bodies." Current Opinion in Cell Biology **17**(3): 326-31.
- Fire, A., S. Xu, et al. (1998). "Potent and specific genetic interference by double-stranded RNA in *Caenorhabditis elegans*." Nature **391**(6669): 806-11.
- Forbush, B. (1984). "Na⁺ Movement in a Single Turnover of the Na Pump." Proceedings of the National Academy of Sciences of the United States of America-Biological Sciences **81**(17): 5310-5314.
- Forbush, B., 3rd (1984). "Na⁺ movement in a single turnover of the Na pump." Proceedings of the National Academy of Sciences of the United States of America **81**(17): 5310-4.
- Forman, J., M. Dietrich, et al. (2007). "Photobiological and thermal effects of photoactivating UVA light doses on cell cultures." Journal of Photochemistry and Photobiology **6**(6): 649-58.
- Furuta, T., H. Torigai, et al. (1993). "New photochemically labile protecting group for phosphates." Chemistry Letters **22**(7): 1179.
- Geibel, S., A. Barth, et al. (2000). "P(3)-[2-(4-hydroxyphenyl)-2-oxo]ethyl ATP for the rapid activation of the Na(+),K(+)-ATPase." Biophysical Journal **79**(3): 1346-57.
- Ghosn, B., F. R. Haselton, et al. (2005). "Control of DNA hybridization with photocleavable adducts." Photochem Photobiol **81**(4): 953-9.

- Gil, J. and M. Esteban (2000). "Induction of apoptosis by the dsRNA-dependent protein kinase (PKR): mechanism of action." Apoptosis **5**(2): 107-14.
- Giraldez, A. J., Y. Mishima, et al. (2006). "Zebrafish MiR-430 promotes deadenylation and clearance of maternal mRNAs." Science **312**(5770): 75-9.
- Givens, R. S., P. S. Athey, et al. (1993). "Photochemistry of Phosphate-Esters - Alpha-Keto Phosphates as a Photoprotecting Group for Caged Phosphate." Journal of the American Chemical Society **115**(14): 6001-6012.
- Givens, R. S., A. Jung, et al. (1997). "New photoactivated protecting groups .7. p-Hydroxyphenacyl: A phototrigger for excitatory amino acids and peptides." Journal of the American Chemical Society **119**(35): 8369-8370.
- Givens, R. S. and B. Matuszewski (1984). "Photochemistry of phosphate esters: an efficient method for the generation of electrophiles." Journal of the American Chemical Society **106**: 6860-6861.
- Givens, R. S. and C. H. Park (1996). "p-hydroxyphenacyl ATP: A new phototrigger." Tetrahedron Letters **37**(35): 6259-6262.
- Givens, R. S., J. F. Weber, et al. (1998). "New photoprotecting groups: desyl and p-hydroxyphenacyl phosphate and carboxylate esters." Methods in Enzymology **291**: 1-29.
- Goeldner, M. and R. S. Givens, Eds. (2006). Dynamic Studies in Biology: Phototriggers, Photoswitches and Caged Biomolecules. Dynamic Studies in Biology: Phototriggers, Photoswitches and Caged Biomolecules, Wiley-VCH.
- Goldman, Y. E., M. G. Hibberd, et al. (1982). "Relaxation of muscle fibres by photolysis of caged ATP." Nature **300**(5894): 701-5.
- Göppert-Mayer, M. (1931). "Über Elementarakte mit zwei Quantensprüngen." Ann Phys **9**: 273–295.
- Gossen, M. and H. Bujard (1995). "Efficacy of tetracycline-controlled gene expression is influenced by cell type: commentary." Biotechniques **19**(2): 213-6; discussion 216-7.

- Gossen, M., S. Freundlieb, et al. (1995). "Transcriptional activation by tetracyclines in mammalian cells." Science **268**(5218): 1766-9.
- Grunweller, A., E. Wyszko, et al. (2003). "Comparison of different antisense strategies in mammalian cells using locked nucleic acids, 2'-O-methyl RNA, phosphorothioates and small interfering RNA." Nucleic Acids Research **31**(12): 3185-3193.
- Gupta, S., R. A. Schoer, et al. (2004). "Inducible, reversible, and stable RNA interference in mammalian cells." Proceedings of the National Academy of Sciences of the United States of America **101**(7): 1927-32.
- Guschlbauer, W. and K. Jankowski (1980). "Nucleoside Conformation Is Determined by the Electronegativity of the Sugar Substituent." Nucleic Acids Research **8**(6): 1421-1433.
- Haase, A. D., L. Jaskiewicz, et al. (2005). "TRBP, a regulator of cellular PKR and HIV-1 virus expression, interacts with Dicer and functions in RNA silencing." EMBO Reports **6**(10): 961-7.
- Hagen, V., S. Frings, et al. (2003). "[7-(dialkylamino)coumarin-4-yl]methyl-caged compounds as ultrafast and effective long-wavelength phototriggers of 8-bromo-substituted cyclic nucleotides." Chembiochem **4**(5): 434-442.
- Haley, B., G. Tang, et al. (2003). "In vitro analysis of RNA interference in *Drosophila melanogaster*." Methods **30**(4): 330-6.
- Hall, A. H., J. Wan, et al. (2006). "High potency silencing by single-stranded boranophosphate siRNA." Nucleic Acids Research **34**(9): 2773-81.
- Hall, A. H. S., J. Wan, et al. (2004). "RNA interference using boranophosphate siRNAs: structure-activity relationships." Nucleic Acids Research **32**(20): 5991-6000.
- Hall, I. H., B. S. Burnham, et al. (1993). "Hypolipidemic activity of boronated nucleosides and nucleotides in rodents." Biomed Pharmacother **47**(2-3): 79-87.
- Hall, I. M., G. D. Shankaranarayana, et al. (2002). "Establishment and maintenance of a heterochromatin domain." Science **297**(5590): 2232-7.

- Hamada, M., T. Ohtsuka, et al. (2002). "Effects on RNA interference in gene expression (RNAi) in cultured mammalian cells of mismatches and the introduction of chemical modifications at the 3'-ends of siRNAs." Antisense & Nucleic Acid Drug Development **12**(5): 301-309.
- Hammond, S. M., E. Bernstein, et al. (2000). "An RNA-directed nuclease mediates post-transcriptional gene silencing in *Drosophila* cells." Nature **404**(6775): 293-6.
- Harborth, J., S. M. Elbashir, et al. (2003). "Sequence, chemical, and structural variation of small interfering RNAs and short hairpin RNAs and the effect on mammalian gene silencing." Antisense & Nucleic Acid Drug Development **13**(2): 83-105.
- Heckel, A. and G. Mayer (2005). "Light regulation of aptamer activity: An anti-thrombin aptamer with caged thymidine nucleobases." Journal of the American Chemical Society **127**(3): 822-823.
- Hobartner, C. and S. K. Silverman (2005). "Modulation of RNA tertiary folding by incorporation of caged nucleotides." Angewandte Chemie-International Edition **44**(44): 7305-9.
- Holen, T., M. Amarzguioui, et al. (2003). "Similar behaviour of single-strand and double-strand siRNAs suggests they act through a common RNAi pathway." Nucleic Acids Research **31**(9): 2401-7.
- Holen, T., M. Amarzguioui, et al. (2003). "Similar behaviour of single-strand and double-strand siRNAs suggests they act through a common RNAi pathway." Nucleic Acids Research **31**(9): 2401-2407.
- Holen, T., M. Amarzguioui, et al. (2002). "Positional effects of short interfering RNAs targeting the human coagulation trigger Tissue Factor." Nucleic Acids Research **30**(8): 1757-1766.
- Hong, J. I., Q. Feng, et al. (1992). "Competition, Cooperation, and Mutation: Improving a Synthetic Replicator by Light Irradiation." Science **255**(5046): 848-850.
- Hopt, A. and E. Neher (2001). "Highly nonlinear photodamage in two-photon fluorescence microscopy." Biophysical Journal **80**(4): 2029-36.

- Hunter, C. P. (2000). "Gene silencing: shrinking the black box of RNAi." Current Biology **10**(4): R137-40.
- Il'ichev, Y. V., M. A. Schworer, et al. (2004). "Photochemical reaction mechanisms of 2-nitrobenzyl compounds: Methyl ethers and caged ATP." Journal of the American Chemical Society **126**(14): 4581-4595.
- Jabri, E. (2005). "P-bodies take a RISC." Nature Structural & Molecular Biology **12**(7): 564.
- Jackson, A. L., J. Burchard, et al. (2006). "Position-specific chemical modification of siRNAs reduces "off-target" transcript silencing." RNA-a Publication of the RNA Society **12**(7): 1197-205.
- Jepsen, J. S. and J. Wengel (2004). "LNA-antisense rivals siRNA for gene silencing." Current Opinion in Drug Discov Devel **7**(2): 188-94.
- Kaplan, J. H., B. Forbush, et al. (1978). "Rapid Photolytic Release of Adenosine 5'-Triphosphate from a Protected Analog - Utilization by Na-K Pump of Human Red Blood-Cell Ghosts." Biochemistry **17**(10): 1929-1935.
- Kawasaki, A. M., M. D. Casper, et al. (1993). "Uniformly Modified 2'-Deoxy-2'-Fluoro Phosphorothioate Oligonucleotides as Nuclease-Resistant Antisense Compounds with High-Affinity and Specificity for Rna Targets." Journal of Medicinal Chemistry **36**(7): 831-841.
- Kawasaki, A. M., M. D. Casper, et al. (1993). "Uniformly modified 2'-deoxy-2'-fluoro phosphorothioate oligonucleotides as nuclease-resistant antisense compounds with high affinity and specificity for RNA targets." Journal of Medicinal Chemistry **36**(7): 831-41.
- Kim, J. K., H. W. Gabel, et al. (2005). "Functional genomic analysis of RNA interference in *C. elegans*." Science **308**(5725): 1164-7.
- Kraynack, B. A. and B. F. Baker (2006). "Small interfering RNAs containing full 2'-O-methylribonucleotide-modified sense strands display Argonaute2/eIF2C2-dependent activity." RNA-a Publication of the RNA Society **12**(1): 163-76.
- Kurreck, J. (2003). "Antisense technologies - Improvement through novel chemical modifications." European Journal of Biochemistry **270**(8): 1628-1644.

- Layzer, J. M., A. P. McCaffrey, et al. (2004). "In vivo activity of nuclease-resistant siRNAs." RNA-a Publication of the RNA Society **10**(5): 766-771.
- Lee, R. C., R. L. Feinbaum, et al. (1993). "The *C. elegans* heterochronic gene *lin-4* encodes small RNAs with antisense complementarity to *lin-14*." Cell **75**(5): 843-54.
- Lee, Y. S., K. Nakahara, et al. (2004). "Distinct roles for *Drosophila* Dicer-1 and Dicer-2 in the siRNA/miRNA silencing pathways." Cell **117**(1): 69-81.
- Leuschner, P. J., S. L. Ameres, et al. (2006). "Cleavage of the siRNA passenger strand during RISC assembly in human cells." EMBO Reports **7**(3): 314-20.
- Lewis, B. P., I. H. Shih, et al. (2003). "Prediction of mammalian microRNA targets." Cell **115**(7): 787-98.
- Li, Z. Y., H. Mao, et al. (2005). "The effects of thiophosphate substitutions on native siRNA gene silencing." Biochemical and Biophysical Research Communications **329**(3): 1026-30.
- Lingel, A., B. Simon, et al. (2003). "Structure and nucleic-acid binding of the *Drosophila* Argonaute 2 PAZ domain." Nature **426**(6965): 465-9.
- Liu, J., M. A. Carmell, et al. (2004). "Argonaute2 is the catalytic engine of mammalian RNAi." Science **305**(5689): 1437-41.
- Liu, J., M. A. Valencia-Sanchez, et al. (2005). "MicroRNA-dependent localization of targeted mRNAs to mammalian P-bodies." Nature Cell Biology **7**(7): 719-23.
- Liu, Q., T. A. Rand, et al. (2003). "R2D2, a bridge between the initiation and effector steps of the *Drosophila* RNAi pathway." Science **301**(5641): 1921-5.
- Lorenz, C., P. Hadwiger, et al. (2004). "Steroid and lipid conjugates of siRNAs to enhance cellular uptake and gene silencing in liver cells." Bioorganic & Medicinal Chemistry Letters **14**(19): 4975-4977.
- Ma, J. B., Y. R. Yuan, et al. (2005). "Structural basis for 5'-end-specific recognition of guide RNA by the *A. fulgidus* Piwi protein." Nature **434**(7033): 666-70.

- Macmillan, A. M. and G. L. Verdine (1990). "Synthesis of Functionally Tethered Oligodeoxynucleotides by the Convertible Nucleoside Approach." Journal of Organic Chemistry **55**(24): 5931-5933.
- Macmillan, A. M. and G. L. Verdine (1991). "Engineering Tethered DNA-Molecules by the Convertible Nucleoside Approach." Tetrahedron **47**(14-15): 2603-2616.
- Manoharan, M. (2003). "RNA interference and chemically modified siRNAs." Nucleic Acids Research Suppl(3): 115-6.
- Manoharan, M. (2004). "RNA interference and chemically modified small interfering RNAs." Current Opinion in Chemical Biology **8**(6): 570-579.
- Martinez, J., A. Patkaniowska, et al. (2002). "Single-stranded antisense siRNAs guide target RNA cleavage in RNAi." Cell **110**(5): 563-574.
- Matranga, C., Y. Tomari, et al. (2005). "Passenger-strand cleavage facilitates assembly of siRNA into Ago2-containing RNAi enzyme complexes." Cell **123**(4): 607-20.
- Matsuura, B., M. Dong, et al. (2005). "Demonstration of a specific site of covalent labeling of the human motilin receptor using a biologically active photolabile motilin analog." Journal of Pharmacology and Experimental Therapeutics **313**(3): 1101-8.
- Matzke, M. and A. J. M. Matzke (2003). "Molecular biology - RNAi extends its reach." Science **301**(5636): 1060-1061.
- Mayer, G. and A. Heckel (2006). "Biologically active molecules with a "light switch"." Angewandte Chemie-International Edition **45**(30): 4900-4921.
- Mayer, G., L. Krock, et al. (2005). "Light-induced formation of G-quadruplex DNA secondary structures." Chembiochem **6**(11): 1966-70.
- McCray, J. A., L. Herbet, et al. (1980). "A new approach to time-resolved studies of ATP-requiring biological systems; laser flash photolysis of caged ATP." Proceedings of the National Academy of Sciences of the United States of America **77**(12): 7237-41.

- McCray, J. A. and D. R. Trentham (1989). "Properties and uses of photoreactive caged compounds." Annual review of biophysics and biophysical chemistry **18**: 239-70.
- McGall, G., J. Labadie, et al. (1996). "Light-directed synthesis of high-density oligonucleotide arrays using semiconductor photoresists." Proceedings of the National Academy of Sciences of the United States of America **93**(24): 13555-60.
- Meister, G., M. Landthaler, et al. (2004). "Human Argonaute2 mediates RNA cleavage targeted by miRNAs and siRNAs." Molecular Cell **15**(2): 185-97.
- Meister, G. and T. Tuschl (2004). "Mechanisms of gene silencing by double-stranded RNA." Nature **431**(7006): 343-9.
- Meldrum, R. A., R. S. Chittock, et al. (1998). "Use of caged compounds in studies of the kinetics of DNA repair." Methods in Enzymology **291**: 483-95.
- Meldrum, R. A., S. Shall, et al. (1990). "Kinetics and mechanism of DNA repair. Evaluation of caged compounds for use in studies of u.v.-induced DNA repair." Biochemical Journal **266**(3): 891-5.
- Mikat, V. and A. Heckel (2007). "Light-dependent RNA interference with nucleobase-caged siRNAs." RNA-a Publication of the RNA Society.
- Miyoshi, K., H. Tsukumo, et al. (2005). "Slicer function of Drosophila Argonautes and its involvement in RISC formation." Genes & Development **19**(23): 2837-48.
- Monroe, W. T. and F. R. Haselton (2004). Gene expression targeting using caged DNA. Dynamic Studies in Biology: Phototriggers, Photoswitches and Caged Biomolecules. F. Weinreich, Wiley Interscience Publishing. Submitted March 2004. **In Press**.
- Monroe, W. T., M. M. McQuain, et al. (1999). "Targeting expression with light using caged DNA." Journal Biological Chemistry **274**(30): 20895-900.
- Monroe, W. T., M. M. McQuain, et al. (1999). "Caged DNA: A novel strategy to induce expression with light." The Federation of American Societies for Experimental Biology Journal **13**(4): A192-A192.

- Morrissey, D. V., K. Blanchard, et al. (2005). "Activity of stabilized short interfering RNA in a mouse model of hepatitis B virus replication." Hepatology **41**(6): 1349-56.
- Morrissey, D. V., K. Blanchard, et al. (2005). "Activity of stabilized short interfering RNA in a mouse model of hepatitis B virus replication." Hepatology **41**(6): 1349-1356.
- Morrissey, D. V., J. A. Lockridge, et al. (2005). "Potent and persistent in vivo anti-HBV activity of chemically modified siRNAs." Nature Biotechnology **23**(8): 1002-7.
- Motamedi, M. R., A. Verdel, et al. (2004). "Two RNAi complexes, RITS and RDRC, physically interact and localize to noncoding centromeric RNAs." Cell **119**(6): 789-802.
- Muratovska, A. and M. R. Eccles (2004). "Conjugate for efficient delivery of short interfering RNA (siRNA) into mammalian cells." FEBS Letters **558**(1-3): 63-8.
- Napoli, C., C. Lemieux, et al. (1990). "Introduction of a Chimeric Chalcone Synthase Gene into Petunia Results in Reversible Co-Suppression of Homologous Genes in trans." Plant Cell **2**(4): 279-289.
- Nguyen, Q. N., R. V. Chavli, et al. (2006). "Light controllable siRNAs regulate gene suppression and phenotypes in cells." Biochimica Et Biophysica Acta-Biomembranes **1758**(3): 394-403.
- No, D., T. P. Yao, et al. (1996). "Ecdysone-inducible gene expression in mammalian cells and transgenic mice." Proceedings of the National Academy of Sciences of the United States of America **93**(8): 3346-51.
- Noma, K., T. Sugiyama, et al. (2004). "RITS acts in cis to promote RNA interference-mediated transcriptional and post-transcriptional silencing." Nature Genetics **36**(11): 1174-80.
- Nykanen, A., B. Haley, et al. (2001). "ATP requirements and small interfering RNA structure in the RNA interference pathway." Cell **107**(3): 309-21.
- Oates, A. C., A. E. Bruce, et al. (2000). "Too much interference: injection of double-stranded RNA has nonspecific effects in the zebrafish embryo." Developmental Biology **224**(1): 20-8.

- Oishi, M., Y. Nagasaki, et al. (2005). "Lactosylated poly(ethylene glycol)-siRNA conjugate through acid-labile beta-thiopropionate linkage to construct pH-sensitive polyion complex micelles achieving enhanced gene silencing in hepatoma cells." Journal of the American Chemical Society **127**(6): 1624-5.
- Okamura, K., A. Ishizuka, et al. (2004). "Distinct roles for Argonaute proteins in small RNA-directed RNA cleavage pathways." Genes & Development **18**(14): 1655-66.
- Ordoukhanian, P. and J. S. Taylor (1995). "Design and Synthesis of a Versatile Photocleavable Dna Building-Block - Application to Phototriggered Hybridization." Journal of the American Chemical Society **117**(37): 9570-9571.
- Padilla, R. and R. Sousa (1999). "Efficient synthesis of nucleic acids heavily modified with non-canonical ribose 2'-groups using a mutant T7 RNA polymerase (RNAP)." Nucleic Acids Research **27**(6): 1561-1563.
- Padilla, R. and R. Sousa (2002). "A Y639F/H784A T7 RNA polymerase double mutant displays superior properties for synthesizing RNAs with non-canonical NTPs." Nucleic Acids Research **30**(24): -.
- Padilla, R. and R. Sousa (2002). "A Y639F/H784A T7 RNA polymerase double mutant displays superior properties for synthesizing RNAs with non-canonical NTPs." Nucleic Acids Research **30**(24): e138.
- Park, C. H. and R. S. Givens (1997). "New photoactivated protecting groups .6. p-hydroxyphenacyl: A phototrigger for chemical and biochemical probes." Journal of the American Chemical Society **119**(10): 2453-2463.
- Parker, J. S., S. M. Roe, et al. (2004). "Crystal structure of a PIWI protein suggests mechanisms for siRNA recognition and slicer activity." EMBO Journal **23**(24): 4727-4737.
- Parker, J. S., S. M. Roe, et al. (2005). "Structural insights into mRNA recognition from a PIWI domain-siRNA guide complex." Nature **434**(7033): 663-6.
- Parrish, S., J. Fleenor, et al. (2000). "Functional anatomy of a dsRNA trigger: differential requirement for the two trigger strands in RNA interference." Molecular Cell **6**(5): 1077-87.

- Pelliccioli, A. P. and J. Wirz (2002). "Photoremovable protecting groups: reaction mechanisms and applications." Photochemical & Photobiological Sciences **1**(7): 441-458.
- Pham, J. W., J. L. Pellino, et al. (2004). "A Dicer-2-dependent 80s complex cleaves targeted mRNAs during RNAi in *Drosophila*." Cell **117**(1): 83-94.
- Pillai, R. S., S. N. Bhattacharyya, et al. (2005). "Inhibition of translational initiation by Let-7 MicroRNA in human cells." Science **309**(5740): 1573-6.
- Pillai, V. N. R. (1980). "Photoremovable Protecting Groups in Organic Synthesis." Synthesis: 1-26.
- Pirrung, M. C. and S. W. Shuey (1994). "Photoremovable protecting groups for phosphorylation of chiral alcohols. Asymmetric synthesis of phosphotriesters of (-)-3',5'-dimethoxybenzoin." Journal of Organic Chemistry **59**(14): 3890-3897.
- Pitsch, S., P. A. Weiss, et al. (1999). "Fast and reliable automated synthesis of RNA and partially 2-O- protected precursors ('caged RNA') based on two novel, orthogonal 2-O-protecting groups, preliminary communication." Helvetica Chimica Acta **82**(10): 1753-1761.
- Prakash, T. P., C. R. Allerson, et al. (2005). "Positional effect of chemical modifications on short interference RNA activity in mammalian cells." Journal of Medicinal Chemistry **48**(13): 4247-4253.
- Puthenveetil, S., L. Whitby, et al. (2006). "Controlling activation of the RNA-dependent protein kinase by siRNAs using site-specific chemical modification." Nucleic Acids Research **34**(17): 4900-11.
- Rajesh, C. S., R. S. Givens, et al. (2000). "Kinetics and mechanism of phosphate photorelease from benzoin diethyl phosphate: evidence for adiabatic fission to an -keto cation in the triplet state." Journal of the American Chemical Society **122**(4): 611-618.
- Rand, T. A., K. Ginalski, et al. (2004). "Biochemical identification of Argonaute 2 as the sole protein required for RNA-induced silencing complex activity." Proceedings of the National Academy of Sciences of the United States of America **101**(40): 14385-9.

- Rehwinkel, J., I. Behm-Ansmant, et al. (2005). "A crucial role for GW182 and the DCP1 : DCP2 decapping complex in miRNA-mediated gene silencing." RNA-a Publication of the RNA Society **11**(11): 1640-1647.
- Reinhart, B. J. and D. P. Bartel (2002). "Small RNAs correspond to centromere heterochromatic repeats." Science **297**(5588): 1831.
- Rhoades, M. W., B. J. Reinhart, et al. (2002). "Prediction of plant microRNA targets." Cell **110**(4): 513-20.
- Rivas, F. V., N. H. Tolia, et al. (2005). "Purified Argonaute2 and an siRNA form recombinant human RISC." Nature Structural & Molecular Biology **12**(4): 340-9.
- Rock, R. S. and S. I. Chan (1998). "Preparation of a water-soluble "cage" based on 3',5'-dimethoxybenzoin." Journal of the American Chemical Society **120**: 10766–10767.
- Romano, N. and G. Macino (1992). "Quelling: transient inactivation of gene expression in *Neurospora crassa* by transformation with homologous sequences." Molecular Microbiology **6**(22): 3343-53.
- Ruvkun, G. (2001). "Molecular biology. Glimpses of a tiny RNA world." Science **294**(5543): 797-9.
- Sarker, A. M., Y. Kaneko, et al. (1998). "Photochemistry and photophysics of novel photoinitiators: N,N,N-tributyl-N-(4-methylene-7-methoxycoumarin) ammonium borates." Journal of Photochemistry and Photobiology A: Chemistry **117**(1): 67-74.
- Sarker, A. M., Y. Kaneko, et al. (1997). "Photoinduced electron-transfer reactions: highly efficient cleavage of C-N bonds and photogeneration of tertiary amines." Journal of Physical Chemistry A **102**(8): 5375-5382.
- Sasaki, T., A. Shiohama, et al. (2003). "Identification of eight members of the Argonaute family in the human genome small star, filled." Genomics **82**(3): 323-30.
- Schade, B., V. Hagen, et al. (1999). "Deactivation behavior and excited-state properties of (coumarin-4-yl)methyl derivatives. 1. Photocleavage of (7-

methoxycoumarin-4-yl)methyl-caged acids with fluorescence enhancement." Journal of Organic Chemistry **64**(25): 9109-9117.

Schoenleber, R. O. and B. Giese (2003). "Photochemical Release of Amines by C,N-Bond Cleavage." Synthetic Letters **2003**(4): 501-504.

Schramke, V. and R. Allshire (2003). "Hairpin RNAs and retrotransposon LTRs effect RNAi and chromatin-based gene silencing." Science **301**(5636): 1069-74.

Schwarz, D. S., G. Hutvagner, et al. (2002). "Evidence that siRNAs function as guides, not primers, in the Drosophila and human RNAi pathways." Molecular Cell **10**(3): 537-548.

Schwarz, D. S., Y. Tomari, et al. (2004). "The RNA-induced silencing complex is a Mg²⁺-dependent endonuclease." Current Biology **14**(9): 787-91.

Sen, G. L. and H. M. Blau (2005). "Argonaute 2/RISC resides in sites of mammalian mRNA decay known as cytoplasmic bodies." Nature Cell Biology **7**(6): 633-6.

Shah, S. and S. H. Friedman (2007). "Tolerance of RNA interference toward modifications of the 5' antisense phosphate of small interfering RNA." Oligonucleotides **17**(1): 35-43.

Shah, S., S. Rangarajan, et al. (2005). "Light activated RNA interference." Angewandte Chemie-International Edition **44**(9): 1328-1332.

Shaw, B. R., D. Sergueev, et al. (2000). "Boranophosphate backbone: a mimic of phosphodiester, phosphorothioate, and methyl phosphonates." Methods in Enzymology **313**: 226-57.

Sheehan, J. C. and K. J. Umezawa (1973). "Phenacyl photosensitive blocking groups." Journal of Organic Chemistry **38**: 3771-3774.

Sheehan, J. C., R. M. Wilson, et al. (1971). "The photolysis of methoxy-substituted benzoin esters. A photosensitive protecting group for carboxylic acids." Journal of the American Chemical Society **93**: 7222-7228.

- Song, J. J., J. Liu, et al. (2003). "The crystal structure of the Argonaute2 PAZ domain reveals an RNA binding motif in RNAi effector complexes." Nature Structural Biology **10**(12): 1026-32.
- Song, J. J., S. K. Smith, et al. (2004). "Crystal structure of Argonaute and its implications for RISC slicer activity." Science **305**(5689): 1434-7.
- Sousa, R. and R. Padilla (1995). "Mutant T7 Rna-Polymerase as a DNA-Polymerase." EMBO Journal **14**(18): 4609-4621.
- Soutschek, J., A. Akinc, et al. (2004). "Therapeutic silencing of an endogenous gene by systemic administration of modified siRNAs." Nature **432**(7014): 173-178.
- Tabara, H., E. Yigit, et al. (2002). "The dsRNA binding protein RDE-4 interacts with RDE-1, DCR-1, and a DExH-box helicase to direct RNAi in *C. elegans*." Cell **109**(7): 861-71.
- Tang, G., B. J. Reinhart, et al. (2003). "A biochemical framework for RNA silencing in plants." Genes & Development **17**(1): 49-63.
- Tang, G. and P. D. Zamore (2004). "Biochemical dissection of RNA silencing in plants." Methods in Molecular Biology **257**: 223-44.
- Tang, X. J. and I. J. Dmochowski (2005). "Phototriggering of caged fluorescent oligodeoxynucleotides." Organic Letters **7**(2): 279-282.
- Tang, X. J. and I. J. Dmochowski (2006). "Controlling RNA digestion by RNase H with a light-activated DNA hairpin." Angewandte Chemie-International Edition **45**(21): 3523-3526.
- Tang, X. J. and I. J. Dmochowski (2007). "Regulating gene expression with light-activated oligonucleotides." Molecular Biosystems **3**(2): 100-110.
- Thirlwell, H., J. E. Corrie, et al. (1994). "Kinetics of relaxation from rigor of permeabilized fast-twitch skeletal fibers from the rabbit using a novel caged ATP and apyrase." Biophysical Journal **67**(6): 2436-47.

- Ting, R., L. Lermer, et al. (2004). "Triggering DNAzymes with light: A photoactive C8 thioether-linked adenosine." Journal of the American Chemical Society **126**(40): 12720-12721.
- Tomari, Y., T. Du, et al. (2004). "RISC assembly defects in the Drosophila RNAi mutant armitage." Cell **116**(6): 831-41.
- Tomari, Y., C. Matranga, et al. (2004). "A protein sensor for siRNA asymmetry." Science **306**(5700): 1377-80.
- Tomari, Y. and P. D. Zamore (2005). "Perspective: machines for RNAi." Genes & Development **19**(5): 517-529.
- van der Krol, A. R., L. A. Mur, et al. (1990). "Flavonoid genes in petunia: addition of a limited number of gene copies may lead to a suppression of gene expression." Plant Cell **2**(4): 291-9.
- Vickers, T. A., S. Koo, et al. (2003). "Efficient reduction of target RNAs by small interfering RNA and RNase H-dependent antisense agents. A comparative analysis." Journal Biological Chemistry **278**(9): 7108-18.
- Volpe, T., V. Schramke, et al. (2003). "RNA interference is required for normal centromere function in fission yeast." Chromosome Research **11**(2): 137-46.
- Volpe, T. A., C. Kidner, et al. (2002). "Regulation of heterochromatic silencing and histone H3 lysine-9 methylation by RNAi." Science **297**(5588): 1833-7.
- Walker, C. J., G. P. Reid, et al. (1988). "Photolabile 1-(2-Nitrophenyl)ethyl phosphate esters of adenine nucleotide analogues." Journal of the American Chemical Society **110**: 7170-7177.
- Wassenegger, M. (2000). "RNA-directed DNA methylation." Plant Mol Biol **43**(2-3): 203-20.
- Wassenegger, M., S. Heimes, et al. (1994). "RNA-directed de novo methylation of genomic sequences in plants." Cell **76**(3): 567-76.

- Wei, C. F., G. A. Alianell, et al. (1983). "Isolation and comparison of two molecular species of the BAL 31 nuclease from *Alteromonas espejiana* with distinct kinetic properties." Journal Biological Chemistry **258**(22): 13506-12.
- Wenter, P., B. Furtig, et al. (2005). "Kinetics of photoinduced RNA refolding by real-time NMR spectroscopy." Angewandte Chemie-International Edition **44**(17): 2600-3.
- Westerfield, M. (2000). The Zebrafish Book, A Guide for Laboratory Use of Zebrafish (Danio Rerio). Eugene, OR, Univ. of Oregon Press.
- Williams, B. R. G. (1997). "Role of the double-stranded RNA-activated protein kinase (PKR) in cell regulation." Biochemical Society Transactions **25**(2): 509-513.
- Yan, X., J. F. Mouillet, et al. (2003). "A novel domain within the DEAD-box protein DP103 is essential for transcriptional repression and helicase activity." Molecular Cell Biology **23**(1): 414-23.
- Yang, M., Y. Li, et al. (2005). "MicroRNAs: Small regulators with a big impact." Cytokine Growth Factor Reviews **16**(4-5): 387-93.
- Yang, W. and T. A. Steitz (1995). "Recombining the Structures of Hiv Integrase, Ruvc and Rnase-H." Structure **3**(2): 131-134.
- Yazbeck, D. R., K. L. Min, et al. (2002). "Molecular requirements for degradation of a modified sense RNA strand by *Escherichia coli* ribonuclease H1." Nucleic Acids Research **30**(14): 3015-25.
- Yazbeck, D. R., K. L. Min, et al. (2002). "Molecular requirements for degradation of a modified sense RNA strand by *Escherichia coli* ribonuclease H1." Nucleic Acids Research **30**(14): 3015-25.
- Yip, R. W., D. K. Sharma, et al. (1985). "Photochemistry of the o-nitrobenzyl system in solution: evidence for singlet state intramolecular abstraction." Journal of Physical Chemistry **89**: 5328-5330.
- Yip, R. W., X. Y. Wen, et al. (1991). "Photochemistry of the o-nitrobenzyl system in solution : identification of the biradical intermediate in the intramolecular rearrangement." Journal of Physical Chemistry **1991**(95): 6078-6081.

- Young, D. D. and A. Deiters (2007). "Photochemical control of biological processes." Organic & Biomolecular Chemistry **5**(7): 999-1005.
- Yuan, Y. R., Y. Pei, et al. (2005). "Crystal structure of A. aeolicus argonaute, a site-specific DNA-guided endoribonuclease, provides insights into RISC-mediated mRNA cleavage." Molecular Cell **19**(3): 405-19.
- Zhang, H. Y., Q. Du, et al. (2006). "RNA interference with chemically modified siRNA." Current Topics in Medicinal Chemistry **6**(9): 893-900.
- Zhang, K., J. E. T. Corrie, et al. (1999). "Mechanism of photosolvolytic rearrangement of p-hydroxyphenacyl esters: evidence for excited-state intramolecular proton transfer as the primary photochemical step." Journal of the American Chemical Society **121**(24): 5625-5632.
- Zhang, K. J. and J. S. Taylor (1999). "A caged ligatable DNA strand break." Journal of the American Chemical Society **121**(49): 11579-11580.
- Zhang, L., R. Buchet, et al. (2004). "Phosphate binding in the active site of alkaline phosphatase and the interactions of 2-nitrosoacetophenone with alkaline phosphatase-induced small structural changes." Biophysical Journal **86**(6): 3873-3881.
- Zhao, Z., Y. Cao, et al. (2001). "Double-stranded RNA injection produces nonspecific defects in zebrafish." Developmental Biology **229**(1): 215-23.
- Zilberman, D., X. Cao, et al. (2004). "Role of Arabidopsis ARGONAUTE4 in RNA-directed DNA methylation triggered by inverted repeats." Current Biology **14**(13): 1214-20.

LETTER OF PERMISSION

From: on behalf of Journals Rights
To: Mattingley Sue
Subject: RE: Special request for Publisher approval -> Fwd: CB&DD manuscript/permission for dissertation

Tom K. Sawyer,

Editor-in-Chief
Chemical Biology and Drug Design

Dr. Sawyer,


I have recently had a manuscript published in Chemical Biology & Drug Design (see citation below). I would like to use a slightly modified version of this manuscript as a chapter of my Ph.D. dissertation, and I need the publisher's expressed written permission. Please let me know if 1) you are willing to give me permission to use the manuscript in the dissertation and 2) if the answer is yes, how do I officially request a letter from you or Blackwell Publishing? I have provided my contact information below.

Thank you,
Richard Blidner
149 EB Doran Building
Dept. Biological & Agricultural Engineering
Baton Rouge, LA 70803
P: 225-578-7369
F: 225-578-3492

Blidner RA, Hammer RT, Lopez MJ, Robinson SO, Monroe WT. Fully 2'-deoxy-2'-fluoro substituted nucleic acids Induce RNA interference in mammalian cell culture. *Chem Biol & Drug Design*. 2007 Aug;70(2):133-22.

Permission is granted for you to use the material you specify below subject to the usual acknowledgements (author, title of material, title of book/journal, ourselves as publisher) and on the understanding that, wherever in the original text we acknowledge another source for the requested material.

Non-exclusive WORLD ENGLISH LANGUAGE
one edition, print and electronic version of publication only.
This permission is granted on the condition that you contact the author for consent should you wish to adapt/modify the material.
This is not the responsibility of Blackwell Publishing.

22 Oct '07 

VITA

Richard Andrew Blidner, son of Bruce and Patricia Blidner, was born February 1, 1979, in Columbus Ohio. He graduated from Westerville South High School in 1997. In May, 2001, he earned his Bachelor of Science degree in Biomedical Engineering with departmental honors from Tulane University School of Engineering in New Orleans, Louisiana. While at Tulane, he held the Founder's Scholarship award and conducted research at the Louisiana State University Health Science Center directed towards an animal model of glaucoma. Afterwards, he attended The Ohio State University and earned a Master of Science degree in Biomedical Engineering in March, 2003. From 2001-2002, he held a university fellowship. After receiving his M.S. degree, he worked as a surgical corneal tissue recovery technician procuring human tissue for research and transplant at the Central Ohio Lyon's Eye Bank in Columbus, Ohio until August, 2003. He then enrolled at Louisiana State University in the interdisciplinary doctorate program of Engineering Science in August, 2003. While at Louisiana State University he held an Economic Development Assistantship from August, 2003, to July, 2007. From July, 2007, to November, 2007, he continued as a Research Assistant in the laboratory of Dr. W. Todd Monroe.